Rockfall triggering and meteorological variables in the Dolomites (Italian Eastern Alps)

Francesca N. Bonometti [1], Giuseppe Dattola [1], Paolo Frattini [1], Giovanni B. Crosta [1]

[1]Department of Earth and Environmental Sciences - DISAT, Università degli Studi di Milano-Bicocca, Milano, 20126, Italy

Correspondence to: Francesca N. Bonometti (f.bonometti2@campus.unimib.it)

Abstract. Alpine areas are ~~undergoing the highest change~~experiencing substantial changes in both temperature and rainfall intensity~~ that represent main rockfall triggering factors. Since few approaches were proposed to analyse it, a new approach using meteorological variable frequencies was developed to comprehend~~, both critical triggers for rockfall events. To better understand these evolving climatic scenarios in the Dolomites from 1970 to 2019 ~~with implication on triggering~~and their implications for historical rockfall ~~events in the Dolomites.~~ occurrences, we developed a novel approach based on the frequency analysis of meteorological variables.

~~The~~Our analysis considered key climate variables~~:~~ including mean air temperature, precipitation, thermal amplitude, freeze~~/~~-thaw cycles, and icing, ~~under different~~examined at various aggregation scales. Results ~~reveal that~~ unequivocally show a significant warming trend, with the highest warming rates ~~were~~(up to 0.3°C per decade) observed during spring~~, while~~. This warming has led to an earlier onset of summer and a delayed end of winter, altering seasonal lengths. We also detected a notable ~~reduction in icing and~~decline in cold-related phenomena, with an estimated decrease of 7.3 freeze-thaw ~~cycles frequency was obtained during spring and autumn. An anticipation of both starting of summer and ending of winter was detected. Analyses with~~ days and 2.2 icing days per decade. Precipitation patterns are changing too, with an increasing frequency of high-intensity rainfall events, particularly in winter, and a reduction in low-intensity events across all seasons. The Rescaled Adjust~~m~~ent~~d~~ Partial Sums (RAPS) method ~~provided valuable insights into~~ further confirmed long-term precipitation ~~long-term~~ trends ~~and fluctuations.~~

~~The analysis showed an increasing trend over last decade (2000-2019) suggesting variation in precipitation~~, revealing that climatic evolution is driven by shifts in variable frequencies ~~over years. The~~rather than just extreme values. Employing a Bayesian method ~~was employed to study~~ , we investigated the conditional probability of ~~meteorological variables~~rockfall occurrences knowing that a meteorological variable is within a given range. Our findings reveal several key correlations: in the last decade high-intensity rainfall correlates with rockfalls in autumn, showing conditional probabilities of 12.4% below 1000 m and 22.2% between 1000-2000 m. Mean air temperature correlates with rockfalls in summer, for instance, with a 12.7% probability for 21-24°C between 1000-2000 m, and in autumn, such as a 2.2% probability for 17.6-20.8°C above 2000m. Temperature amplitude shows high rockfall probabilities in spring, reaching 28.6% for 8.8-9.9°C below 1000 m, and in winter, with a 5.8% probability for 9-10°C between 1000-2000 m. Beyond these meteorological links, rockfall frequency exhibits three main peaks: November, February-April, and August. Regarding rockfall source aspect, north component has significant increment from 1970-1999 to 2000-2025 (from 4% to 12% +3%) above 2000 m, a pattern likely linked to permafrost thawing. This study underscores the critical influence of changing climate dynamics on rockfall ~~events. Rockfalls and high intensity rainfall are correlated in autumn, while with mean temperature at different altitudes in summer and autumn. Higher values probability of temperature amplitude characterises spring, while autumn seasons are interested to high temperature variation values. Finally, it was observed strong dependency of the freeze-thaw cycles and icing periods by regional timeseries.~~activity in Alpine environments, providing quantitative links between specific meteorological shifts and rockfall occurrence.

1 Introduction

Rockfalls are ~~a type of instantaneous collapse~~sudden and dangerous landslide~~, involving the detachment of a~~ events where rock ~~block (or several~~ blocks~~)~~ detach from ~~a vertical or sub-vertical cliff, followed by rapid down-slope motion characterised by~~steep cliffs and move rapidly downslope through free-falling, bouncing, rolling, and ~~local~~ sliding ~~phases~~ (Varnes, 1978). These phenomena ~~can involve a wide range of volumes and are extremely hazardous~~pose significant hazards to human lives, structures, and ~~infrastructures~~infrastructure, varying widely in volume and impact (Bunce et al., 1997; Crosta and Agliardi, 2004; Hilker et al., 2009; Volkwein et al., 2011; Zhao et al., 2017).

~~Various~~ Numerous intrinsic and external parameters, ~~highly variable over~~which vary considerably in space and time, can trigger rockfalls (Volkwein et al., 2011~~), including~~). These include earthquakes (Valagussa et al., 2014), intense rainfall (Palladino et al., 2018), snowmelt, permafrost degradation (Ravanel et al., 2017), freeze-thaw cycles (Matsuoka and Sakai, 1999), and ground temperature oscillations (Luethi et al., 2015; Palau et l., 2024; Stoffel et al., 2024), both in cold and warm conditions. ~~Therefore, it is important to consider them when understanding~~Understanding the evolution of slopes in response to climate change, and its impact on ~~rock fall~~rockfall frequency and seasonality, is therefore crucial (Davies et al., 2001; Fischer et al., 2006; Stoffel and Huggel, 2012; Corò et al., 2015; Palau et al., 2024).

~~Climate change has caused a~~Mountain regions, particularly the Alps, have experienced significant ~~increase in~~ temperature ~~in mountain areas (Pepin et al., 2022) and the Alpine area~~increases over the last 150 years (Pepin et al., 2022; Schär et al., 2004), with annual mean warming rates in the Alps of ~~about~~approximately 0.5°C per decade since 1980 (Böhm et al., 2001; Allen and Huggel, 2013~~) beyond the average global~~). These accelerated changes~~. These changes are particularly impactful~~ in the Alpine environment~~, leading to increase rockfalls.~~ exacerbate rockfall activity. The ~~effects~~impacts of climate change in the ~~Alpine area include~~Alps manifest as: (i) ~~potential~~ a substantial rise in temperature ~~rise~~ (Beniston, 2006; Brunetti et al., 2009; Gobiet et al., 2014), (ii) increased frequency and intensity of ~~phenomena such as~~extreme events like floods, droughts, rockfalls, and landslides (Gariano and Guzzetti, 2016; Palladino et al., 2017), and (iii) ~~increased frequency of~~more frequent medium and extreme precipitation events~~(~~, particularly during autumn and winter (Krautblatter and Moser, 2009~~), especially during autumn and winter (~~; Schmidli and Frei, 2005). A direct consequence of global warming is the ~~increased~~accelerated degradation of permafrost ~~(~~in many high-mountain, steep rock slopes environments (Noetzli et al., 2003; Gobiet et al., 2014; Draebing et al., 2019; Manent et al., 2024~~) in many steep rock slopes in high-mountain environments (~~; Salzmann et al., 2007~~), which can affect~~). This degradation significantly impacts slope stability ~~at different scales. Gruber and Haeberli (2007) highlighted that~~ , as warming air temperatures at high altitudes ~~lead to permafrost degradation, affecting the stability of steep rock walls at different timings, magnitudes, and depths, as well as the~~ alter the thermal and hydraulic conditions of the rock mass~~. Davies et al. (2001) suggested that warming air temperatures alter the~~ (Gruber and Haeberli, 2007) and reduce rock mass shear strength by modifying active layer thickness and fracture conditions~~, reducing rock mass shear strength (~~ (Davies et al., 2001; Krautblatter et al., 2013).

The widespread effects of changing mean and extreme temperatures~~,~~ and precipitation are ~~likely~~expected to ~~be widespread, influencing~~influence both the ~~occurrence (in terms of~~ temporal frequency~~)~~ and ~~the~~ magnitude of future mass movements across the Alps. ~~Therefore, it is necessary to analyse the relationship between meteorological variables and rockfall events. Many~~Numerous studies ~~in the literature~~ have ~~demonstrated~~established the relationship between rockfall occurrence and climate conditions in the Alpine environment. For instance, ~~Frayssines and Hantz (2006) and D'Amato et al. (2016)~~correlations have been found ~~a correlation between rockfalls and~~ with freeze-thaw cycles~~, while Delonca et al. (2014) found a correlation with~~ (Frayssines and Hantz, 2006; D'Amato et al., 2016), rainfall and minimum temperature~~. Seasonality also plays a role in rockfall occurrence, with Maciotta~~ (Delonca et al., 2014), and seasonality. Macciotta et al~~.~~., (2015, 2017) ~~noting~~highlighted the importance of freeze-thaw in early spring ~~and~~, while Perret et al. (2006) observ~~ing~~ed a positive correlation ~~between rockfall events and~~ with temperature in early summer. ~~Studying~~More recently, Stoffel et al. (2024) analyzed a 100-year rockfall time-series~~, at a degrading slope~~ in the Swiss Alps, ~~Stoffel et al (2024) found~~revealing that interannual and decadal ~~trends indicate~~

that rockfall activity correlates with summer air temperatures, and increases increasing with warmer temperaturesconditions. This pattern, observed during the Early Twentieth Century Warming (ETCW) and since the mid-1980s, strongly suggests that degrading permafrost contributes to slope instability and rockfalls, with interannual variations affected by other factors (e.g. snow cover, ground heat, and soil moisture).) influencing interannual variations.

To characterise the possible relationships between different climate variables and the triggering of slope failures, Previous research, such as that by Paranunzio et al. (2015, 2016, 2019), Viani et al. (2020), and Paranunzio and Marra (2024)), proposed a nonparametric method by analysingto characterize relationships between climate variables and slope failures by analyzing climate anomalies associated with different time aggregations associated with the events. Their . This method involves, based on ranking all values of a climatic variable (V) recorded over the years values (in ascending order withfor a chosenspecific scale aggregation. Each rockfall has n values of V_i, with i from 1 to n, associated with different years, where i is the i-th value of V in the ranked sample. The associated) and computing a probability P(V) is calculated assuming variable V to be a significant triggering factor at an *alpha* level. This methodof anomalies, links an extreme value of a climate variablues with a rockfall event without consideringevents, but does not fully account for their frequency. However, during periods of climate change, variations in frequency occur across the entire range of meteorological variables, not just at their extremes. These changes can also influence the onset of rockfalls.

The aim of this workstudy is therefore to calculate the spatial and temporal frequency variation in time and space of differentvariations of various climate variables in the eastern Italian Eastern Alps, in order to understand the climate evolution in the area and its influenceimpact on the distribution of rockfall frequency distribution.at different elevations. To achieve this, end, we propose a new method basedthat builds on Paranunzio'sParanunzio's (2015) methodology (2015) is proposed with improvements to address previous limitations regarding rockfall eventto include the frequencies, applying it to a large of both anomalous and non-anomalous climate variables affecting rockfall events. This refined method was applied to a comprehensive database of rockfall events within the study area.

This paper is organized as follows: Section 2 illustratesdetails the study area and the collection of rockfall and climate data. Section 3 describes the methodology used for climate analysis and rockfall characteriszation. Section 4 presents the results of the analyses. Section 5 discusses some issues with previous work. Finally, the conclusion reports on the correlation between climate change and rockfall events.

2 Case study

2.1 Study area

The study area, located encompassing approximately 24.500km^2 in the eastern Italian Alps, spans 24.500km^2 and includes the Trentino-Alto Adige Region, andalong with the provinces of Belluno (Veneto region), Pordenone and Udine (Friuli Venezia Giulia region). This area encompassesis home of the Dolomites region, a group of carbonate platforms located informing a south-vergent Neogene thrust-and-fold belt within the eastern part of Southern European Alps, a south-vergent Neogene thrust-and-fold belt, which constitutes a structural unit of the Alpine chain (Doglioni, 1987, Bosellini et al., 2003). The Dolomites are separated from the Austroalpine Unit by theThe Periadriatic Lineament, a major fault system of Oligocene-Neogene age. In the northernmost sector of the Bolzano Province (i.e., Aurina Valley), a little, separates the Dolomites from the Austroalpine Unit. A small portion of the Tauern tectonic window is present, where the lower Penninic Unit crops out, is also present in the northernmost sector of Bolzano Province (Aurina Valley) (Dal Piaz et al., 2003; Coroò et al., 2015).

The bedrock of the study area consists of various lithologies, ranging. It ranges from Permian terrigenous deposits including , such as the Val Gardena Sandstone (sandstone with conglomerates) and the Bellerophon Formation (dolostone with chalks (i.e., Val Gardena Sandstone, Bellerophon Fm.),gypsum), to early Cretaceous carbonate rocks characterised by grey dolostone with oolites, breccias, limestone and claystone (i.e., . These carbonate formations include the Werfen Fm.,Formation, Serla

Dolostones, Contrin ~~Fm.,~~Formation, Marmolada Limestone, Sciliar ~~Fm.,~~Formation, Cassiano Dolostones, Raibl ~~Fm., Formation, and~~ Dolomia Principale ~~Fm.).~~Formation, characterized by grey dolostone with oolites, breccias, limestone and claystone. These successions ~~dominate~~are prevalent in the province of Belluno, Trento, Pordenone and Udine. In the central ~~part of the~~ Trentino-Alto Adige region, the "Gruppo Vulcanico Atesino" ~~consisting of~~comprises volcanic rocks (pyroclastic flow, with subordinate domes and lavas~~),~~) that can reach a thickness of ~~2000m of~~2000 metres. Additionally, ~~in~~ the province of Bolzano, ~~micaschists, phyllites and gneisses are present,~~ particularly ~~to the~~ north and northwest of the Periadriatic Lineament ~~(Coro~~, features micaschists, phyllites and gneisses (Corò et al., 2015) (Figure 1).

The local morphology is primarily controlled by the geological and structural ~~setting of the area, characterised~~settings, characterized by rock types with varying mechanical properties (Frattini et al., 2008). These rocks ~~were initially severely folded or faulted~~underwent significant folding and ~~then uplifted~~faulting, followed by uplift during ~~the~~ various phases of the Alpine orogeny. ~~Furthermore, the landscape was significantly reshaped during~~ Pleistocene glaciations~~.~~ furtherly dramatically reshaped the landscape. Throughout the study area, the landscape is ~~prominently~~distinctly marked by landforms ~~(e.g.,~~such as cirques and U-shape valleys~~),~~ sculpted by ~~the~~ glacial tongues that occupied the region during the Last Glacial Maximum (LGM) and retreated to the highest valleys during the Late glacial period (Bassetti and Borsato, 2015).

The topography of the study area is very irregular, characterized by valleys situated at an altitude less than 400 m, such as Val d'Adige, Valsugana, Riva del Garda e Valle del Piave, and peaks up to altitudes of over 3000 m, such as Ortles (3900 m), Presanella Group (3500 m), Marmolada (3350 m), Antelao (3264 m). In literature at these altitudes it is declared the presence of permafrost (i.e., a portion of soil or rock that remains at a temperature below freezing for at least two consecutive years). In the study area, thanks to the Alpine Permafrost Index Map (APIM) (Boeckli et al., 2011), it could be observed the presence of permafrost at altitudes above 2500 m for north-facing walls and above 2700 m for south-facing walls. The distribution of permafrost with the orientation of the rock walls shows a more frequency towards walls with orientations approximately ia a range between 300° and 50° N.

The region's climate is alpine with continental characteristics and exhibits significant local variations due to microclimates. The Belluno Valley and the Po basin in the Friuli Venezia Giulia Region are influenced by humid breezes from the Adriatic Sea (Desiato et al., 2005). In contrast, the internal mountainous areas experience a typically continental climate, characterised by cold winters and mild summers. Rainfall mainly occurs as brief summer thunderstorms, whereas autumn rainfall is more prolonged (Coro et al., 2015; Frattini et al., 2008).

2.2 Data collection

To ~~analyse~~investigate the relationship between climate variation and ~~its relation with~~ rockfall events~~,~~ (as reported in Sect. 3~~,~~), a ~~complete~~comprehensive record of meteorological variables and rockfall data ~~is required.~~was essential. The ~~descriptions and~~ methods used ~~to obtain these~~for data acquisition are detailed below.

2.2.1 Meteo-climatic time-series

~~Time~~Meteorological time-series ~~of meteorological~~ data ~~from weather stations~~ were collected from the SCIA website (https://scia.isprambiente.it/~~(https://scia.isprambiente.it/). Some weather stations were excluded to~~; Desiato et al., 2011; Padulano et al., 2021). To ensure a homogeneous dataset~~;~~, only weather stations ~~containing~~with complete daily time-series of climatic variables were ~~considered. Consequently,~~included. This selection process resulted in 277 out of 1244 weather stations ~~were~~being selected (Figure 1~~(Fig. 1).~~). The ~~chosen~~selected climatic variables ~~included~~were total daily rainfall, daily minimum temperatures, and daily maximum temperatures. The daily time-series ~~spanned~~covered the period from January 1, 1970, to December 31, 2019.

~~A dataset for~~For each climatic variable a dataset was generated, containing: (i) an identification code for ~~the stations~~each station, (ii) the~~ir~~ coordinates of each station, and (iii) ~~their~~ daily values ~~of~~ for the respective climatic variable~~s~~.

2.2.2. Rockfall catalogue

A new rockfall dataset was ~~created~~compiled from ~~5503~~5628 events ~~extracted~~gathered from various sources: (i) 543~~1~~72 from the Italian Landslide Inventory project (IFFI https://idrogeo.isprambiente.it/~~),~~; Trigila et al., 2007), (ii) 10~~1~~12 rockfalls from the Geomorphological impacts of Climate change in the Alps (GeoClimAlp https://geoclimalp.irpi.cnr.it/~~)~~; Nigrelli et al., 2024) database, (iii) 18 from ~~the~~Gruppo Rete Ferroviaria Italiana (RFI) dataset, and (iv) 66 from online news sources (https://www.ildolomiti.it/~~.~~; https://www.ladige.it/; https://www.guidedolomiti.com/tag/frane-crolli/). To establish a correlation between climatic variables and rockfall events, it ~~is essential~~was crucial to have information on the day, month, and year of occurrence. Therefore, 2971 events (out of ~~5503 events, 2971 with~~the initial 5628) were considered, as complete date information was available for these events (Figure 1~~were considered (Fig. 1).~~). A comprehensive dataset was generated for these events, including: identification code (ID), coordinates (x, y, z), date of event (dd/mm/yyyy), and the associated three closer weather station.

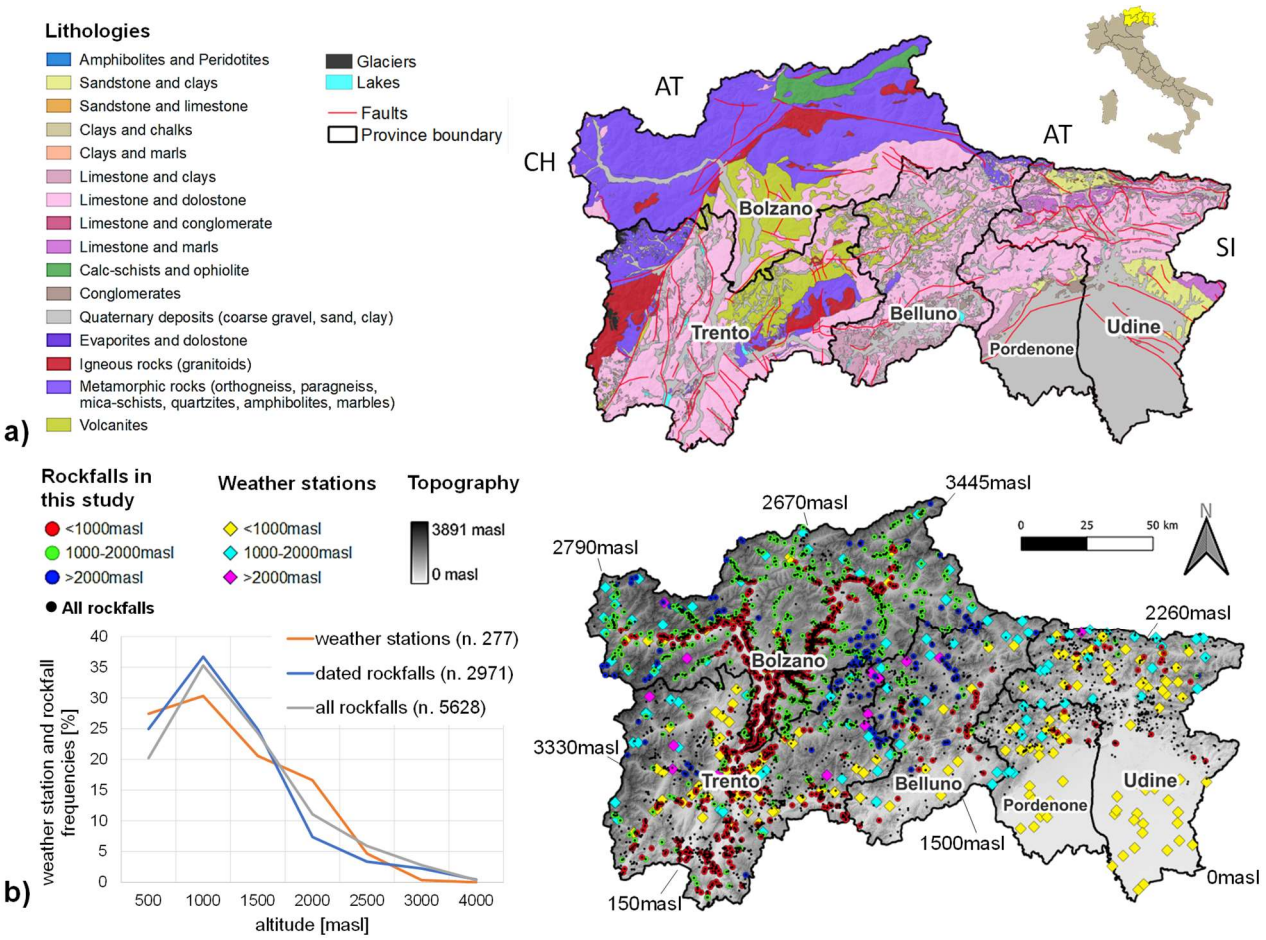

Figure 1~~:~~. (a) Geological setting of the study area (lithology modified from regional open source data). (b) Location and distribution according to altitude of 277 weather station (diamonds), 5628 rockfall data (black dots) and 2971 dated rockfall events (dots) used in the analyses. Meteorological stations: 87 in Trento Province, 46 in Bolzano Province, 30 in Belluno Province, 37 in Pordenone Province and finally 77 in Udine Province. The monitoring network consider~~at~~ed from SCIA are: Idrografica, Regionale and Sinottica. Rockfall events are located: 41~~0~~3 in Trento Province, 2391 in Bolzano Province, 13~~0~~2 in Belluno Province, 9 in Pordenone Province and 29 in Udine Provinces.

3 Methods

The proposed method ~~involves assessing~~aims to assess both the variation of climatic conditions in an area and the effects of this variation on rockfall occurrence. ~~In this~~This analysis~~,~~ computes the frequency of meteorological data ~~is computed~~ by ~~extrapolating from the meteo-stations' time-series to create a~~creating sampled time-series~~, using~~ from recorded weather station data, a procedure ~~discussed~~detailed in the following sub-sections. Differently from Paranunzio et al. (2015, 2016), which ~~identified~~focused on identifying anomalies in ~~the analysed~~ meteorological variables time series, this method ~~focuses~~

~~on~~emphasizes the frequency of statistical samples of meteorological variables within their characteristic value ranges defined as the interval between the maximum and minimum values ~~ranges.~~ obtained from the used time series.

The *measured meteorological variables* from the weather station ~~employed~~used in this study were ~~the same as~~consistent with those in Paranunzio et al. (2015, 2016~~), namely~~): daily minimum air temperature T_0, daily maximum air temperature T_1, and daily precipitation R.

~~The *derived*~~*Derived meteorological variables* included: daily mean air temperature, T_m, and daily air temperature amplitude, $T_a = (T_1 - T_0)$. To analyse the effects induced by both freeze~~/~~-thaw cycles and icing, two Boolean variables were introduced: freeze~~/~~-thaw cycle, C_{FT}, which is 1 if the cycle occurs ($T_0 \leq 0°C$ and $T_1 > 0°C$), and icing, I, which is true (1) if both T_0 and T_1 are negative. These derived climatic variables were ~~chosen~~selected based on previous studies indicating their potential to trigger rockwall instabilities in alpine environment (Douglas, 1980; Sandersen et al., 1996; Matsuoka and Sakai, 1999; Frayssines and Hantz, 2006; Letortu 2013; ~~d~~D'Amato et al., ~~2015; Maciotta~~2016; Macciotta et al., 2017).

3.1 Computed time-series of meteorological variables

~~Since the time-series of aforementioned variables refer to daily~~Daily measurements~~,~~ of meteorological variables do not directly capture the effects of multi-day ~~quantities cannot be directly obtained from them.~~processes. To ~~overcome~~address this ~~limitation~~, *computed time-series* ~~(obtained~~were derived from the original data ~~through~~using various computational methods~~)~~ ~~were derived using the following procedure, which considers~~ that account for multi-day ~~effects (~~aggregation ~~scale, S_a~~scales (S_a). ~~Let us consider~~Consider a time series of ~~one of the above-mentioned~~a meteorological variable~~s~~:

$$(D_i, V_i) \quad i = 1, \cdots, n_t \tag{1}$$

where V_i ~~is~~represents the meteorological variable value, D_i is the corresponding date, and n_t is length of the time-series (i.e., the number of record values ~~of reported in the~~). Computed time-series~~). It is possible to derive the computed time-series~~ can be derived using three basic procedures: mean, addition and subtraction.

~~In case of~~For the mean procedure, the new time-series ~~can be~~is obtained by computing the average ~~following~~as shown in Eq.(2):

$$\bar{V}_i = avg\left(\left[V_{i-S_a}; V_i\right]\right) \quad i = \mathrm{S_a}, \cdots, n_t \tag{2}$$

where avg is the average operator, $\bar{V}_i$ is the mean of the values within the closed interval $\left[V_{i-S_a}; V_i\right]$. Consequently, the mean time-series ~~h~~takes the ~~following~~ form:

$$(D_i, \bar{V}_i) \quad i = \mathrm{S_a}, \cdots, n_t \tag{3}$$

~~In case of~~For the addition ~~the~~procedure, new values are computed as indicated in Eq. (4):

$$V_i^a = \sum_{j=1}^{S_a-1} V_{i+1-S_a+j} \quad i = \mathrm{S_a}, \cdots, n_t \tag{4}$$

~~and the~~The resulting new time-series ~~has the form expresses~~is expressed as in Eq. (5):

$$(D_i, V_i^a) \quad i = \mathrm{S_a}, \cdots, n_t \tag{5}$$

Finally, in the subtraction procedure, the new values are computed using the following formula:

$$\Delta V_i = V_i - V_{i-S_a} \quad i = \mathrm{S_a} + 1, \cdots, n_t \tag{6}$$

and the new time-series ~~h~~takes the form:

$$(D_i, \Delta V_i) \quad i = \mathrm{S_a} + 1, \cdots, n_t \tag{7}$$

For the C_{FT} (freeze-thaw cycle) and I (icing) time-series, the computed time-series ~~coincides~~align directly with the original ones ~~since no aggregation scale is considered for these~~, after that they are aggregated as the other meteorological variables.

3.2 Sampled time-series

Once the computed time-series were obtained, ~~the~~ *sampled time-series* were derived ~~from them~~ using ~~the~~a reference date set D_r and ~~the~~a temporal scale S_t. ~~Denoting~~Let D_e be a ~~chosen~~selected date. ~~t~~The set of reference dates $\boldsymbol{D}_r$ set is defined ~~with~~by Eq. (8):

$$\boldsymbol{D}_r = \{D_i \mid D_i = D_e + k365days\} \quad (8)$$

This set ~~contains~~includes the chosen date and ~~the~~ corresponding dates with same day and month but from different years ~~of the chosen date.~~. The number of years used for the analysis depends on the dates available in the computed time-series ~~dates~~. The sample time-series is then obtained from the computed time-series using the following condition:

$$(D_i, V_i^s) = (D_i, V_i^c) \quad D_i \in [D_r - S_t; D_r + S_t] \quad (9)$$

~~in which~~In this context, $D_r \in \boldsymbol{D}_r$ ~~are~~represent the reference dates ~~and~~, V_i^c is the value ~~of~~from the computed time-series according to the procedures ~~proposed~~outlined in the previous sub-section, and V_i^s is the value ~~of~~in the sample time-series.

3.4 Bayesian method

The influence of a weather variable on rockfall events can be analy~~s~~zed using the Bayesian method (Bayes. 1763~~),~~) to ~~obtain~~determine the conditional probability of rockfall occurrence (Rf) under the condition that a meteorological variable ~~to act as a trigger for a rockfall (Berti et al., 2012).~~is within a given range. Consider a time series of a meteorological variable, ~~with~~where its range is divided into specific intervals. Let ~~R represents~~Rf represent the set of rockfall events under analysis, and M_i the set of recorded data falling within a specific $i-th$ interval~~. The probability can be obtained as follows:~~ of the meteorological variable.

~~$P(R|M_t) = P(M_t|R)\frac{P(R)}{P(M_t)}$~~ The conditional ~~(10)~~

~~where $P(R|M_t)$ is the~~ probability $P(Rf|M_i)$ that rockfall events ~~are~~occur, conditioned ~~by~~on the meteorological variable being within the range $i-th$, can be obtained as follows:

$$P(Rf|M_i) = P(M_i|Rf)\frac{P(Rf)}{P(M_i)} \quad (11)$$

~~(R)~~where $P(Rf)$ is the overall rockfall daily probability, calculated dividing the number of rockfall events by the number of days of observation; $P(M_i)$ is the daily probability of the meteorological variable falling within the $i-th$ range, ~~and finally,~~ calculated dividing the number of days with the variable within that range by the number of observation days; and P~~$(M_t|R)$~~$(M_i|Rf)$ is the probability of the meteorological variable being in the $i-th$ interval when a rockfall event occurs, calculated as the number of rockfall events occurred with the variable within that range divided by the total number of rockfall events.

To apply this method ~~to the aforementioned variables~~, a time series of the selected meteorological variable for the study area ~~under consideration~~ must be used. This involves averaging the time-series data from all considered stations. For each day ~~of~~within the measurement interval, the value of the meteorological variable is the mean of the values from all stations included in the analysis. After processing this new time-series with the proposed approach, a sample time-series is obtained, which is then used in the Bayesian method. For the ~~case of~~ icing and freeze~~/~~-thaw time-series, both spatial mean, maximum and

minimum values of the maximum and minimum temperatures were considered~~, taking into account both spatial mean, maximum and minimum values~~.

3.5 Climate analysis

~~Considering all~~For the ~~meteo-~~climate analysis, only meteorological stations ~~in the area those~~ with time-series ~~covering a range of~~spanning five decades (1970-2019) were selected~~. To perform a climate analysis, ~~, aligning with climatological standards established by the World Meteorological Organization (WMO~~) ~~establishes the *climatological standards,* (WMO~~, 1989~~) namely averages of~~). While WMO generally recommends 30-year periods for climatological ~~data computed for consecutive periods of 30 years. They~~normals, it also ~~introduce~~acknowledges *provisional normals* ~~(WMO, 1989), which are short period means~~ based on observations extending over at least ten years at continental or global scales~~. Based on this consideration~~ (WMO, 1989). Given the restricted study area, a ten-year interval was deemed sufficient ~~for the restricted area considered in this study.~~. Therefore, only meteo-stations with complete time-series from 1970 to 2019 were ~~chosen for~~included in the following analyses.

The ~~above procedure was~~procedures outlined in previous sections were employed to ~~obtain~~derive both ~~the~~ calculated and sampled time-series, using an aggregation scale $S_a = \{0,7,30,90\}$ and a temporal scale $S_t = 45$ days. For the C_{FT} and I variables, ~~the time~~an aggregation scale $S_a = \{7\}$ and a temporal scale $S_t = \{15,45\}$ ~~was~~were used. The results were then grouped into five decades~~, and for~~. For each decade, the values ~~for~~of each variable were divided into ten bins, and their corresponding frequencies were computed. For the C_{FT} and I variables, the frequency of persistence was computed, ~~where the persistence of C_{FT} and I were~~ defined as the number of continuous days ~~in~~for which C_{FT} and I are respectively true. ~~The aim of this~~This computation ~~was~~aimed to ~~check the~~evaluate temporal variations in the frequency of each variable ~~over time~~.

3.6 Rockfall and climate indices

The ~~aforementioned~~described method requires ~~the time-series of the~~ meteorological ~~variables~~ variable time-series as input. However, ~~the location of the~~ rockfall event locations often differs from ~~that of the meteo-stations, and consequently, the~~weather station locations, meaning direct meteorological time-series for that precise ~~point is not known. Therefore,~~rockfall source are typically unavailable. To overcome this, two methods were used to derive the necessary time-series ~~was derived from the time-series recorded at the meteo-stations using two methods~~.

The first ~~methods involve assessing the distance between the meteo-stations and the rockfall event source,~~method involves selecting the time-series associated with the closest meteo-station~~, as follows~~ to the rockfall source:

$$V_{rf}(t) = V_n(t) \tag{12}$$

where $V_{rf}(t)$ is the rockfall source time-series, and the $V_n(t)$ is the time series for the closest ~~time-series~~ weather station. ~~This method is the same as that employed by Paranunzio et al. (2015).~~ This approach, however, does not account for the fact that meteorological variables ~~change according to (i)~~vary significantly with both elevation and ~~(ii)~~ spatial location. These variations are ~~significant~~crucial because weather stations and rockfall sources typically have different elevations and spatial locations~~.~~ ~~Therefore, the time series from~~, meaning that a single weather ~~stations~~ station's time series may not ~~be representative of~~accurately represent the rockfall ~~source~~ site. To address ~~this issue~~these limitations, the following procedure was ~~used in this study.~~adopted. First, the weather ~~station points~~ stations were connected ~~by~~using a Delaunay triangulation ~~that considers,~~ considering only their horizontal coordinates. ~~Consequently, the~~Each rockfall source point ~~belongs to~~then falls within one of the triangles of ~~the Delaunay~~this triangulation. The vertices of the~~is~~ triangle are three weather stations, referred to as nodal weather stations, which are associated with that specific rockfall event source. The time series from these nodal weather stations were subsequently used to calculate the time series at the rockfall event source.

To obtain the rockfall site weather time-series, two corrections were ~~employed~~applied. The ~~first correction, the~~ altitude correction~~, involved adjusting the~~ adjusts temperature time-series values using the following mathematical expressions Eq. (12):

$$V_i^*(t) = V_i(t) - c(z_{rf} - z_i) \quad (13)$$

~~wh~~Here $V_i(t)$ is the variable value recorded by the nodal weather stations, z_i is the nodal weather elevation, z_{rf} is the rockfall elevation, c is the vertical gradient correction~~,~~ (with $c = 0.0065°C/m$ according to Stull, 2000), and $V_i^*(t)$ ~~are~~represents the corrected weather variable values. ~~According to (Stull, 2000) $c = 0.0065°C/m$.~~This simple linear approach, which is based on a constant vertical gradient, has been used despite the fact that is expected that warming in mountain regions depends on elevation (Pepin et al., 2015; Nigrelli et al., 2018; Pepin et al., 2022).

The spatial correction ~~involves computing~~computes the site weather time-series ~~according to~~based on the spatial positions of the nodal stations using the following relationship:

$$V_{rf}(t) = N_1(x,y)V_1^*(t) + N_2(x,y)V_2^*(t) + N_3(x,y)V_3^*(t) \quad (14)$$

where $N_i(x,y)\ i = 1,2,3$ are the weight functions ~~depending~~that depend on the ~~weather stations's~~ positions of the nodal weather stations, and (x,y) represents the coordinates of the rockfall event source. The weight functions, ranging between 0 and 1, were computed by imposing a linear interpolation between the weather stations' values according to their spatial positions. This correction was applied to temperature ~~and rainfall variables.~~. Figure 2 provides a schematic representation of the rockfall source, P, and the surrounding weather stations (S_1, S_2 and S_3) forming a triangle used in the time-series computations.

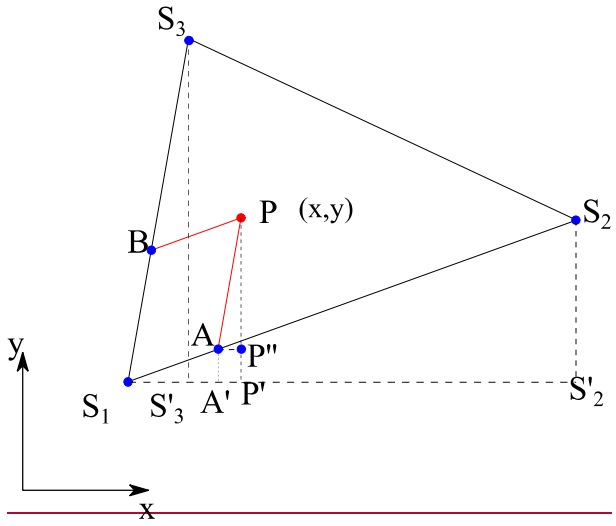

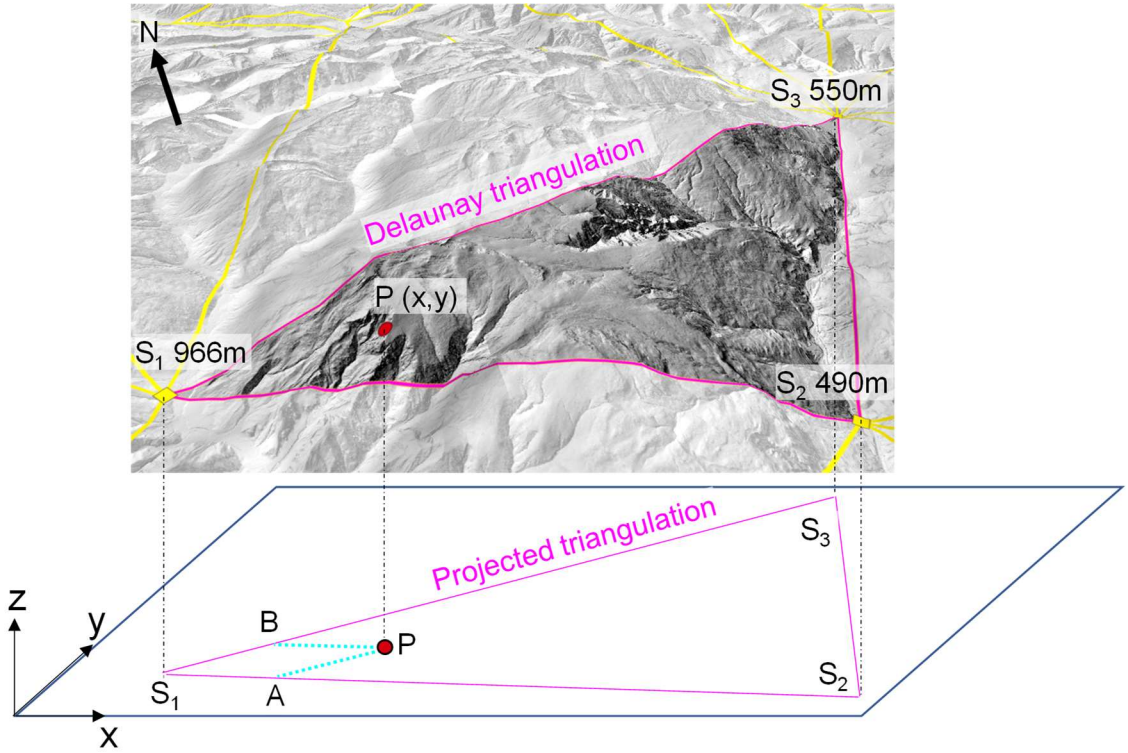

Figure 2~~:~~. Schematic representation of the rockfall source point P and the weather stations (S_1, S_2 and S_3) positions forming a triangle used int time-series computations. Points A and B are the inclined projections of the point P along the edges $\overline{S_1S_3}$ and $\overline{S_1S_2}$.

Once $V_{rf}(t)$ was computed for all meteorological variables, the computed time-series and sampled time-series were subsequently obtained. This triangulation approach partially compensates for the problem of sparse weather stations that may be distant from the landslide points. However, it assumes an even spatial distribution of weather stations and a linear trend in the variables, both of which may not be accurate in complex terrain.

3.7 Rescaled Adjusted Partial Sums (RAPS)

To visualize long-term trends, fluctuations, and periodicities climatic records, the Rescaled Adjusted Partial Sums (RAPS) approach, proposed by Garbrecht and Fernandez (1994), was employed. This method is a powerful tool for analyzing time series data, particularly in hydrology and meteorology, as it facilitates the detection of irregularities and fluctuations (e.g., temperature, precipitation) that might not be evident using traditional analysis techniques. RAPS involves rescaling the partial sums of deviations from the mean of a time series, enabling the identification of significant changes or trends over time. It provides a visual representation and analysis of cumulative deviations from the mean, scaled by the standard deviation, to reveal underlying patterns and trends in the data. This technique is particularly effective for identifying breakpoints and subperiods within the data, making it valuable for studying long-term climatic trends and periodicities (Garbrecht and Fernandez, 1994, Durin et al., 2022). Mathematically, the RAPS value at time k can be expressed with the following Eq. (14):

$$RAPS_k = \sum_{t=1}^{k} \frac{Y_t - \bar{Y}}{S_y} \quad (15)$$

where $RAPS_k$ is the rescaled adjusted partial sum at time ($t = 1,2,..,k$) represents the individual data points in the time series, $\bar{Y}$ is the mean of the time series, and S_y is the standard deviation of the time series.~~attained~~ In this study, the RAPS method was utilized to compare its conclusions with those obtained from the proposed approach.

4 Results

Rockfall events are initiated by various mechanisms that ~~generate~~ contribute to rock mass degradation, ~~which in turn leads~~leading to a progressive reduction in rock mass strength~~,~~. This is particularly prevalent in areas with steep slopes ~~and,~~ sparse vegetation, or ~~with~~ permafrost. This study specifically focuses on the effects of meteorological variables in triggering rockfall events. Over ~~the~~recent decades, observed changes in climate conditions have ~~led to~~resulted in variations in meteorological variables, thereby altering degradation rates and the probability of ~~triggering rockfalls.~~rockfall initiation. Consequently, this ~~affects~~influences the temporal and spatial distribution of rockfall events. Using the method~~o~~logy proposed in the Sect. 3, the following analysis demonstrates the impact of climate change on rockfall ~~events~~occurrences.

~~Eighteen~~For the purpose of this work, three sets of meteorological stations ~~out of the total 277~~ were considered.

Set A comprises all 277 selected stations and was used for the Bayesian method to analyse the frequency of climate ~~analysis, based on those with~~variables.

Set B contains 18 stations chosen from the ~~longest records covering~~original 277. These stations were specifically selected because they have a complete time series spanning the entire period from 1970 to 2019~~. The results are presented~~ with no data gaps. Results for mean air temperature and precipitation are presented at a 90-day aggregation scale, while ~~a 7-day aggregation scale was used to assess the frequency of~~ results for freeze-thaw cycles~~. This choice was made to observe~~ are presented at 7-day scale. This enabled the observation of detailed short-term changes ~~and avoid~~while avoiding overlap with other months. Additional results are provided in the supplementary materials for completeness (S1). ~~The analysis of rockfall events was performed using data from all 277 stations. The frequency of climate variables associated with rockfall events is shown for an aggregation scale of 0 days, while results for other aggregation scales are reported in~~

Set C consists of 12 weather stations with complete time series. These stations were selected to analyse long-term trends at different elevations (below 1000 m, between 1000 and 2000 m, and above 2000 m a.s.l.). To ensure the ~~supplementary materials (S2).~~selected stations were homogeneous, four stations were chosen for each elevation range. Two distinct periods were considered: 1970–2019 for stations below 2000 m and 1985–2019 for stations above 2000 m a.s.l..

4.1 Climate analysis

4.1.1 Rainfall

Rainfall is a ~~significant~~critical triggering factor for rockfalls, ~~especially~~particularly when ~~its~~exhibiting high intensity ~~is very high, as water infiltrates~~. Water infiltration into rock mass discontinuities~~, affecting both the onset of rockfalls (Delonca et al., 2014; Palladino et al., 2018) by increasing water~~ pressure, ~~the melting of~~melts ice within fractures, ~~the erosion of~~erodes discontinuity infillings, and ~~the dissolution of~~dissolve cementing materials, all of which contribute to the onset of rockfalls (Delonca et al., 2014; Palladino et al., ~~(~~2018; Nissen et al., 2022).

The evolution of rainfall ~~over~~was analyzed across different decades~~,~~ and seasons, ~~and at~~utilizing a 90-day aggregation scale ~~was analysed, and the~~ . The results, presented in terms of frequency, are ~~reported~~displayed in Fig. 3. Apart from minor fluctuations between ~~different~~ decades, particularly noticeable above 2000 meters of elevation during spring (~~shown~~illustrated in supplementary materials, Fig.S2), a general trend shows an increase in the frequency of ~~low and~~ high-height rainfall ~~intensity~~ events ~~decreases and increases, respectively. The largest increase in high-intensity frequencies occurs~~, concomitantly leading to a proportional decrease in low-height events. The most substantial increase in the frequency of large rainfall amounts is observed during the winter and autumn seasons. This behaviour becomes more ~~evident~~pronounced with increasing aggregation scale, as the cumulative effect of three months of accumulated rainfall ~~are added up (see the results of other aggregation scales in the~~ is considered (refer to supplementary materials~~,~~ S1.1 for results at other aggregation scales).

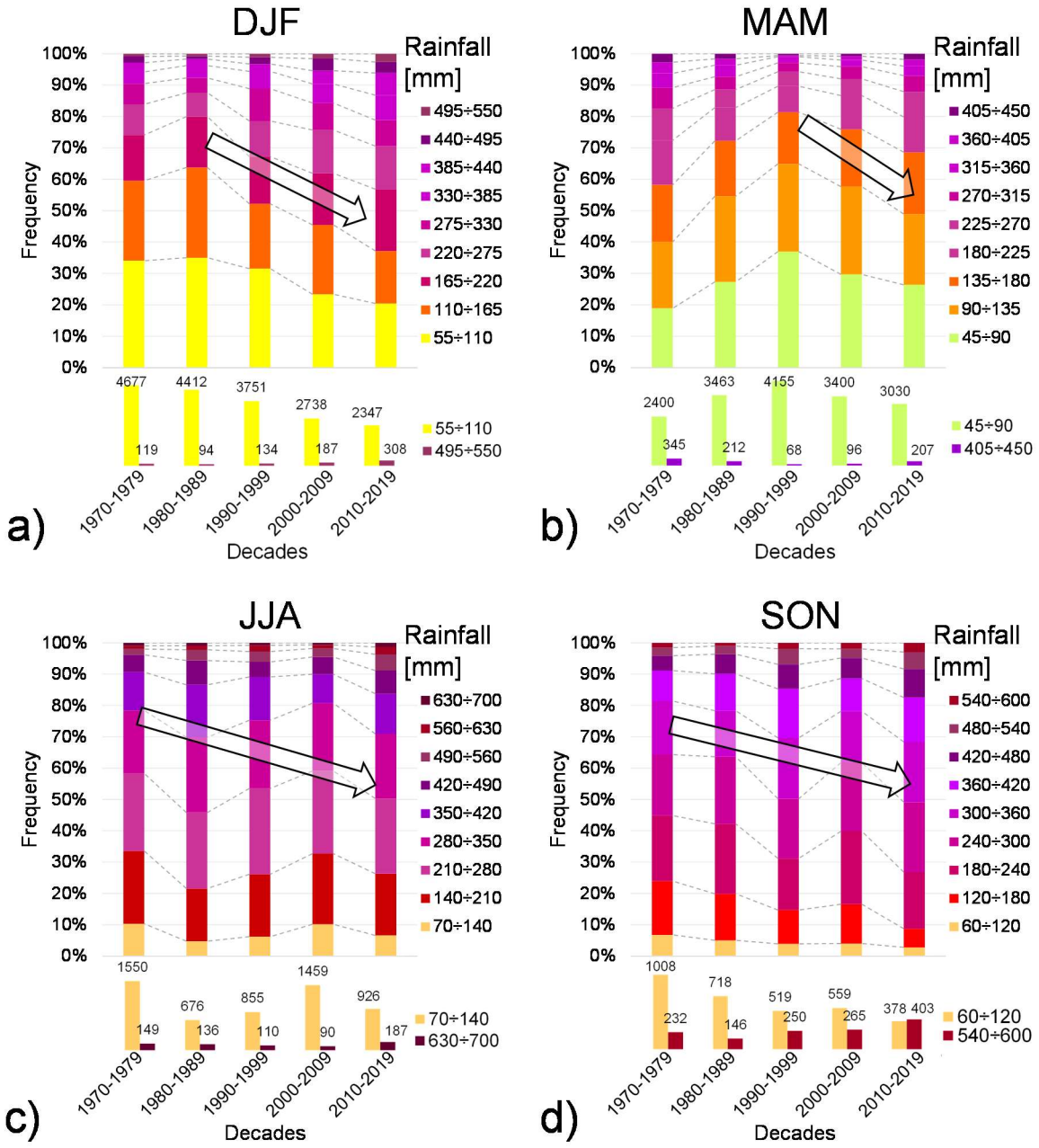

Figure 3~~:~~. Frequency distribution of ~~accumulated~~ rainfall height with an aggregation scale of 90 days ~~considering all altitudes~~ during (a) winter (DJF), (b) spring (MAM), (c) summer (JJA) and (d) autumn (SON). ~~The arrow illustrated~~ Arrows indicate a possible frequency trend~~. For~~ associated with each ~~graph, frequenciessub~~-interval of rainfall. Frequencies of the maximum and minimum rainfall ranges are zoomed in ~~in~~at the bottom of each graph for clarity.

Analogous insights were derived from the RAPS method analysis. For this study, RAPS analysis was carried out for the three altitude ranges, utilizing the 12 meteorological stations in Set C. For stations below 1000 m (Figure 4a) the RAPS values decrease from 1985 to 2008, followed by a sharp increase in the most recent years, indicating that rainfall tended to be higher than the mean value after 2008. A notable exception was observed in 2002, which documented a significant peak (red arrow in Figure 4a), likely corresponding to high rainfall events in May and November (as reported by Bollettino meteorologico e valanghe, Ufficio idrografico di Bolzano; Protezione Civile Provincia Autonoma di Trento). For stations between 1000m and 2000m (Figure 4b), a progressively increasing trend in rainfall is suggested by the downwards parabolic trend of the RAPS. Finally, above 2000m (Figure 4c), the RAPS plot exhibits a V-shape, reaching a minimum in 2007, followed by a sharp increase in the last decade.

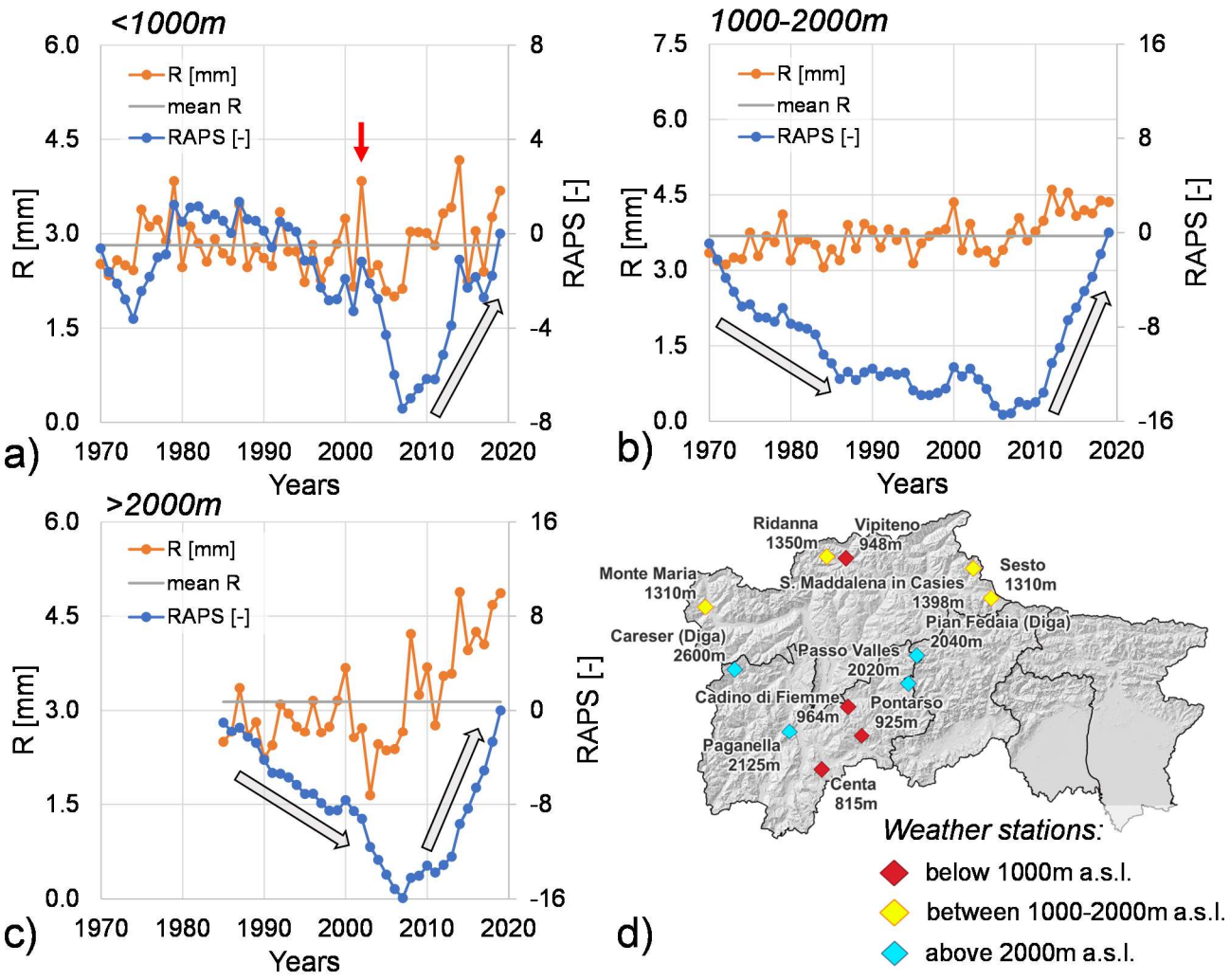

Figure 4. Annual mean rainfall values and Rescaled Adjusted Partial Sums (RAPS): (a) altitudes below 1000m (1970-2019); (b) altitudes between 1000-2000m (1970-2019); and (c) altitudes above 2000m (1985-2019). The red arrow in (a) indicates extraordinary events of 2002. (d) Spatial distribution of the 12 meteorological stations considered (Set C).

4.1.2 Air mean temperature

Air temperature ~~varies~~exhibits variations on yearly, seasonal~~ly~~, monthly, and daily scales, with weather stations recording ~~the~~daily maximum and minimum ~~daily~~ temperatures. The ~~onset~~initiation of ~~a rockfall~~rockfalls can be ~~associated with~~significantly linked to these temperature variations ~~during the~~, both within a single day and ~~over time.~~overextended periods. For ~~the purpose of~~ this analysis, ~~the variation of~~ variations in temperature over ~~time (~~periods longer than one day~~) is~~ are represented by the mean air temperature, while ~~within a day,~~ intra-day variations are captured by the air temperature amplitude ~~is used.~~(section 4.1.4).

Figure 5~~In ,~~ illustrates the frequencies of the 90-day mean temperature ~~at a 90-day aggregation scale are reported for~~ across the four seasons~~,~~ and five decades~~, and all altitudes. A reduction in the frequency associated with~~. A consistent trend of reduced for low temperatures and an ~~increase in the~~increased frequency ~~of~~for high temperatures is observed over the decades. ~~For~~Across all seasons and ~~at all~~ altitudes (~~see~~as detailed in supplementary materials, S1.2), the results indicate a slight warming trend in the study area, with a particularly significant frequency increase observed during the autumn season.

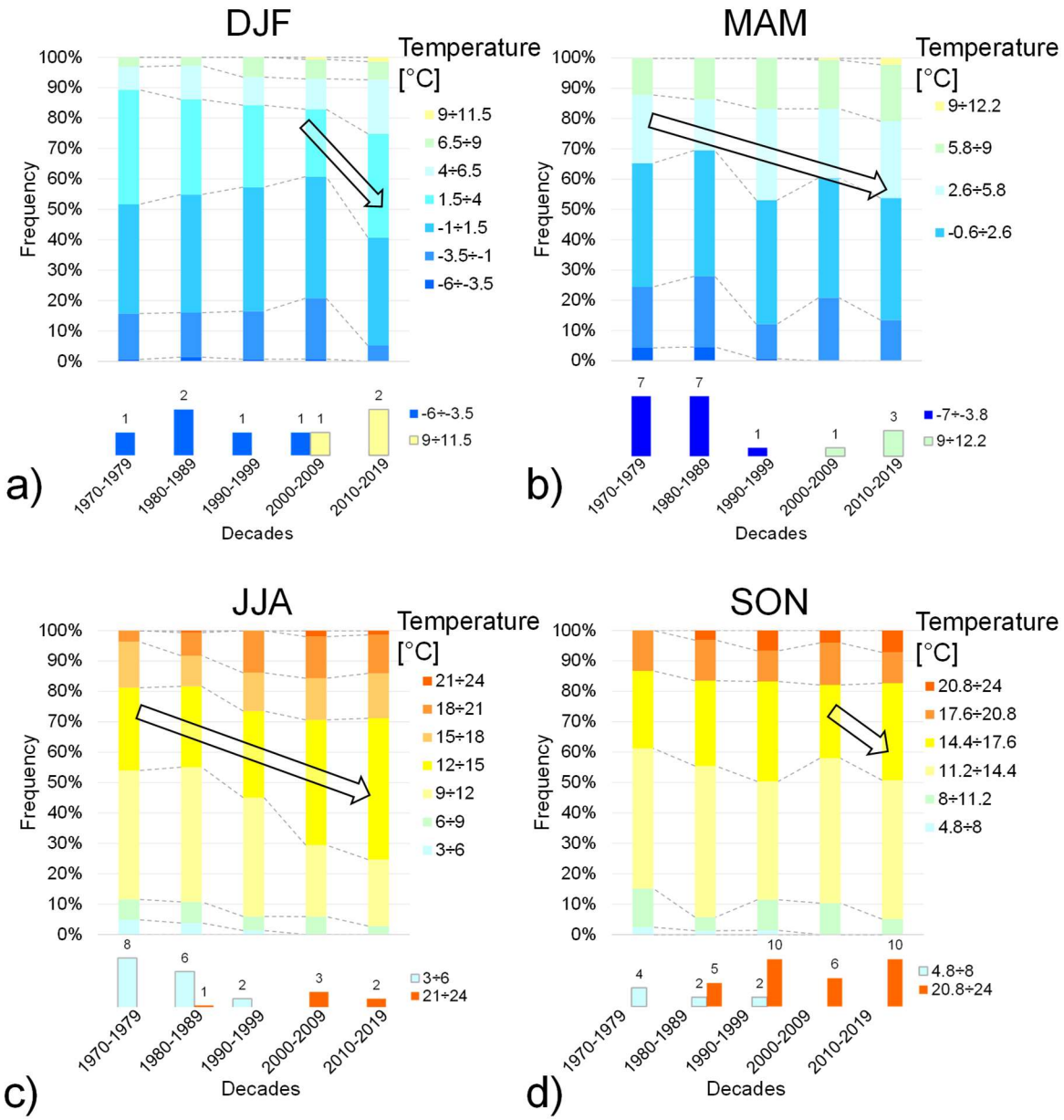

Figure 5~~:~~. Frequency distribution of mean temperature with an aggregation scale of 90 days ~~considering all altitudes during in the following seasons~~during: (a) winter (DJF), (b) spring (MAM), (c) summer (JJA) and (d) autumn (SON). ~~The arrow illustrated~~Arrows indicate a possible frequency trend~~. For~~ associated with each ~~graph, frequencies~~sub-interval of mean temperature. Frequencies of the maximum and minimum temperature ranges are zoomed in ~~in~~at the bottom of each graph.

Based on the methodology by Nigrelli and Chiarle (2023), and using the 12 stations selected for an overlapping period from 1985 to 2019, the annual average warming rates were calculated. For minimum temperature, the rates ranged between 0.23°C and 0.51°C per decade, while for maximum temperature, they ranged between 0.17°C and 0.37°C per decade (Figure 6). The highest warming rates were identified during the spring period above 2000m, with maximum increases of approximately 0.65°C for maximum temperature and 0.62°C per decade for minimum temperature.

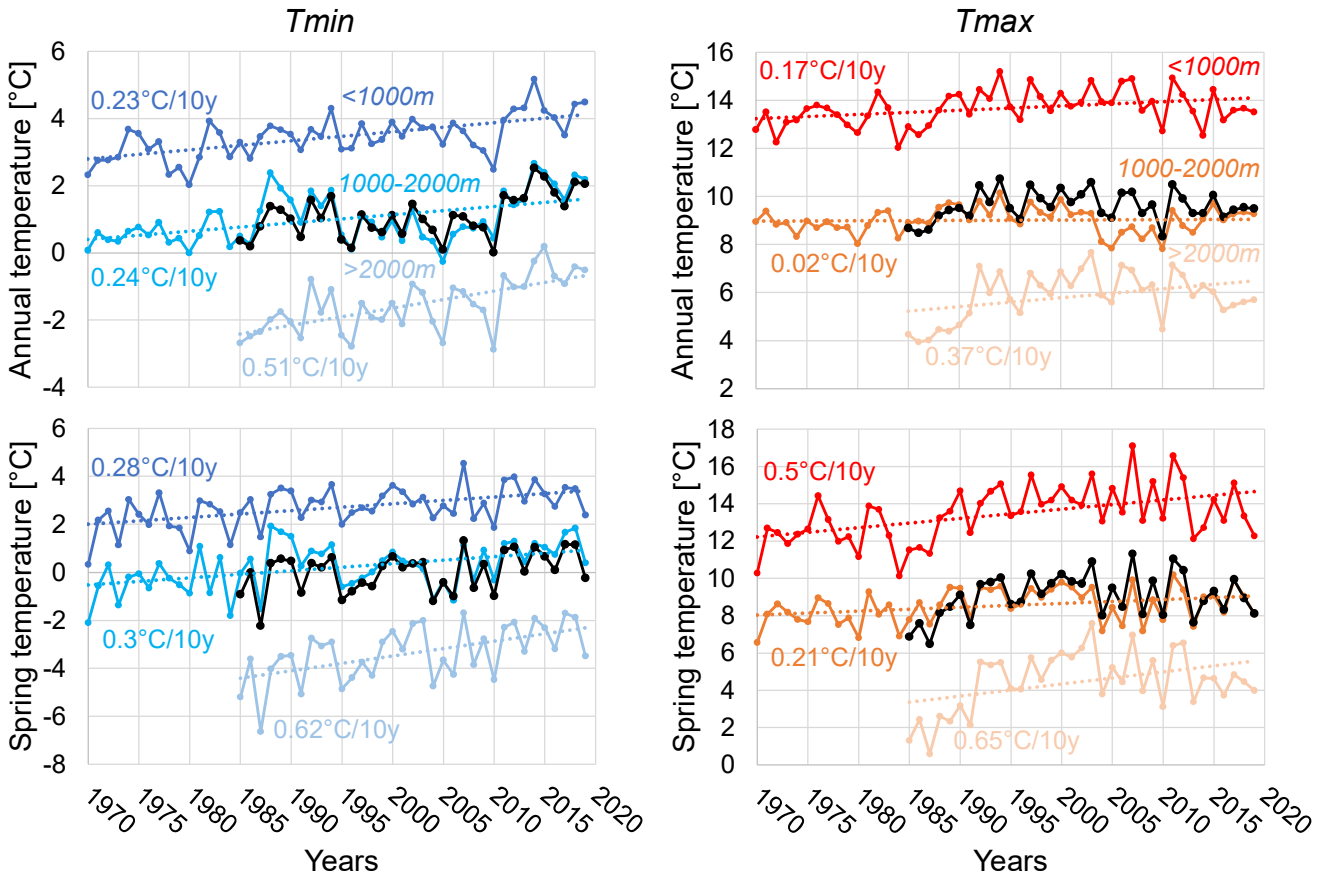

Figure 6. Annual and spring T_{min} and T_{max} trends considering 12 weather stations from 1970 to 2019 for case study. The lack line shows the mean time-series.

To corroborate the conclusion regarding the shifting of winter and spring seasons, an analysis similar to Wang et al (2021) was performed. Considering the 12 weather stations with full time-series (Set C) from 1970 to 2019, an increase in mean temperature of approximately 1.5°C in winter and 3°C in summer was observed (Figure 7a-c). During the spring and autumn seasons, an increase in mean temperature of about 3°C and 2°C, respectively, was noted. Furthermore, this analysis revealed a shift in the onset of spring by 30 days and autumn by 20 days, consequently causing a change in the length of these two seasons (Figure 7b-d), with a more significant change occurring during spring.

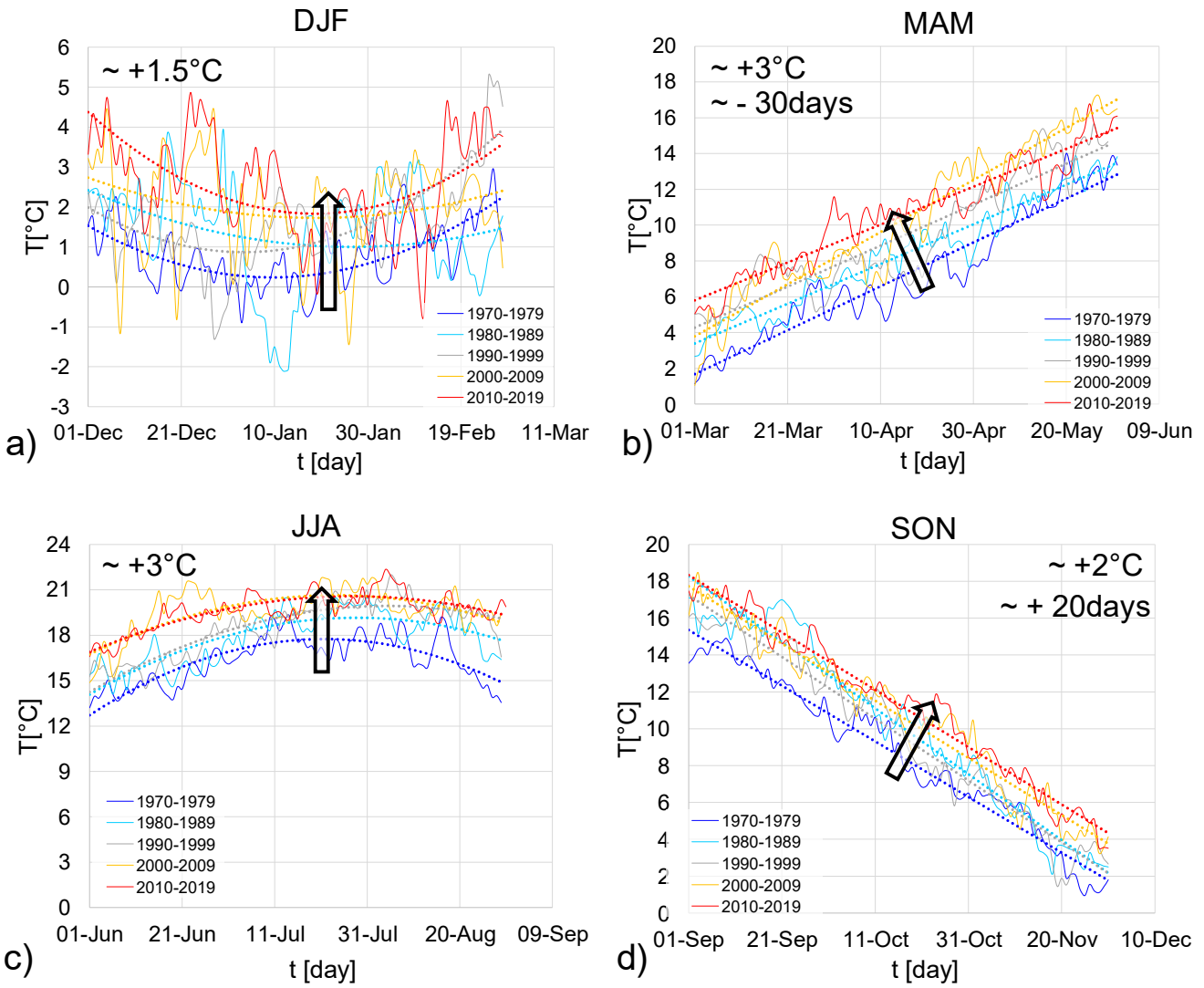

Figure 7~~.~~. Daily time series of air mean temperature over 1970-2019 during: (a) winter (DJF), (b) spring (MAM), (c) summer (JJA) and (d) autumn seasons (SON).

4.1.3 Temperature variation

Air mean temperature variation~~,~~ is defined as the difference between the ~~air~~ mean air temperature on a given day and the corresponding ~~air~~ mean air temperature assessed on a preceding day, as determined by the chosen ~~according to the~~ aggregation scale. Figure 8~~In~~ illustrates the frequencies of temperature variation with an aggregation scale of 6 days for the four seasons ~~are shown~~. No significant changes in temperature variation are evident over the decades ~~are evident, except for some slight,~~ apart from minor fluctuations. ~~Therefore,~~This suggests that temperatures ~~over the years~~ change gradually from one season ~~with the subsequent one keeping the same evolution~~ to the next across the years, maintaining a consistent evolution throughout all decades. This conclusion ~~is consistent~~ holds true when considering other aggregation scales, as shown in the supplementary materials (S1.3). ~~Comparing~~When comparing the highest and lowest values of temperature variation, ΔT, an increase in the ~~range between~~ 8÷10°C range during winter in the last decade was observed (Figure 8a). ~~In~~Conversely, in summer, a reduction of frequencies of ~~extremes~~extreme temperature variation values was ~~observed~~noted (Figure 8c).

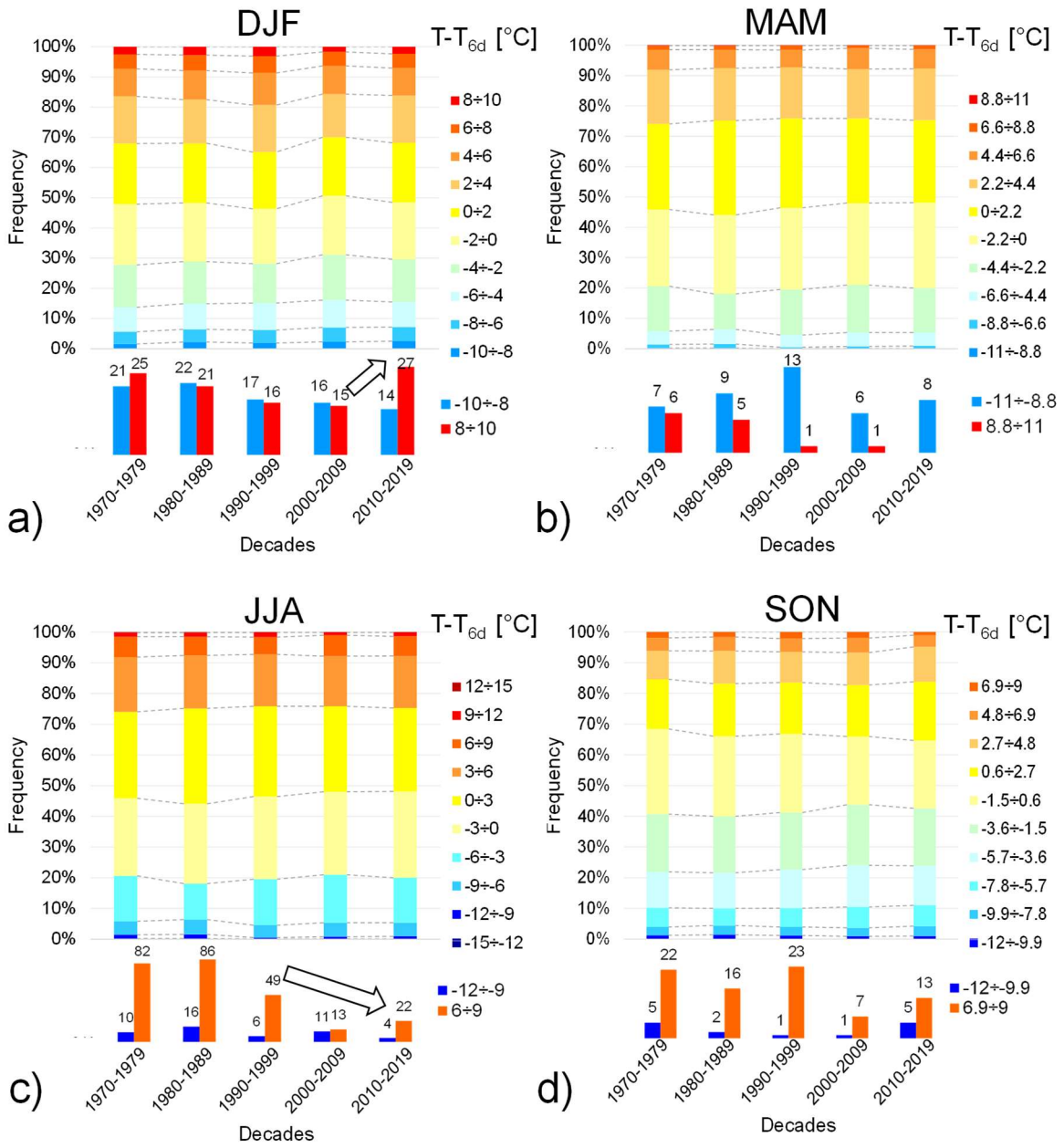

Figure 8~~:~~. Frequency distribution of mean temperature difference with an aggregation scale of 6 days ~~at all elevations during in the following seasons~~during: (a) winter (DJF), (b) spring (MAM), (c) summer (JJA) and (d) autumn (SON). ~~The arrow illustrated~~Arrows indicate a possible frequency trend~~. For~~ associated with each ~~graph, frequencies~~sub-interval of temperature variation. Frequencies of the maximum and minimum temperature-difference ranges are zoomed in at the bottom of each graph.

4.1.4 Temperature amplitude

The results concerning temperature amplitude frequencies, considering different decades and seasons, are shown in Figure 9. In all seasons, except winter, an increase in the frequencies of maximum temperature amplitude and a reduction in frequencies of the lowest range ~~frequencies~~ were observed. This indicates that on many days, there ~~can be~~is a significant difference between ~~the~~ minimum and maximum temperatures, averaging 11°C. Conversely, during the winter season, the opposite trend was ~~observed~~noted: low temperature amplitude ranges increased, while high ones decreased over the last decade. This suggests that ~~there is not much~~the difference between minimum and maximum temperatures tends to be less pronounced in winter.

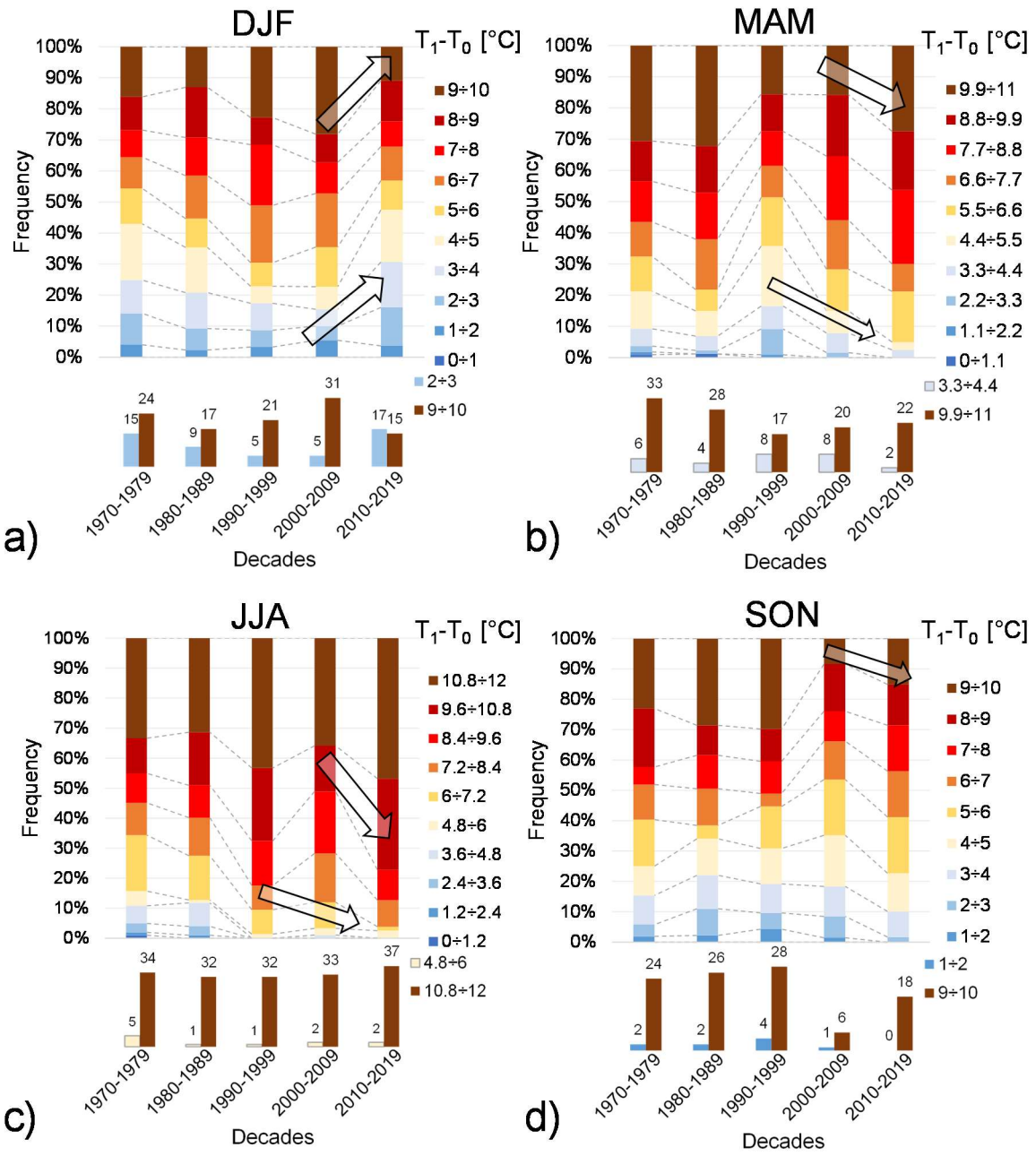

Figure 9~~:~~. Frequency distribution of daily air temperature amplitude with an aggregation scale of 90 days, and at all elevations, during ~~in the following seasons~~: (a) winter (DJF), (b) spring (MAM), (c) summer (JJA) and (d) autumn (SON). ~~The arrow illustrated~~Arrows indicate a possible frequency trend~~. For each graph, frequencies of~~ associated with each sub-interval of temperature amplitude. Frequencies of the maximum and minimum temperature amplitude ranges are zoomed in at the bottom of each graph.

4.1.5. Freeze-Thaw cycle

As the frequen~~cies~~y of high temperatures ~~increase,~~increases, so does the number of days with maximum and/or minimum daily temperatures above zero ~~also rises~~. This shift alters the persistence of icing in the area, consequently affecting the onset and frequency of ~~the~~ freeze/thaw cycles, and ~~increasing~~ leading to an increase in the number of ice-free days ~~with no ice~~. Specifically, freeze/thaw cycles accelerate ~~the~~ rock mass degradation ~~processes~~ by reducing cohesion at the ice-rock interface. To ~~study~~investigate these effects, the persistence of bo~~the~~ icing and freeze/thaw cycles ~~were analysed, with~~was analyzed. The results for freeze/thaw cycles ~~shown in ,~~ considering different elevations at a 7-day aggregation scale are presented in Figure 10~~.~~. For each elevation, two key months were ~~considered~~selected, as ~~these are~~ representing periods when freeze/thaw cycles ~~either stop~~typically cease or ~~begin~~commence.

TheOverall, the results indicate that, ina general, decrease in the persistence and frequency of freeze-thaw cycles have decreased over the years. This means, signifying a reduction in the number of consecutive days with freeze/thaw experiencing these cycles has reduced. Analysing. When analyzing different altitude ranges,: for elevations below 2000m2000 m (Figure 10a, b, c and d), this reduction in persistence is observed in March/April and October. Due to warming, high frequencies with low persistence are observed in March/April during the last decade, as freeze/thaw cycle days are notno longer consecutive. Similarly, in October at low altitudes (Figure 10b), freeze/thaw cycles occur less frequently and tend to disappear. At medium altitudes between 1000m1000 m and 2000m2000 m (Figure 10c and d), an increase in frequencies with one-day persistence is recorded, indicating. This indicates that freeze/thaw cycles are becoming more discontinuous, often separated by days withwhere the minimum temperature remains above zero. Above 2000m2000 m (Figure 10e and f), a significant decrease in cycle frequency is observed in June and September. In September, many frequencies of consecutive days of freeze/thaw cyclesdays with low persistence (e.g., 2 days) are noted. In contrast, during past decades, freeze/thaw cycles at these altitudes were less frequent but more continuous. These variations acrossobserved at different elevations are duecan be attributed to the linear decrease in temperature with increasing altitude, which. This delays the end of the summer months and advancesbrings forward the end of the winter months at higher elevations. Similar patterns can be observed at other aggregation scales, as shown in the supplementary materials (S1.5).

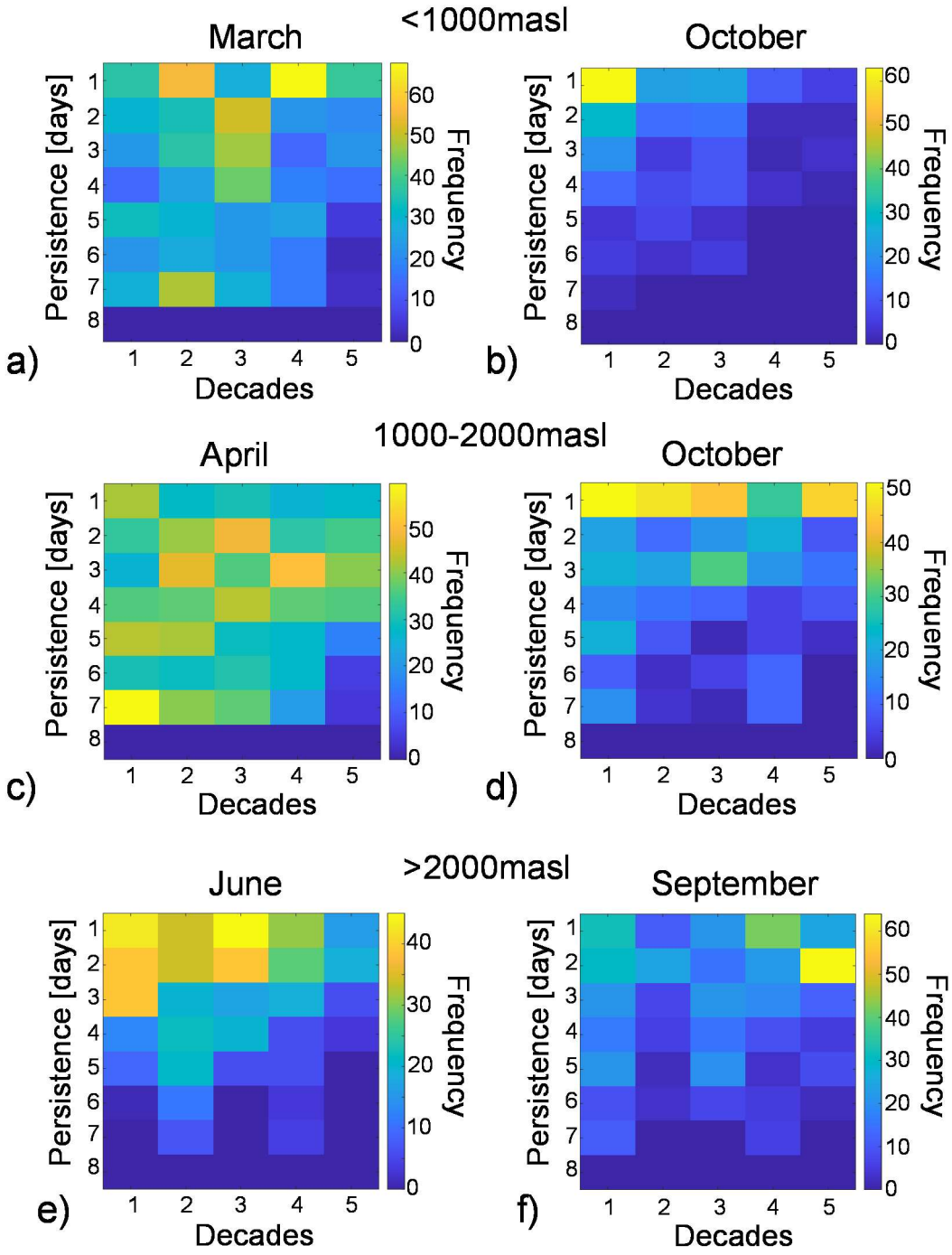

Figure 10~~:~~. Heatmaps of freeze-thaw cycle frequency during thawing and freezing period: (a-b) below ~~1000m asl~~1000 m a.s.l, (c-d) between ~~1000m-2000m asl~~1000 m-2000 m a.s.l and (e-f) above ~~2000m asl~~2000 m a.s.l.

4.1.6 Icing

Figure 11 ~~shows~~ illustrates the persistence and frequency of icing for the spring and autumn seasons at elevations above ~~2000m~~2000 m, using a 7-day aggregation scale. Lower elevations ~~a~~were not considered, as no relevant icing phenomena ~~a~~were present at these altitudes during the studied decades. The results indicate ~~that in April and November, there is only~~ a reduced frequency of 7-day persistence~~.~~ in both April and November. In April and October, there is an increase in 1-day persistence, while ~~in May,~~ a reduction in persistence is noted in May. Consequently, ~~the variation in frequencies implies that~~while the total number of icing ~~days~~ changes only slightly, ~~but they are~~their occurrence is increasingly interspersed with ~~days without~~ ice-free days. This phenomenon is primarily ~~due to~~driven by an increase in maximum daily temperatures, which ~~causes~~leads to a transition from pervasive icing to more frequent freeze/thaw cycles. To further verify this transition, Figure 12 plots the persistence of freeze/thaw cycles for the same months and aggregation scale. A global increase in the frequency and persistence

of freeze/thaw cycles is observed, indicating that some days that would traditionally experience icing ~~days~~ are ~~converted into~~now undergoing freeze/thaw cycles ~~days~~.

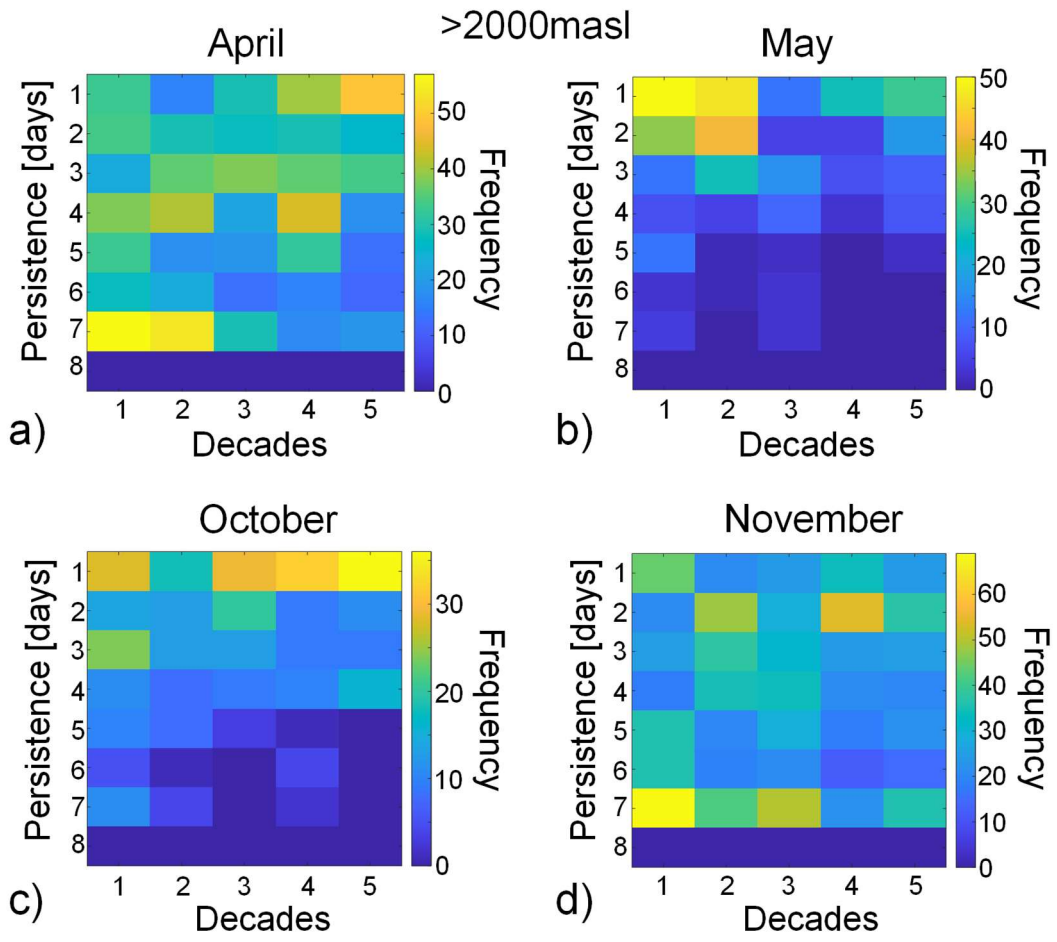

Figure 11~~:~~. Heatmaps of icing frequency above ~~2000m asl~~2000 m a.s.l: during (a-b) spring season and (c-d) autumn season.

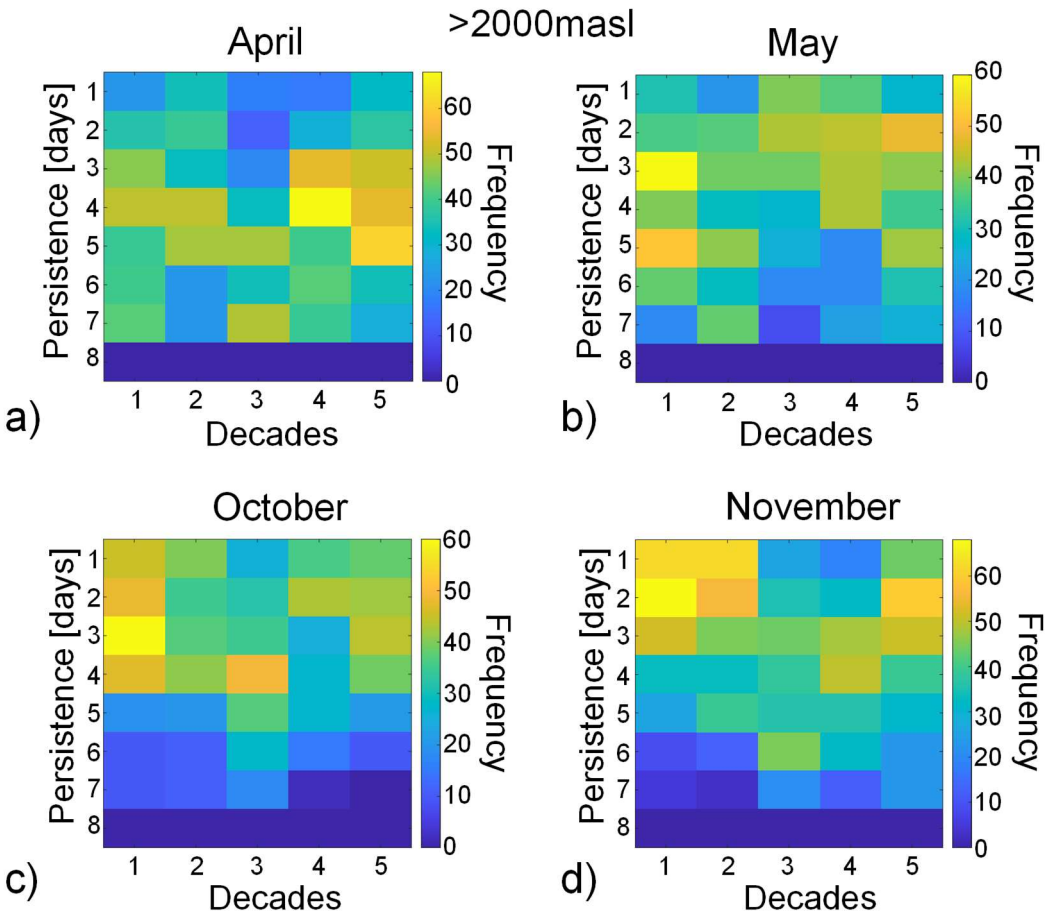

Figure 12~~:~~. Heatmaps of freeze-thaw cycle frequency above ~~2000m~~2000 m a.s.l. during (a-b) spring season and (c-d) autumn season.

Considering the same weather stations used for the calculation of the temperature trends and employing the approach outlined by Nigrelli and Chiarle (2023), the analysis reveals a decrease of approximately 7.3 freeze-thaw days and about 2.2 icing days per decade (Figure 13a). From the seasonal analysis, while the overall trend is generally decreasing, above 2000 m, freeze-thaw (FT) cycles show an increase at a rate of 3.3 days/10 years in winter and 2.7 days/10 years in spring (Figure 13b-c). Furthermore, in winter above 2000 m, a loss of 2.1 ice days per decade is calculated (Figure 13e).

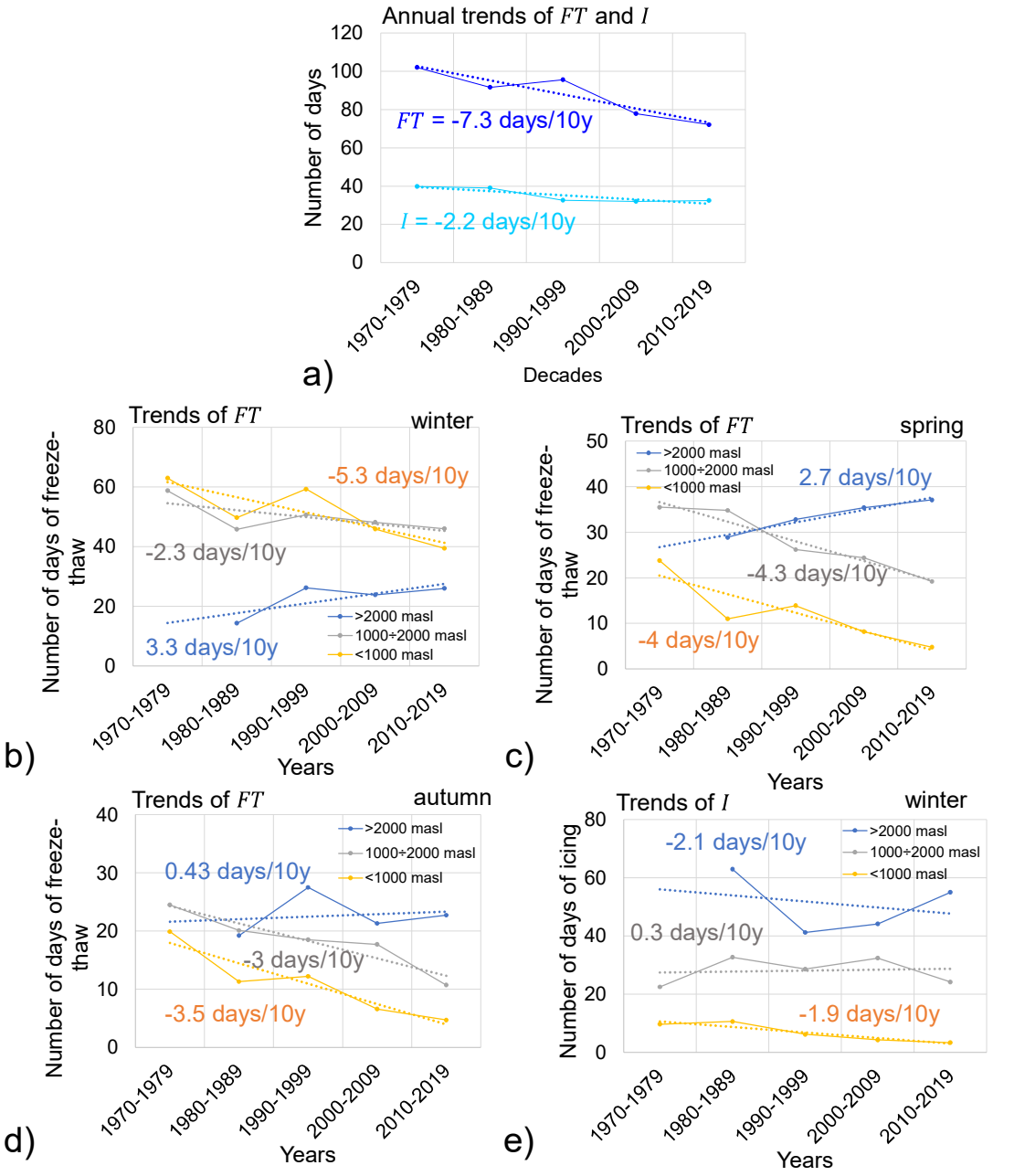

Figure 13. Annual and seasonal freeze-thaw (FT) and icing (I) trends relative to altitudes for this case study during 1970 to 2019. (a) considering 12 weather stations; (b) FT trends during winter season; (c) FT trends during spring season; (d) FT trends during autumn season; (e) I trends during winter season.

4.2 Rockfall events distribution

From ~~the~~an initial dataset of 5480 rockfalls that occurred between 1970 and 2019, ~~2971 rockfalls~~ 2971events were extracted for detailed analysis. Recent rockfalls occurred from 2020 until 2025 were added to them in Figure 14~~analysis. .~~ The results obtained ~~by~~through the proposed approach are discussed below.

Figure 14~~In a~~, displays the number of recorded rockfall events ~~is shown~~ alongside the number of active weather stations. ~~The~~While the graph suggests an apparent increase in rockfall frequency over the past two decades~~. However, as highlighted by~~, it is important to acknowledge that this increase could be partly attributed to improvements in the accuracy, completeness, and documentation of recording method of rockfall events at all elevations in recent years (Huggel et al., ~~(~~2012~~),;~~ Sass and Oberlechner ~~(~~, 2012~~),;~~ Rupp and Damm ~~(~~, 2020~~) and;~~ Bajni et al. ~~(~~., 2021~~), this increase could be attributed to improvements in the accuracy, completeness and the level of documentation at all elevations and for all rockfall events in recent years.~~).

Figure 14b shows the monthly frequency of rockfalls, revealing three main peaks: in November, during the February-March-April period, and in August. The altitudinal distribution of rockfalls events (Figure 14c) referred to the number of events

recorded in that decade, shows a ~~concentration below 1500m each year.~~frequency a reduction of the frequency with increasing the altitude (apart the altitude between 500 m and 1000 m). For elevations above ~~1500m~~1000 m, an increase in relative frequency (since in every decade the number of events changes) is observed ~~over~~across the decades. However, in recent decades, a relative frequency decrease is noted below ~~1000m, while a relative increase is observed above 1500m. Regarding~~ 1000 m.

To study the variation of the aspect of ~~the~~ rockfall source during the different decades, the rockfall dataset was split up in two sub-datasets: one grouping the events from 1970 to 1999 (group A) and the second one collecting the events from 2000 to 2025 (group B). This subdivision was carried out in this way and not for decades because the number of rockfall events in the first two decades was too small. In this way they were aggregate to obtain a significant statistical number of events for the two groups. The obtained results are reported in the Figure 14~~(d), 70% of events below 1000m occur on broadly south-facing slopes. In contrast, 50% of rockfalls above 2000 meters occur on north-northwest facing slopes, and 35% of events between 1000~~ d where the percentage of rockfall event for different aspect classes (8 sectors) are reported for different elevation and for two groups. The percentage changes for the different elevation and for the two considered groups. For elevation below 1000 m, the predominant percentage is SE in the first group while in the second one is the W. For altitude between 1000 m and 2000 ~~meters occur on south-southeast facing slopes. Above 2000m, this~~ m, in the first group the S and E orientations are more frequent in the group A while in the group B the difference between the aspect classes reduces and S and SE remains still the more important.

Finally, for altitude greater than 2000 m, for group A the predominant component is W while for the group B the W component reduces significantly, the S, SW and SE reduces slightly while the N component has significant increment. This pattern ~~can~~, especially on north-facing cliffs, could be attributed to permafrost thawing, which predominantly ~~affects higher~~ is present at elevations ~~on north-facing cliffs~~higher than 2500 m (Noetzli et al 2003, Noetzli and Gruber 2009).

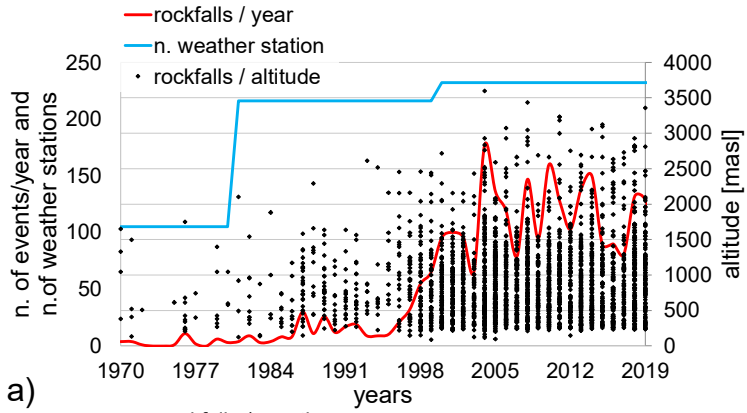
rockfalls / year
n. weather station
rockfalls / altitude
n. of events/year and n.of weather stations
altitude [masl]
years
a)

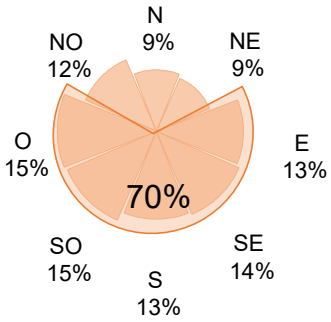
N 9%
NE 9%
E 13%
SE 14%
S 13%
SO 15%
O 15%
NO 12%
70%

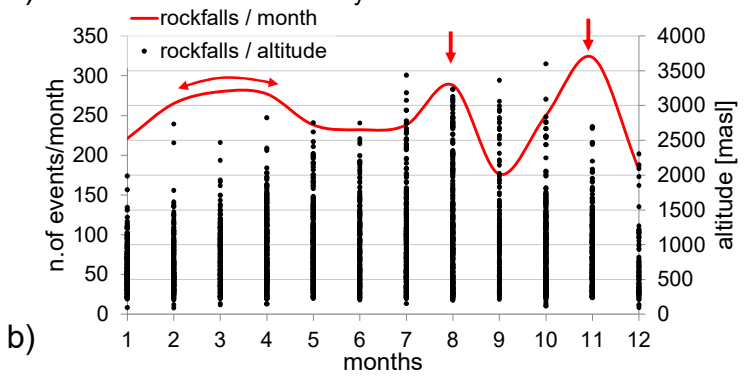
rockfalls / month
rockfalls / altitude
n.of events/month
altitude [masl]
months
b)

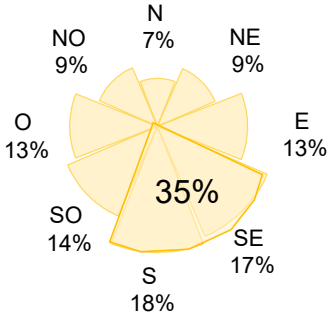
N 7%
NE 9%
E 13%
SE 17%
S 18%
SO 14%
O 13%
NO 9%
35%

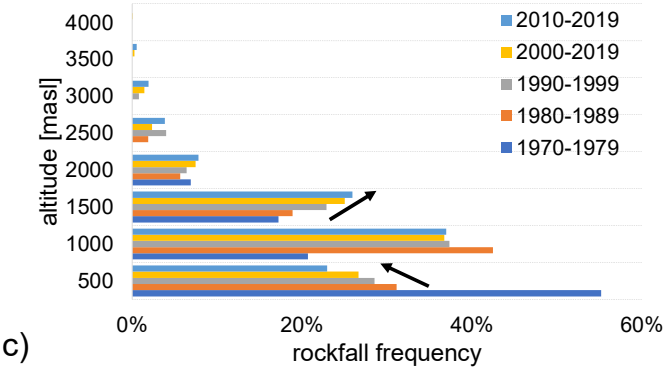
2010-2019
2000-2019
1990-1999
1980-1989
1970-1979
altitude [masl]
rockfall frequency
c)

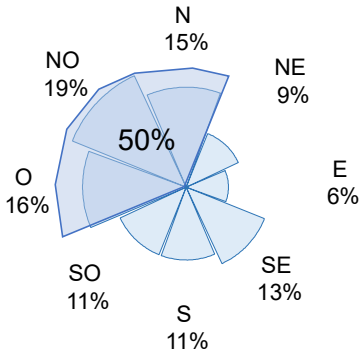
N 15%
NE 9%
E 6%
SE 13%
S 11%
SO 11%
O 16%
NO 19%
50%
d)

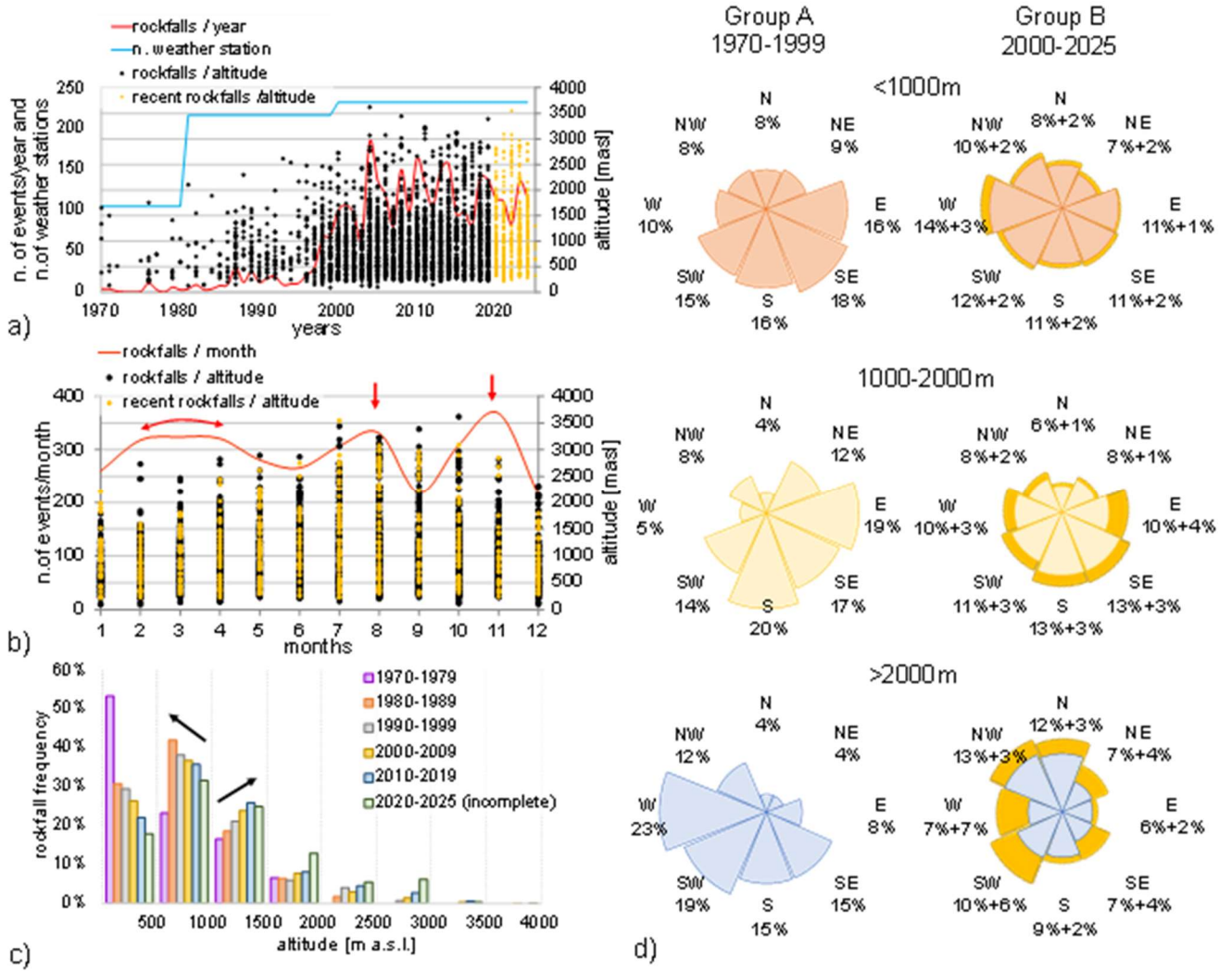

Figure 14~~:~~. Analysis of ~~2971~~ rockfall events from 1970 to 20~~19~~25: (a) ~~distribution of~~ annual frequency of rockfalls ~~regarding~~(red line), distribution of rockfall events relative to altitude~~, the red line is the number of rockfalls/year~~ (black and ~~blue line the~~yellow dots), number of active weather stations~~;~~ (blue line); (b) monthly frequency of rockfall events ~~regarding to altitude~~ relative for all years~~, the~~ (red line ~~is the number of rockfalls/month;~~), altitude distribution for all years for the different months (yellow and black dots); (c) rockfall event~~s~~ distribution in terms of altitude and decades; (d) ~~frequency of rockfall~~ comparison rockfalls frequencies occurrence in terms of aspect classes ~~and~~ for different altitudes (0-1000 m, 1000-2000 m and greater than 2000 m) between 1970-1999 (left side) and 2000-2025 (right side). Rockfalls frequencies from 2020 to 2025 are represented in the yellow areas.

4.3. Rockfalls and climate variables

The ~~aim of this~~ sub-section aims to assess the ~~correlation~~specific relationship between rockfall events and ~~weather~~various meteorological variables. ~~Since~~Given that weather variables ~~vary over time and space~~exhibit spatio-temporal variability, the analysis ~~was~~is presented in terms of elevation range, season, and aggregation scale. The same climate variables and their defined ranges, as used in the climate analysis, were considered, using the same ranges. For ~~simplicity~~sake of brevity, only the ~~more important~~most significant results ~~were illustrated~~ are shown here~~, while~~. Comprehensive tables containing all the analysed conditional ~~probability analysed~~probabilities are ~~shown~~provided in the supplementary materials (S2).

4.3.1 Rainfall

Figure 15 ~~shows~~ presents the conditional probabilities of ~~cumulative~~ rockfall events under the condition that rainfall is within a given range. Specifically, Figure 15~~obtained from weather stations below 1000masl~~ a illustrates these probabilities for the autumn season at elevations below 1000 m a.s.l. with $S_a = 90\ days$, while Figure 15~~a and~~ b shows the probabilities for autumn season at elevations between 1000-~~2000masl~~2000 m a.s.l. with $S_a = 30\ days$.

In ~~these two~~both cases, an increment ~~of~~in conditional probability is observed for the ~~values with~~ highest ~~intensity~~values of total rainfall~~, are shown~~ in the last decade~~; with~~, reaching 12.4% below ~~1000m~~1000 m and 22.2% between 1000-~~2000m of probability. Observing results with~~ 2000 m. When considering other aggregation scales and altitudes~~,~~ (detailed in supplementary materials S2.1), the highest probabilities associated with rainfall ~~are present again~~continue to occur during autumn season, specifically with ~~an~~a 7-days aggregation scale ~~of 7 days~~ below ~~2000m~~2000 m and ~~with~~a daily aggregation scale below ~~1000m. Therefore, for high rainfall values in the autumn season there could be a~~1000 m. These findings suggest a potential correlation between rockfall events and high ~~intensity~~total rainfall values during the autumn season. Furthermore, it is not~~abled~~ that in ~~the past~~earlier periods, rockfalls ~~had~~showed a higher probability of occurrence with ~~a~~ daily and weekly aggregation scales, whereas in the last decade ~~the~~, probabilities are higher with ~~a~~ monthly and quarterly aggregation scales.

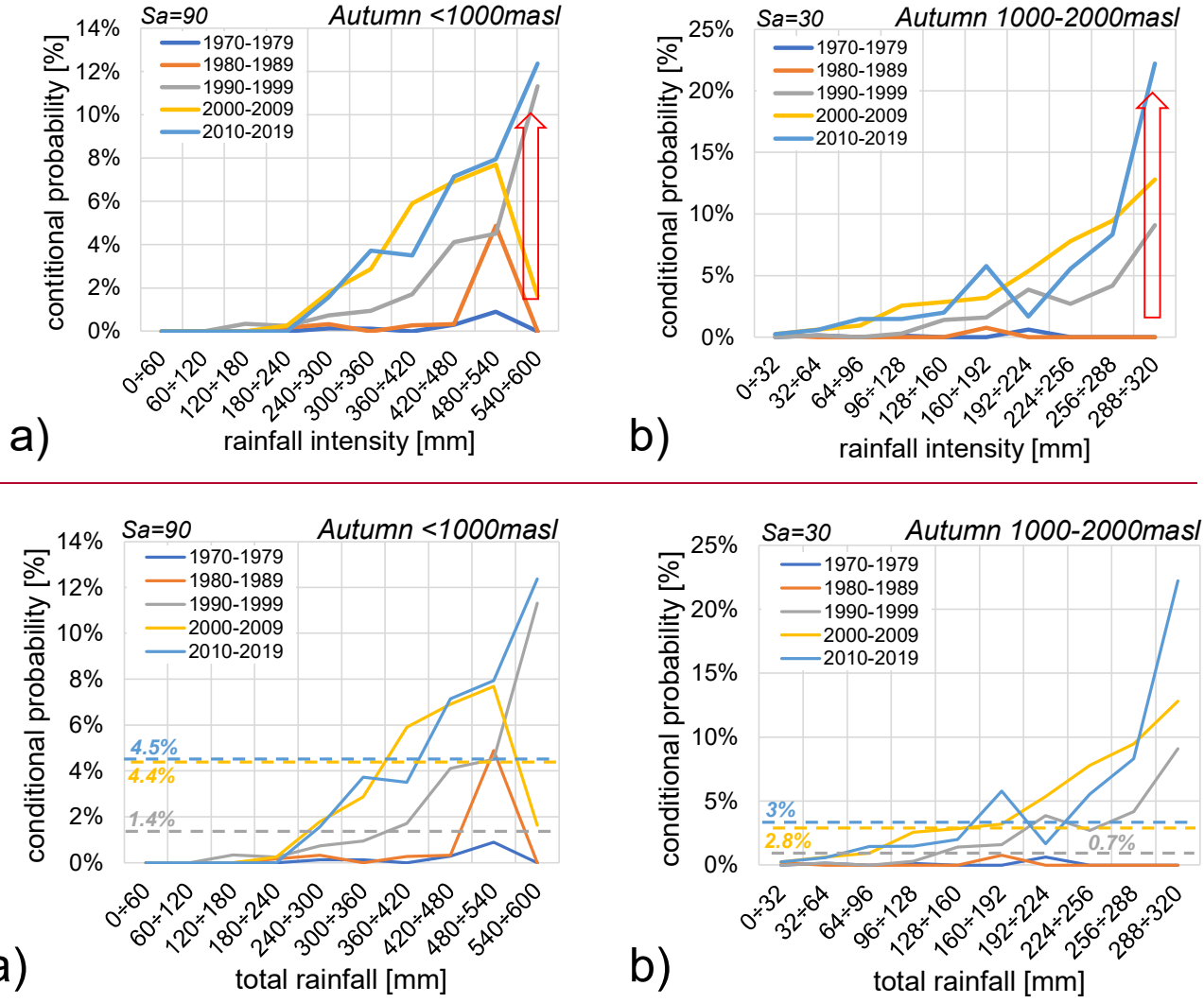

Figure 15~~: (a).~~ Conditional probabilities of rockfalls trigger~~s~~ed by rainfall~~s~~ from 1970 to 2019 during autumn season~~.~~: (a) below ~~1000m~~1000 m a.s.l. considering an aggregation scale S_a = 90~~.~~ *days*; (b) between 1000-~~2000m considering~~ 2000 m a.s.l. with an aggregation scale S_a = 30~~.~~ *days*. Rockfall probabilities are represented by the coloured dotted lines according to the decade as shown in the legend.

4.3.2 Mean air temperature

Figure 16a shows a conditional probability of 12.7% ~~of~~for rockfall events triggered by mean weekly air temperatures at elevations between 1000-~~2000m for~~ 2000 m a.s.l. during the summer season. Figure 16b illustrates a probability of 2.2% ~~of~~for rockfall ~~event~~events triggered by monthly temperature at elevations above ~~2000m~~2000 m a.s.l. during the autumn season. ~~Analysing~~ A comprehensive analysis of all the results in the supplementary materials (S2.2), rockfall probability increased during decades particularly in the last two decades with higher probabilities in winter and spring below 1000m, in summer

between 1000m and 2000m and in autumn above 2000m. These results imply a possible correlation between rockfall events and increasing temperatures in accordance to climate analysis.

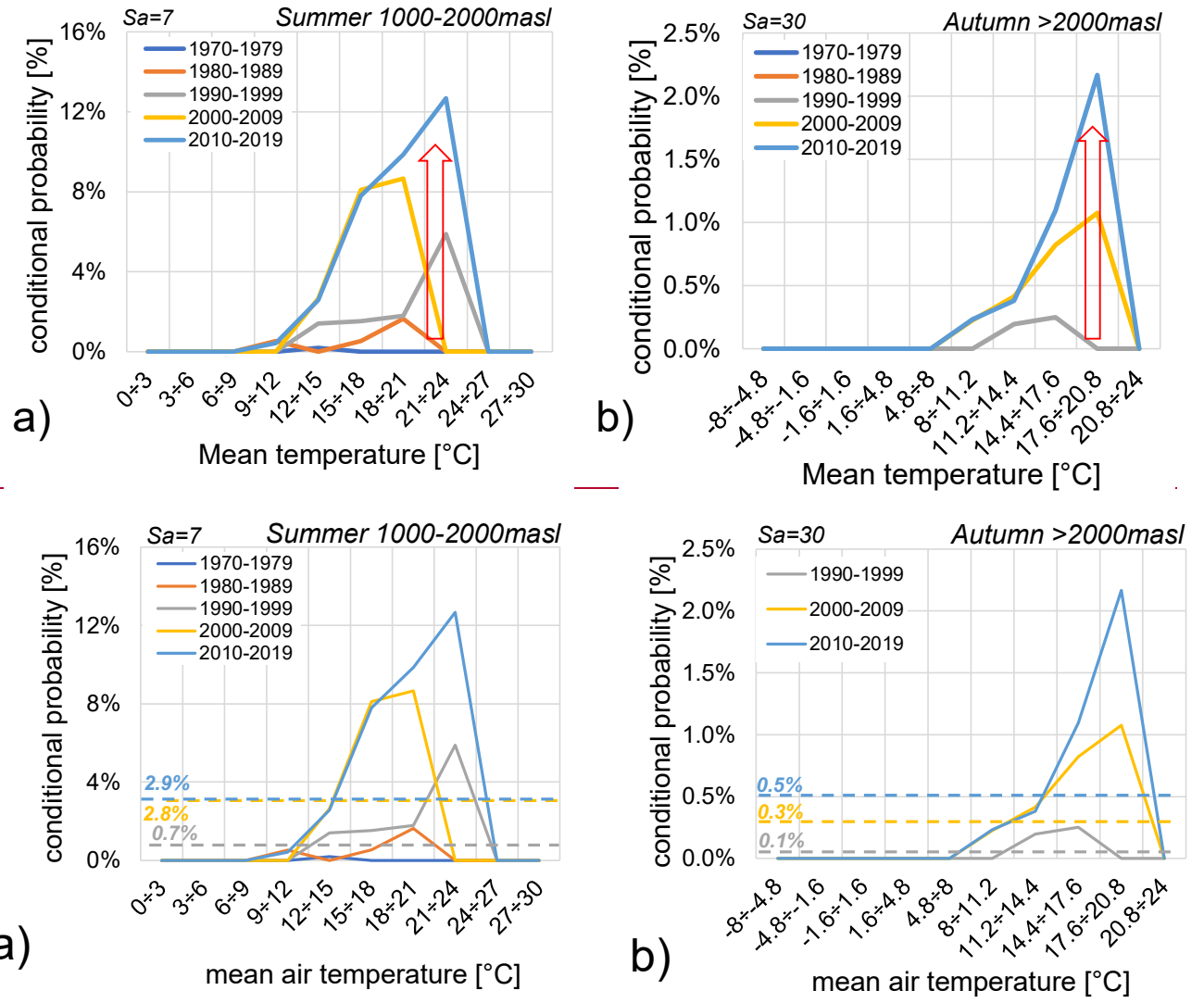

Figure 16~~: (a).~~ Conditional probabilities of rockfalls trigger~~sed~~ by mean temperature values from 1970 to 2019~~: (a)~~ during summer season between 1000-~~2000m considering~~2000 m a.s.l. with an aggregation scale $S_a = 7\ days$. (b) ~~Conditional probabilities of rockfall from 1970 to 2019~~ during autumn season above ~~2000m.~~ 2000 m a.s.l. with an aggregation scale $S_a = 30\ days$. Rockfall probabilities are represented by the coloured dotted lines according to the decade as shown in the legend.

4.3.3 Temperature amplitude

In Figure 17 the conditional probabilities of rockfall events conditioned by monthly air temperature amplitude ($Tmax - Tmin$) are presented. Specifically, Figure 17a shows these probabilities during ~~(a)~~the spring season below ~~1000masl~~1000 m a.s.l.~~,~~ and ~~(b)~~Figure 17b shows them during the winter season between ~~1000masl and 2000masl are presented.~~ 1000-2000 m a.s.l.. Observing Figure 17a, ~~28.6% of~~a probability ~~correspond~~of 28.6% corresponds to ~~range of~~a temperature amplitude range of 8.8°C to 9.9°C. Figure 17b ~~shows~~indicates a 5.8% ~~of~~ probability that rockfall are conditioned by temperature amplitude ~~with a~~ range of 9°C to 10°C. All results ~~present~~consistently show higher ~~values of~~ probability values in the last two decades ~~with,~~ especially for temperature amplitude ranges greater than 6.6°C during spring and ranges from 9°C to 10°C in winter, ~~except~~ with the exception of cases where $Sa = 0$. ~~So~~This suggests that higher probabilities of rockfall events are ~~found~~generally associated with ~~hi~~larg~~h~~est ranges of temperature amplitude.

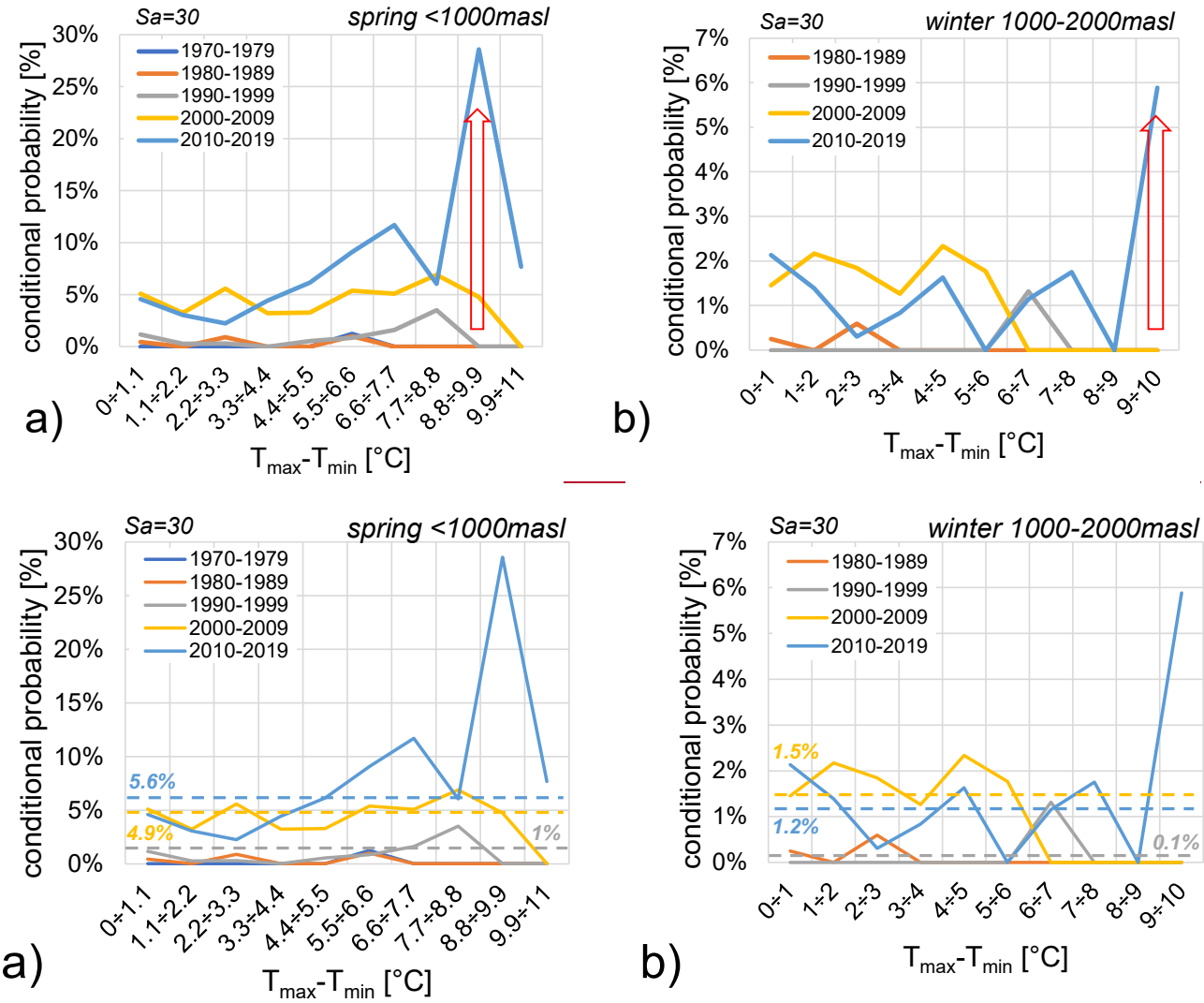

Figure 17~~:~~. Conditional probabilities of rockfalls conditioned by ranges of temperature amplitude from 1970 to 2019~~:~~ (a) during spring season below ~~1000m and~~1000 m a.s.l.; (b) during winter season between ~~1000m-2000m.~~ 1000 m-2000 m a.s.l.. Rockfall probabilities are represented by the coloured dotted lines according to the decade as shown in the legend.

4.3.4 Air mean Temperature variation

Figure 18~~In~~ illustrates the conditional probabilities of rockfalls caused by temperature variation. Figure 18 ~~(1)~~a shows results with a 1-day aggregation scale during summer between 1000-2000 m a.s.l., while Figure 18~~2000masl and (2)~~b shows results with ~~an~~a 6-day aggregation scale ~~of 6 days~~ during spring season below ~~1000masl are shown. Altitudes~~1000 m a.s.l.. At altitudes between ~~1000m~~1000 m to ~~2000m show~~2000 m, a probability of 14.3% for rockfalls is observed with temperature ~~variation of~~variations ranging from -9°C to -6°C. Below ~~1000m~~1000 m, rockfalls are more probable (20%) for temperature ~~range~~variations ranging between 8.8°C to 11°C. ~~Temperature~~Notably, temperature variation frequencies do not change significantly over the decades, implying that temperature variation can be considered stable from a climate perspective.

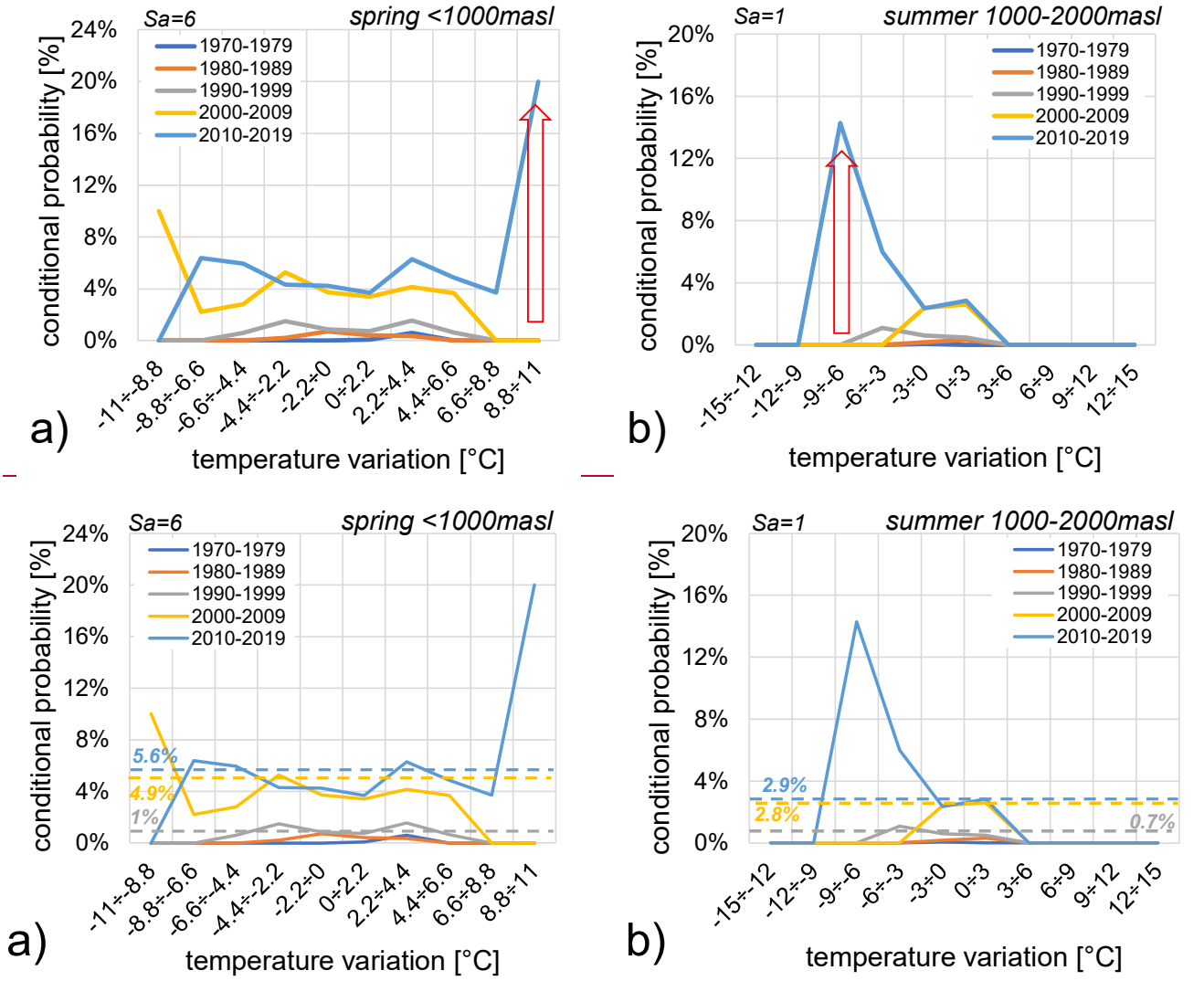

Figure 18~~:~~. Conditional probabilities of rockfalls from 1970 to 2019 during: (a) summer season between 1000-~~2000masl~~2000 m a.s.l. and (b) during spring season below ~~1000m of altitude~~1000 m a.s.l.. Rockfall probabilities are represented by the coloured dotted lines according to the decade as shown in the legend.

4.3.5 Freeze-Thaw cycle and icing

~~As the~~The Bayesian analysis for ~~this weather variable~~freeze-thaw cycles and icing relies on three temperature time-series ~~of~~ (maximum, mean, and minimum ~~temperatures)~~ obtained through regionalization, ~~the results are~~thus significantly ~~influenced by this process.~~influencing the results. To ~~illustrate~~demonstrate this, we compare the results for minimum and mean temperature time-series with a 7-day aggregation scale, focusing on two specific cases: (i) winter at altitudes below 1000 m ~~.~~a.s.l. (Figure 19) and (ii) spring between 1000 m ~~.~~a.s.l. and 2000 m ~~.~~a.s.l. (Figure 20).

Equation (10) ~~shows~~indicates that the conditional probability of a rockfall event ~~(P(M|R)) depends~~$(P(Rf|M))$ is dependent on the frequency of freeze-thaw cycles (~~F/T~~FT) and icing events. As the conditional probability ranges from 0 to 1, variations in the numerator (i.e., the frequency of ~~F/T~~FT and icing events) have a more significant impact on the overall trend of ~~P(M|R)~~$P(M|Rf)$ than variations in the denominator~~. This is particularly evident~~, especially when ~~F/T~~FT and icing events exhibit similar trends over consecutive days.

In Figure 19(a-b), where icing events are more prevalent than ~~F/T~~FT cycles, ~~P(M|R)~~$P(Rf|M)$ increases with increasing icing events and decreases with increasing ~~F/T~~FT cycles. Conversely, in Figure 19(c-d) where ~~F/T~~FT cycles are more frequent, the opposite trend is observed.

Similar trends are ~~observed~~noted in Figure 20, with the specific behaviour depending on the relative frequency of ~~F/T~~FT and icing events. For instance, in Fig. ~~1~~620(a-b), ~~P(M|R)~~$P(Rf|M)$ increases with increasing ~~F/T~~FT events and decreases with increasing icing events.

The contrasting trends observed in the two examples can be attributed to the varying influence of overall rockfall probability. Below 1000 m ~~.~~a.s.l., the rockfall probability ~~is~~remains relatively stable, ~~while~~whereas between 1000 m ~~.~~a.s.l. and 2000 m ~~.~~a.s.l., it tends to increase over time.

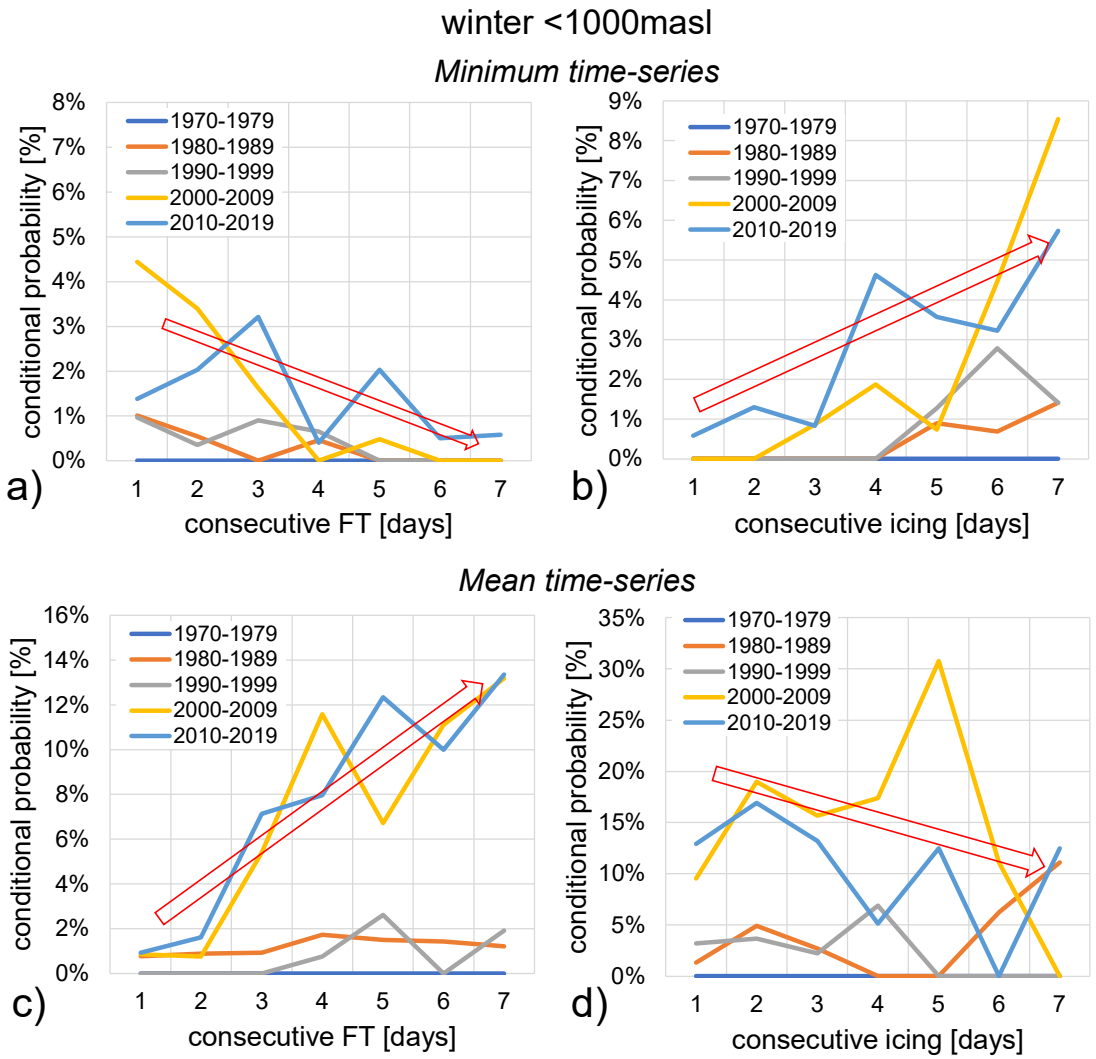

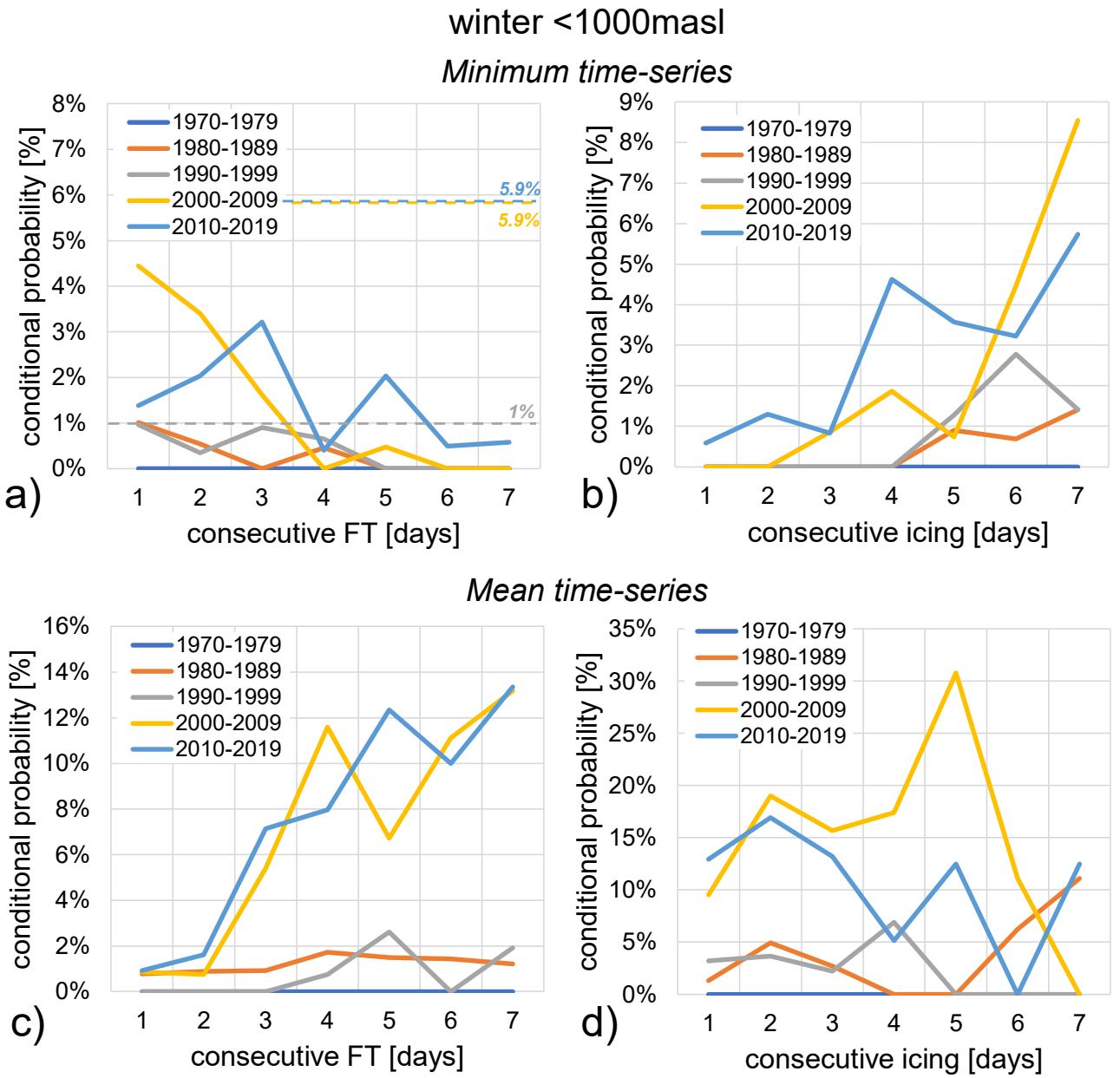

Figure 19~~**: Consecutive**~~**. Conditional probabilities of rockfalls during winter below** ~~**1000masl**~~**1000 m a.s.l. from 1970 to 2019 with** ~~**an**~~**a 7 days aggregation scale** ~~**of 7 days.**~~**:** (a and c) trigger~~**ed**~~ by freeze-thaw cycles with minimum and ~~**medium**~~**mean** times-series~~**.**~~**:** (b and d) trigger~~**ed**~~ by icing with minimum and maximum time-series. Rockfall probabilities are represented by the coloured dotted lines according to the decade as shown in the legend.

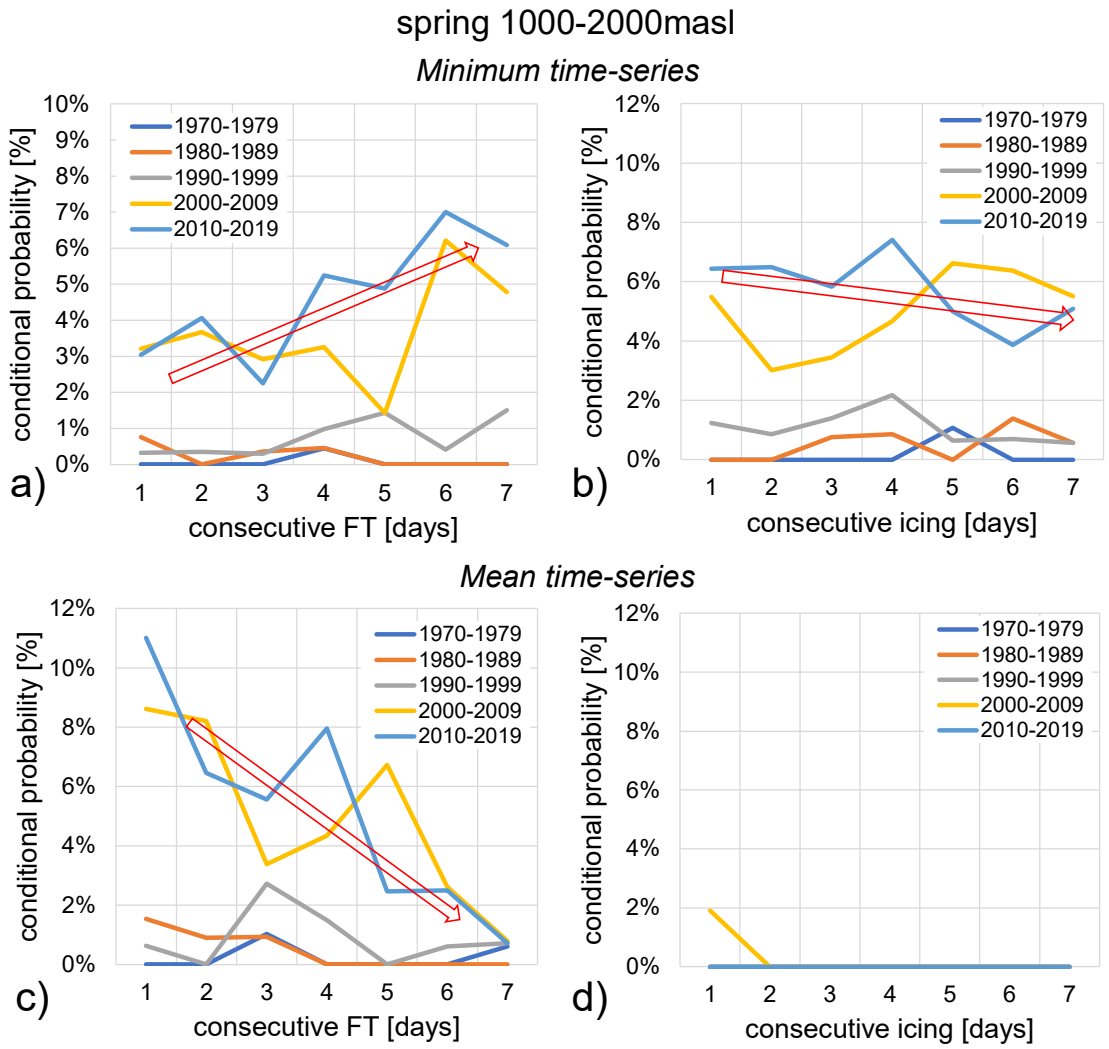
spring 1000-2000masl
Minimum time-series
conditional probability [%]
1970-1979
1980-1989
1990-1999
2000-2009
2010-2019
a)
consecutive FT [days]
b)
consecutive icing [days]
Mean time-series
c)
d)

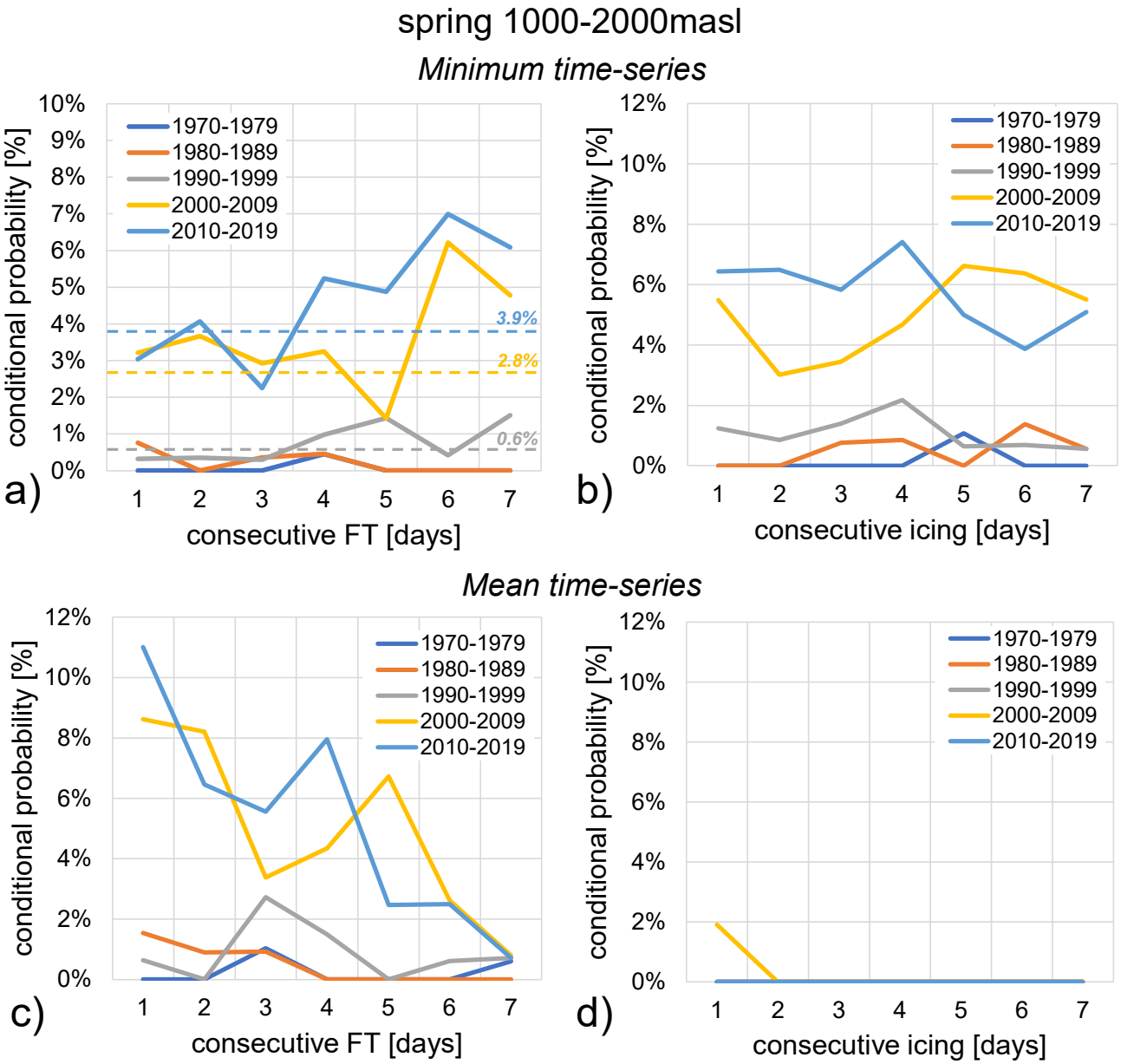

Figure 20~~: Consecutive~~. Conditional probabilities of rockfalls during spring between ~~1000masl~~1000 m a.s.l. and ~~2000masl~~2000 m a.s.l. from 1970 to 2019 with ~~ana~~ 7 days aggregation scale ~~of 7 days~~. (a and c) trigger~~ed~~ by freeze-thaw cycles with minimum and ~~medium~~mean times-series. (b and d) trigger~~ed~~ by icing with minimum and maximum time-series. Rockfall probabilities are represented by the coloured dotted lines according to the decade as shown in the legend.

5 Discussion

5.1 Climate

~~Climate~~Global and regional climate variations, particularly concerning temperature trends, have been extensively monitored ~~by many authors in terms of temperature rates over different years.~~and reported. For instance, Gobiet et al. (2014) ~~reported~~documented increasing temperature in the alpine region from 1980 onwards, with annual mean warming rates of 0.5°C per decade. ~~They~~Their projections also ~~noted~~suggest that the 21st-century temperature changes ~~are expected to affect~~will impact not only rising values but also ~~in~~ seasonal cycles. Similarly, in the Swiss Alps, Allen and Huggel (2013) observed an increase in both the values and frequencies of maximum temperature, T_{max}, ~~at~~with a rate of 0.49°C per decade during summer season. Ceppi et al (2012) reported a comparable rate of 0.46 °C/decade, ~~and~~while Beniston (2006) found that winter minimum temperatures, T_{min}, below ~~1000m~~1000 m elevation increased by ~~about~~approximately 4°C for the period 1961-1990, ~~while~~with summer temperatures ~~are~~ projected to exceed current values by 5.5–6°C. It is ~~worth noticing~~noteworthy that during the Early

Twentieth Century Warming (ETCW, 1916-1945) a maximal global warming trend of 0.47°C/30 years was observed (Bengtsson et al., 2004). The climate reports for the current study area consistently align with these broader findings. The ZAMG (2015) ~~show a~~ climate report ~~about~~for a subregion of ~~alpine arch (Tirolo, Altoadige~~the Alpine arc (Tyrol, South Tyrol and Belluno~~). From the results of this report, normal~~) indicates typical climate fluctuations ~~are presents~~ until 1980, ~~whereas,~~followed by a distinct warming trend from 1980 to 2010 ~~is marked a warming trend.~~. Seasonally, ~~the following trends were~~this report noted: (i) minimal warming in spring and summer; (ii) less variation in autumn temperatures, and (iii) milder winters. Consequently, the number of warm days in summer ha~~ves~~s increased, while icing or frost days have decreased. Nigrelli and Chiarle (2023) further stated that during the most recent ~~normal~~ climatological normal period (1991-2020), the annual average minimum temperature was -2.4 °C, with a warming rate of 0.4 °C per decade, and the annual average maximum temperature was 4.4 °C with a warming rate of 0.5 °C per decade. Summer and autumn temperatures ~~showed the highest warming rates, about 0.6 °C per decade. In this study, to calculate temperature annual averages, 12 weather stations with full time series, were considered in order to observe a trend during time. Since the chosen stations were distributed at different altitudes, two periods were considered to have complete time series: 1970-2019 for stations below 2000m, and 1985-2019 for stations above 2000m.~~ exhibited the highest warming rates, approximately 0.6 °C per decade.

~~Considering all stations and analysing overlapping period from 1985 to 2019, the annual average warming rate for minimum and maximum temperature is 0.28°C per decade and 0.15°C per decade, respectively (a). The highest warming rates were found during the spring period with a maximum increase for maximum temperature of about 0.33°C per decade. Analysing stations~~In this work, by analysing stations characterized by altitudes, an annual warming rate of 0.51°C per decade ~~is~~was found above ~~2000m~~2000 m (Figure 6~~d); however~~). However, for this ~~latter~~specific rate, ~~consideration should be given~~it is crucial to consider the shorter ~~period considered. Analysing~~time period used for analysis at these higher altitudes. When analysing stations by seasons, the maximum temperature warming rate ~~happened, also for~~, in this case, also occurred during spring season~~.~~, consistent with some regional observations.

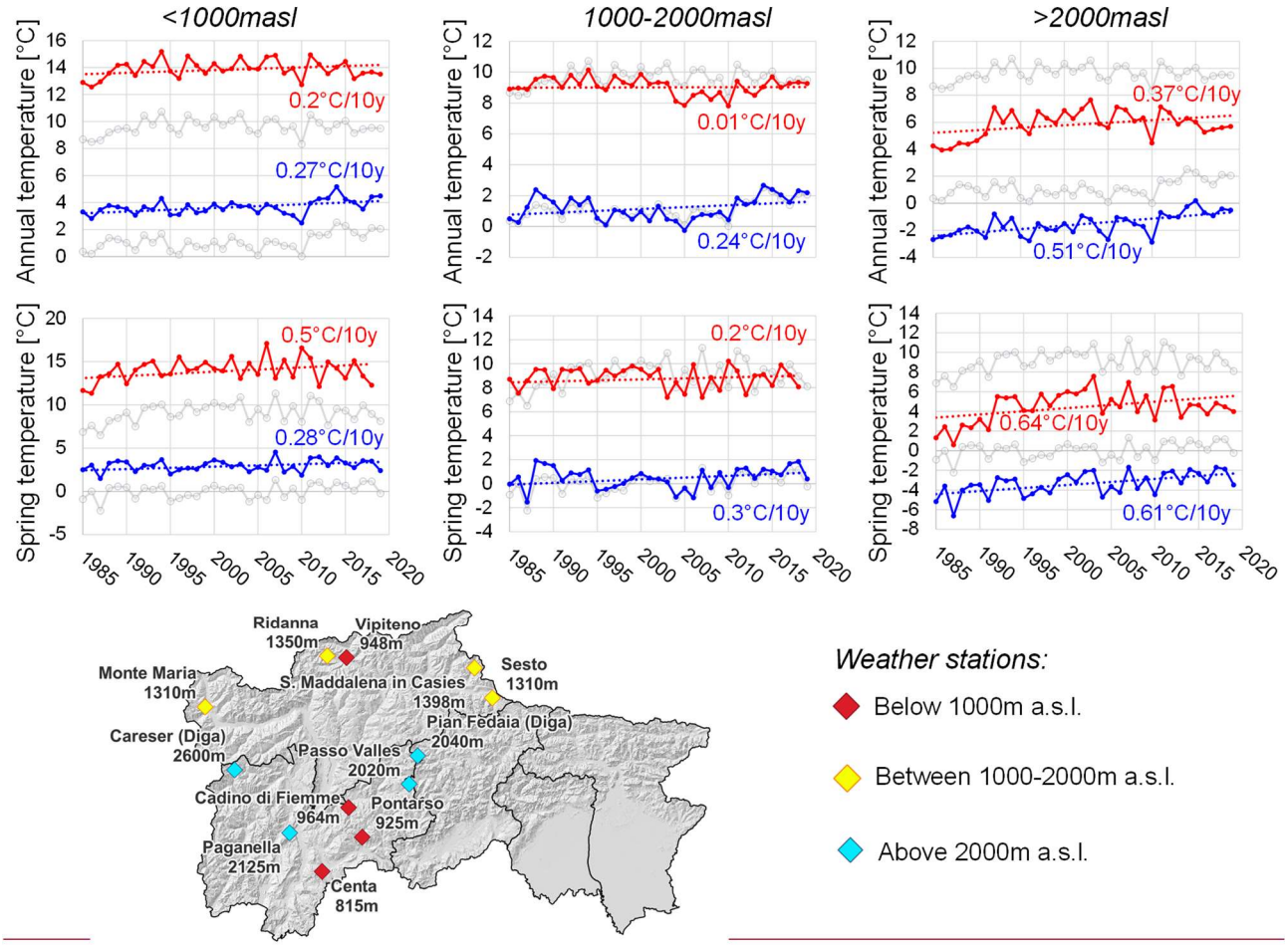

~~**Figure : Annual and spring T_{max} and T_{min} trends considering 12 weather stations from 1985 to 2019 for case study; location of weather stations considered are shown below. The maximum and minimum annual and spring values computed by using data of all weather stations are plotted in grey**~~

~~In this work, an increase in the frequency of high air mean temperatures over the decades is revealed, particularly at altitudes between 1000m and 2000m during the spring season, at all elevation in summer, and below 1000m in autumn, with a 90-day aggregation scale. These results align with the warming trend observed across the entire alpine region by the aforementioned authors.~~

~~Water~~Regarding water availability, several studies suggest a potential decline in some regions ~~may decline~~ due to reduced precipitation and a decrease in snowpack and snow~~-pack and snow~~ season duration in many mountain ~~regions~~areas (Beniston, 2003). In the Swiss Alps, ~~at~~for instance, elevations below ~~1200m, there has been~~1200 m have experienced a reduction in ~~the~~ total snow amount ~~of snow~~ and ~~the duration of the~~ snow season by ~~about~~approximately 100 days since the mid-1980s. Beniston (2006) additionally noted that for every 1°C increase in temperature, the snowline rises by about ~~150m~~150 m. Nigrelli and Chiarle (2023) observed a decrease in the Alps in the number of icing days (days when the maximum temperature is below 0 °C) by 6 days p~~ver~~ery decade, and the number of freeze-thaw cycle days (days when the minimum temperature is below 0 °C) by 9 days per decade. As observed in the Figure 13~~every decade. Considering the same weather stations used for the calculation of the temperature trends, a decrease of about 7.3 freeze-thaw days and about 2.2 icing days every decade (a). From the seasonal analysis, generally the trend is decreasing, however above 2000m FT cycles increase at a rate of 3.3days/10y and 2.7days/10y in winter and spring respectively (b-c). In winter above 2000m, a loss of 2.1 ice days per decade is calculated (e).~~

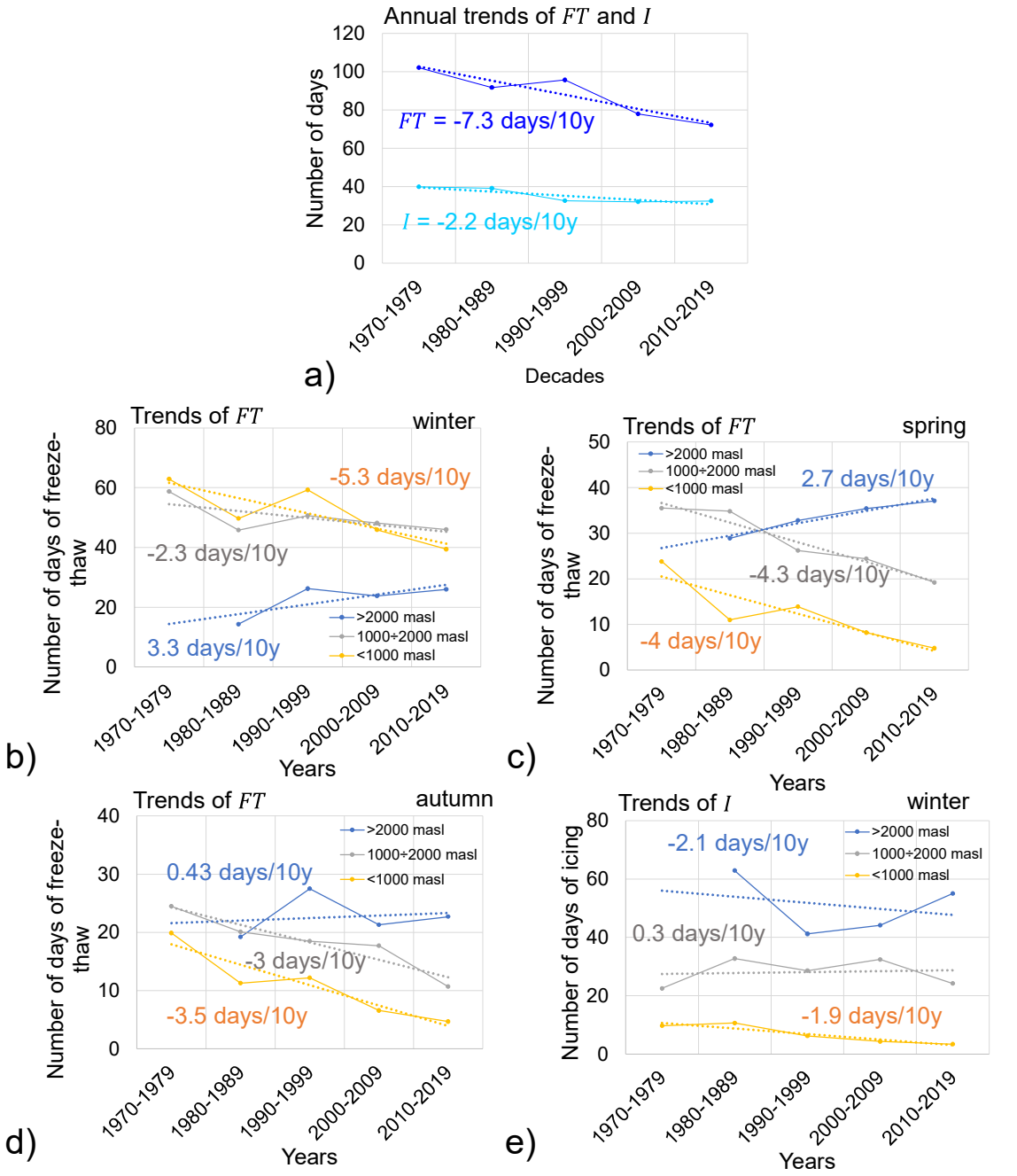

705 ~~**Figure : Annual and seasonal freeze-thaw and icing trends regarding to altitudes for this case study during 1970 to 2019. (a) considering 12 weather stations; (b) trends of FT during winter season; (c) trends of FT during spring season; (d) trends of FT during autumn season; (e) trends of I during winter season.**~~

~~Similar results in terms of reduction in the persistence and frequency of freeze/thaw and icing cycles were also found. Below 2000m, the freeze/thaw cycles persist less and stop earlier in the decades, ceasing in the early spring and reappearing in~~ 710 ~~November. Above 2000m, the frequencies of ice days decrease in May during the last decade, while in October, they appear more frequently but with shorter daily durations, leading to a delay in the onset of the winter season.~~

~~Therefore, it can be~~ similar results were concluded ~~that springs and autumns are getting warmer, and summers have increasing frequencies of high temperature values, leading to an anticipation of summer and a delayed onset of winter. Indeed, considering the 12 weather stations with full time series illustrated before, from 1970 to 2019 an increase temperature of about 1.5°C in~~ 715 ~~winter and 3°C in summer is observed (a-e). During the spring and autumn seasons, an increase in mean temperature of about 3°C and 2°C respectively, is observed, along with a shift in onset of 30 days for spring and 20 days for autumn, thus causing a change in the length of these two seasons (b-d), with a more significant change during spring~~in this work in which a local region was considered.

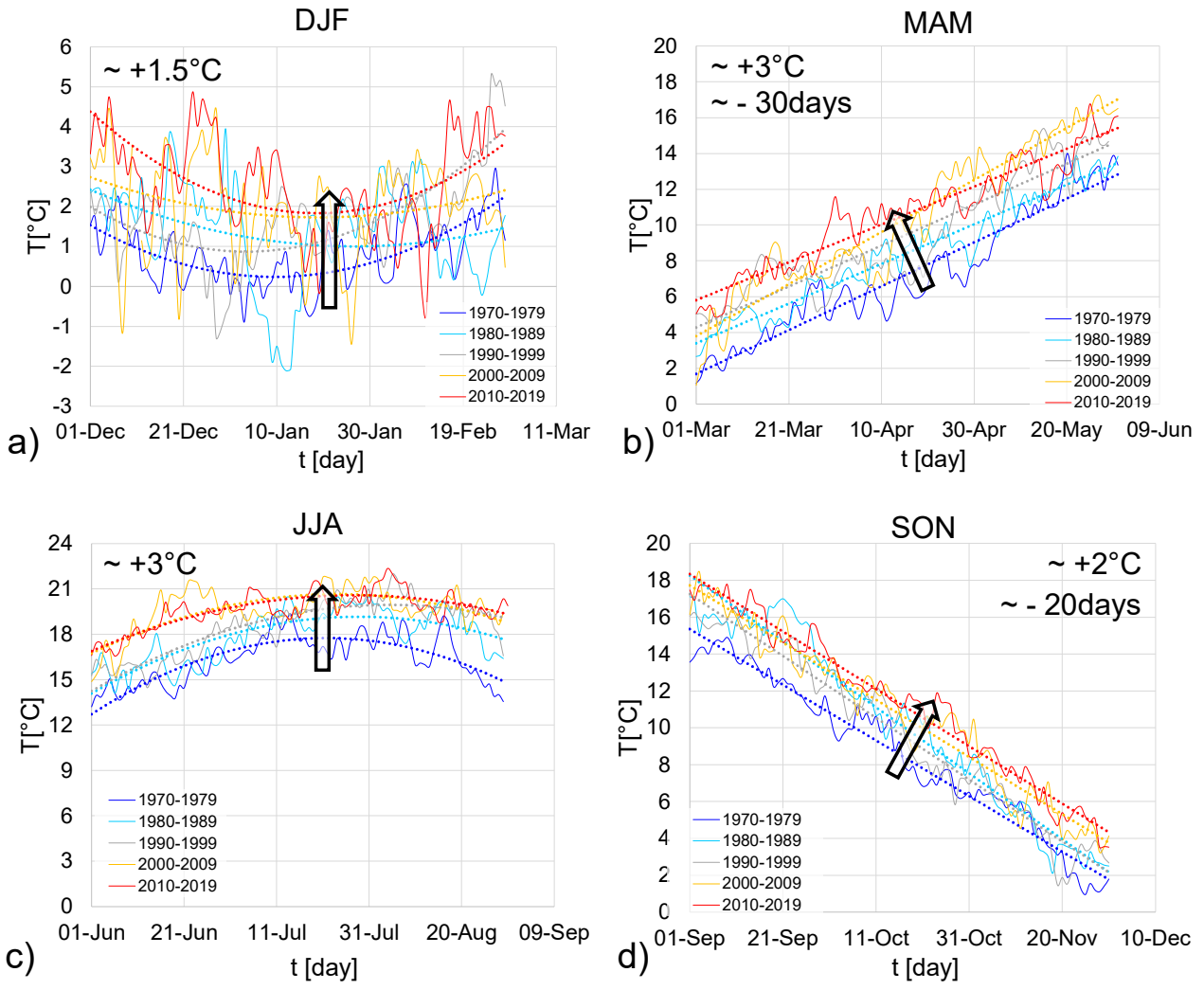

~~Figure : Daily time series of air mean temperature over 1970-2019 during: (a) winter (DJF), (b) spring (MAM), (c) summer (JJA) and (d) autumn seasons (SON).~~

Wang et al (2021) achieved similar results on a global scale~~. They observed that~~ , observing significant changes in the length of the four seasons between 1952 and 2011~~, the length of the four seasons changed~~: spring and summer started earlier by 1.~~6days/10years and 2.~~6 days/10 years and 2.5 days/10 years, respectively, while the onset of autumn and winter was delayed by 1.7 days/10 years and 0.5 days/10 years, respectively. This conclusion was also observed in our work, as shown in Figure 7~~10years, respectively, while the onset of autumn and winter was delayed by 1.7days/10years and 0.5days/10years, respectively~~, even though our analysis focused on a local scale and a 50-year time range.

~~Regarding~~Concerning rainfall, ~~the~~our results indicate that high-intensity rainfall events are becoming more frequent~~,~~. This finding is consistent with ~~findings by~~ Schmidli and Frei (2005) and Widmann and Schär (1997), who ~~stated that~~ reported an increase in mean precipitation ~~increased in~~during the 20th century during, particularly in fall and winter. Beniston (2006) noted that precipitation patterns in the Swiss Alps have changed, with winter precipitation decreasing marginally (2–3%) while summer precipitation is projected to decrease by 15–20% in most parts of the ~~a~~Alpine chain. According to Christensen and Christensen (2003), reductions in average summer precipitation may be accompanied by a sharp increase in short but heavy precipitation events. Gobiet et al. (2014) also stated that precipitation generally decreases in summer and increases in winter. ~~In this work, however, precipitation increases significantly~~The RAPS method, applied in our study (Figure 4~~the winter season, while summer variations are modest over the decades.~~

~~To visualize~~), further confirmed these results by showing long-term trends ~~changes in climatic records, fluctuations and periodicities in precipitation,~~ similar to those identified by Garbrecht and Fernandez (1994~~) used the Rescaled Adjusted Partial Sums (RAPS).~~

The Rescaled Adjusted Partial Sums (RAPS) method is a powerful tool for analysing time series data, particularly in hydrology and meteorology. This method supports the detection of irregularities and fluctuations within a time series (e.g., temperature, precipitation) that might not be apparent using traditional analysis techniques. RAPS involves rescaling the partial sums of deviations from the mean of a time series, allowing for the identification of significant changes or trends over time and it helps in visualizing and analysing the cumulative deviations from the mean, rescaled by the standard deviation, to detect underlying patterns and trends in the data. It is particularly effective for identifying breakpoints and subperiods within the data, making it valuable for studying long-term climatic trends and periodicities (Garbrecht and Fernandez, 1994, Durin et al., 2022). Mathematically, the RAPS method can be expressed with the following Eq. (14):

$$RAPS_k \sum_{t=1}^{k} \frac{Y_t - \bar{Y}}{S_y} \quad (16)$$

Where $RAPS_k$ is the rescaled adjusted partial sum at time ($t = 1,2,..,k$) represents the individual data points in the time series, $\bar{Y}$ is the mean of the time series, and S_y is the standard deviation of the time series.

Garbrecht and Fernandez (1994)), who studied 90-year annual rainfall (1902-1991) in Bryan County, Oklahoma, and found two major trends: a generalidentified distinct periods of decrease from (1902 to -1966,) followed by an increase from (1967 to -1991. This application shows), which corresponded to occurrences of floods and droughts events defined by fluctuations in the RAPS.

In this work, RAPS analysis by altitude, was performed considering the 12 meteorological stations (). Below 1000m a general decrease from 1985 to 2008 was observed, followed by an increasing trend. During autumn, many fluctuations were observed. In 2002, a sharp increase is noted, likely corresponding to high rainfall events in May and November (Bollettino meteorologico e valanghe, Ufficio idrografico di Bolzano; Protezione Civile Provincia Autonoma di Trento). Between 1000m and 2000m, the trend is decreasing because time series remains below the mean value until 2005. After this date, an increment is observed in RAPS. Above 2000m, a general decrease until 2006 was recorded, followed by an increasing trend. During spring, many fluctuations were observed.

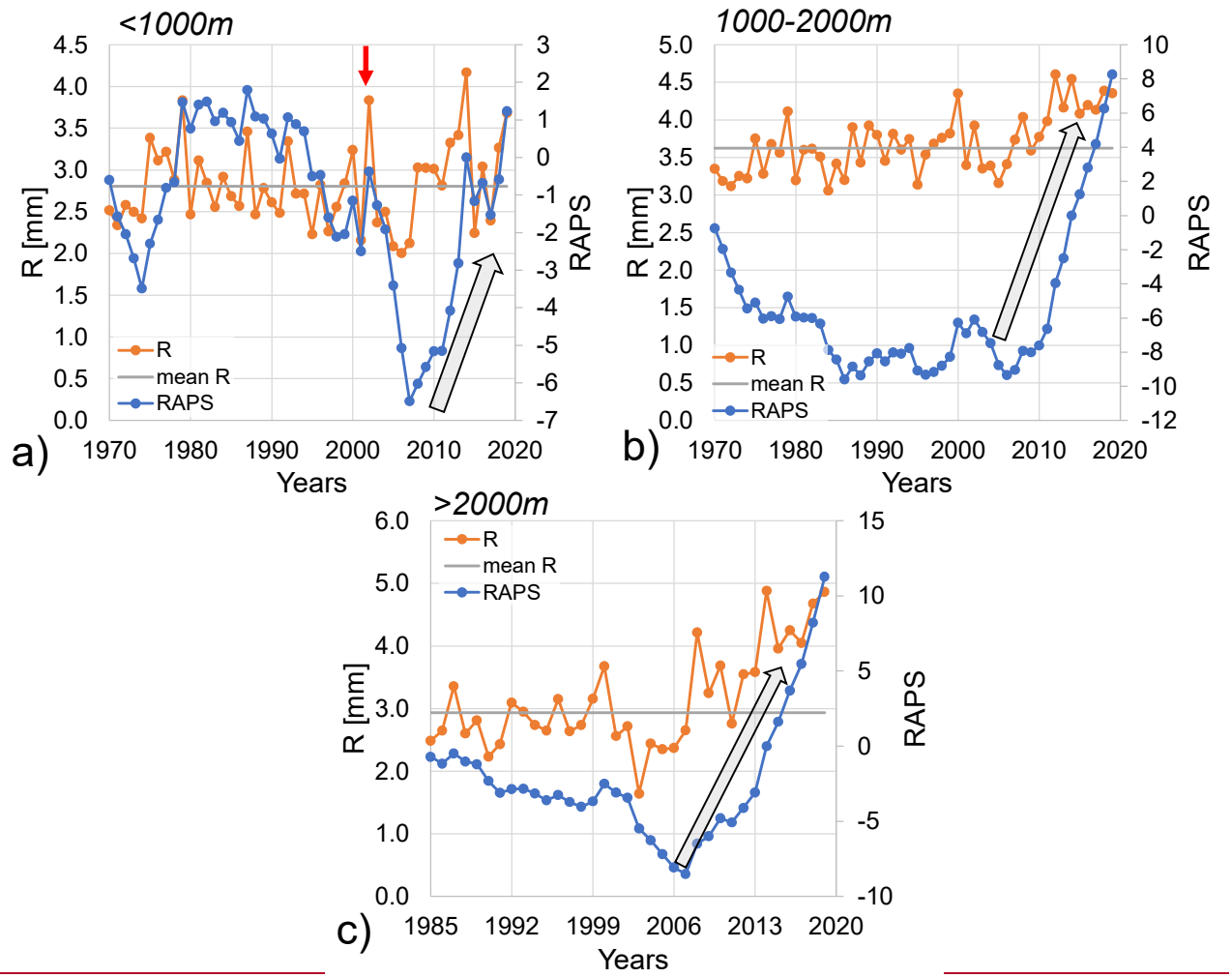

~~Figure : Annual mean rainfall values and Rescaled Adjusted Partial Sums: (a) below 1000m from 1970 to 2019; (b) between 1000-2000m from 1970 to 2019; (c) above 2000m from 1985 to 2019. The red arrow shows extraordinary events of 2002~~.

5.2 Rockfall

Rockfall frequency typically exhibits seasonal variability~~. Previous studies in the Alps have reported diverse~~, and this study's findings align with various seasonal patterns~~: Coro~~ reported in previous Alpine research. For instance, Corò et al. (2015) identified in the Alps rockfall frequency peaks in October-November, June-July~~,~~ and March~~;~~. Bajni et al. (2021) observed primary peaks in spring and minor peaks in January in the Aosta Valley; while Frayssines and Hantz (2006) found a primary peak in winter and a secondary peak in April in the French Alps~~; and~~. Similarly, Perret et al. (2006) ~~noted~~ highlighted early spring seasonality in ~~early spring~~ the rockfall frequency in the Swiss Alps. ~~This~~Consistent with these observations, our study ~~similarly~~ reveals distinct rockfall peaks in November, February, April, and August (Figure 14~~.~~b).

Climate variables significantly influence rockfall occurrence. ~~A strong correlation exists~~Our analysis indicates a relationship between winter rockfalls and precipitation, particularly daily rainfall events exceeding 31.5 mm. Summer rockfalls above 2000 m are potentially linked to mean air temperatures exceeding 9°C, while spring rockfalls between 1000 m and 2000 m correlate with mean air temperatures ranging from 5.8°C to 15.4°C. Additionally, rockfalls exhibit a correlation with winter temperature amplitudes between 1°C and 7°C at elevations between 1000 m and 2000 m, and summer temperature amplitudes between 10.8°C and 12°C above 2000 m.

Air temperature plays a crucial role in rockfall initiation, particularly during warmer months. Elevated temperatures can accelerate snowmelt, ~~infiltrating~~facilitating water infiltration into rockwall discontinuities and thereby triggering rockfalls, especially at the onset of summer and autumn (Allen and Huggel, 2013). Furthermore, air temperature directly influences other critical mechanisms such as icing and freeze-thaw cycles (Noetzli et al., 2003; Salzmann et al., 2007; Manent et al., 2024).

The impact of freeze-thaw (FT) cycles on rockfall occurrence has been ~~previously~~extensively investigated. Frayssines-Hantz (2006) observed a correlation between rockfalls and frequent temperature fluctuations around the freezing point in early spring and late autumn at elevations between 1000 m and 2000 m. D'Amato et al. (2016) reported an increase in rockfall frequency during freeze-thaw episodes, particularly during thawing periods. This study confirms these findings, with an increased rockfall frequency observed in winter below 1000 m during FT cycles lasting 1 to 3 days, and in spring between 1000 m and 2000 m. A slight increase in rockfall frequency was also observed during icing periods lasting 1 to 5 days.

The methodology employed in this study for obtaining the sampled time-series was inspired by the work of Paranunzio et al. (2015). Consequently, ~~a comparison of~~ comparing between our frequency and the anomaly results ~~with those~~ reported by Paranunzio et al. (2015) is essential. Paranunzio et al. (2015) concluded that four out of five case studies in the Piedmont region could be attributed to meteorological anomalies, such as temperature rise or heavy precipitation. In a subsequent study, Paranunzio et al. (2016) found that in 85% of cases across the Western and Eastern Alps, at least one climate variable has anomaly ~~was associated with~~values at rockfall occurrence, with most events linked to short-term temperature anomalies. Precipitation was identified as a contributing factor in only 15% of rockfall events at weekly, monthly, and quarterly aggregation scales.

~~The~~ To further validate our approach, we adapted and tested the method of Paranunzio et al. (2016) ~~was adapted and tested~~ in this study, ~~and~~comparing the results ~~were compared~~ obtained with its method to those obtained using ~~the~~our proposed method~~.~~ ~~The~~ starting in both cases from the dataset reported in this work. We analyzed the same climate variables (precipitation and mean air temperature~~, temperature variations over different days, and precipitation) were analyzed~~) at identical aggregation scales (daily, weekly, monthly, and quarterly~~) for~~). Additionally, we investigated temperature variations (ΔT) over 1, 3, and 6 days prior to the event. The non-exceedance probability P(V) was calculated ~~with~~ and an event is considered anomalous when its non-exceedance probability is less than $\alpha/2$ or is greater than $1.0 - \alpha/2$ being α a significance level ~~(~~that is equal to α=0.2~~).~~

~~The~~ as indicated in Paranunzio et al. (2016). The obtained results are reported in Figure 21~~indicate that 50% where the frequencies of rockfalls were associated with at least one anomaly. Positive temperature anomalies were more frequent than precipitation anomalies (Fig. 21). Daily and weekly temperature anomalies were more frequently cold (negative) than hot (positive), while monthly and quarterly anomalies were more frequently hot than cold. Regarding the season of occurrence, rockfalls were slightly more frequent in autumn (for positive anomalies) and spring (for negative anomalies). All anomalies were more frequent below 1000 m asl, and small~~the anomalous events ~~(<100m3) predominated. Conversely, large-magnitude events were more frequent with positive anomalies. Finally, numerous events occurred in non permafrost areas, while in~~

~~permafrost areas, rockfalls were more strongly controlled by permafrost-favorable conditions than other factors.~~

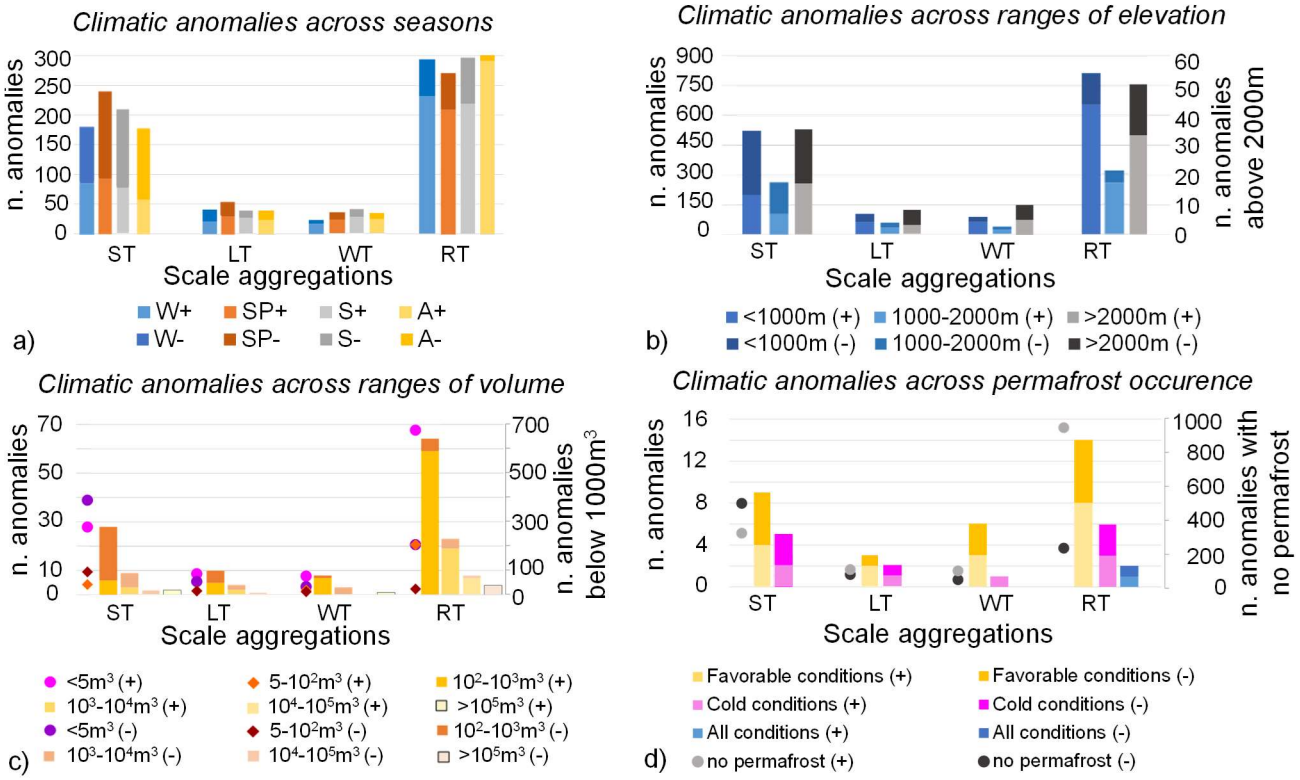

~~Figure : Distribution of rockfalls~~are reported according to ~~controlling factors and aggregation scales: (a) season of occurrence (W=winter; SP=spring; S=summer; A=autumn); (b)~~the corresponding meteorological variables. For all considered variables the frequencies of anomalous events increase with the decades and more frequent anomalous events are located in the middle of the range of ~~elevation; (c) range~~the considered values for each variable. This result could be due to the definition of non-exceeding probability that was estimated ordering the recorded data values. This implies that the first values in the rank could be relative higher but not the highest in the meteorological station. In contrast the conditional probability has greater values for high values of ~~volume; (d) expected permafrost occurrence in detachment zone. The aggregation scales are: ST= short-term~~meteorological variables. This difference is attributed to the method employed for computing the conditional probability in which the meteorological probability is computed for all ranges even those in which the rockfall events did not occurred. Finally, temperature variations have to peaks one associated to negative values and another one to positive. This result is attributed to the fact that the same temperature variation could occur for increasing temperature~~; LT= long-term~~ (temperature~~; WT= widespread~~ variation positive) and for decreasing temperature~~; R= precipitations. Positive anomalies are assigned with (+)~~ (temperature variation negative) and since the anomalous events correspond to a symmetric value of non-exceeding probabilities (positive and negative ~~with (-).~~anomalies) two peaks appeared.

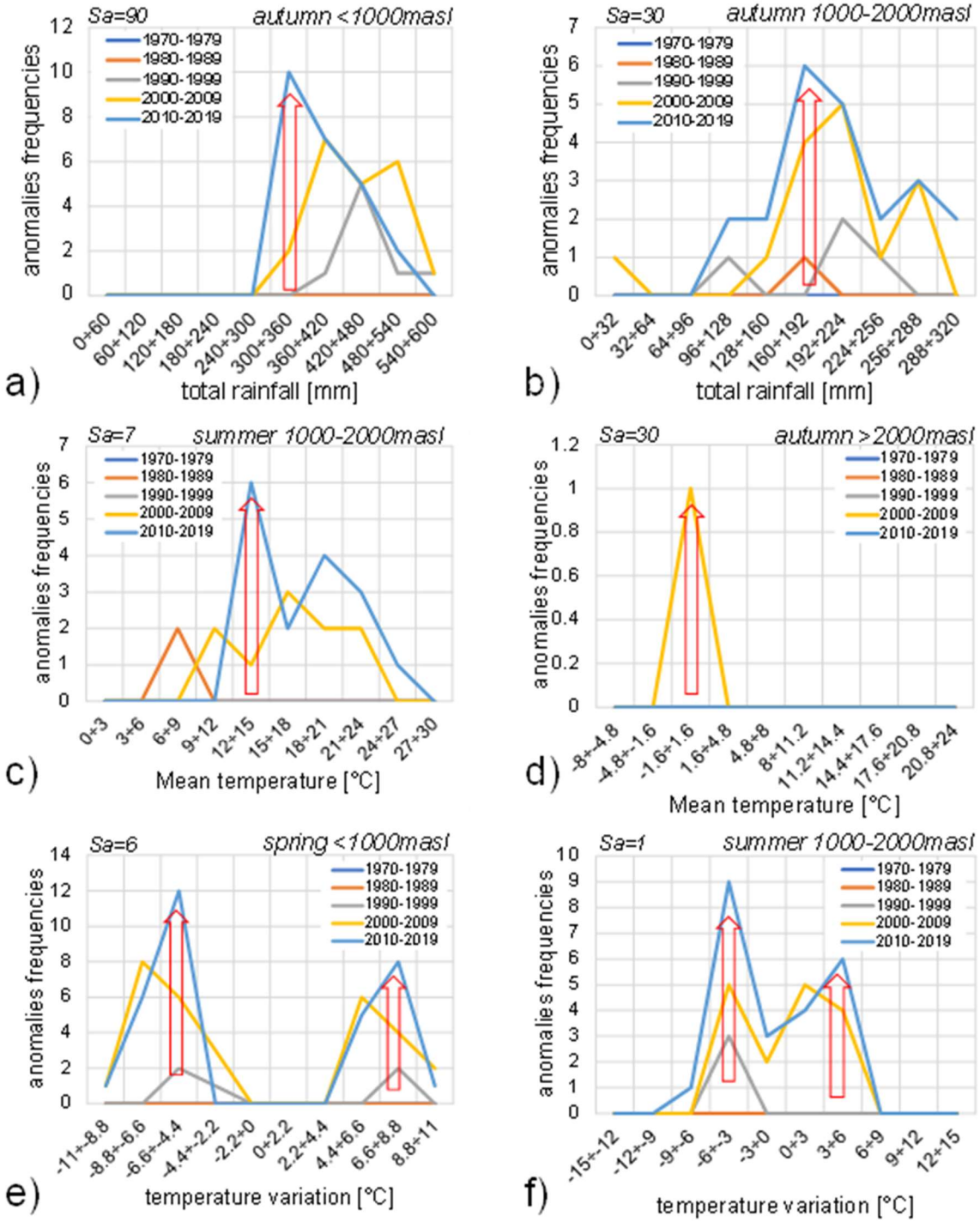

Figure 21 Distributions of anomaly frequencies by using Paranunzio et al. (2015) method, categorized by climate variable and aggregation scale as applied in this analysis. Only results for rainfall, temperature amplitude and temperature variation, as presented in Section 4.3, are reported.

Due to the complexity of meteorological but also lithological and morphological conditions under which the rockfall occurred, this analysis does not allow to unravel into detail the mechanisms why a weather variable has different effects according to the season or elevation. For such detail, it should be necessary to constrain the analysis by considering only rockfalls occurring on single lithological and morphological settings through a detailed multitemporal survey that allows to focus on specific weather variables, e.g. thermal stress (Collins and Stock, 2016; Gasc-Barbier et al., 2024; Fei et al., 2025), freeze-thaw (D'Amato et al., 2016), or rainfall (Weidner et al., 2024).

6 Conclusion

This study ~~confirms~~analyzed meteorological data from 1970 to 2019, confirming a significant warming trend in the ~~a~~Alpine region, consistent with previous research ~~by analysing data from 1970 to 2019. The annual mean warming rate from.~~ Specifically, for the period 1985-2019 ~~for,~~ the study area ~~is~~ recorded an annual mean warming rate of 0.28°C per decade for minimum temperature ~~at 0.28°C per decade~~ and 0.15°C per decade for maximum temperature ~~at 0.15°C per decade. Notably, the~~ . The highest warming rates were notably observed during the spring period, with a maximum increase of ~~about~~ 0.~~33~~3°C per decade. ~~Springs~~These trends indicate that springs and autumns are ~~getting~~becoming warmer, summers are experiencing increasing frequencies of high temperature values, and winters are ~~becoming~~growing milder. This overall warming leads to an earlier onset of summer and a delayed onset of winter, consequently altering the length of these seasons.

Significant changes in precipitation patterns were also observed~~, with an~~. There is a clear increase in high-intensity rainfall events, particularly in winter, ~~while~~alongside a reduction in low-intensity rainfall was recorded across all seasons. This finding aligns with established observations ~~in the literature~~ for the Alpine region in the existing literature. Conversely, summer precipitation variations were modest, contrasting with some previous projections for the area.

A notable decline in both icing and freeze-thaw cycles days ~~are observed, specifically is estimated~~was identified. Quantitatively, this study estimates a decrease of 7.3 days of freeze-thaw cycles and 2.2 ~~days of~~ icing days every decade.

The Rescaled Adjusted Partial Sums (RAPS) method provided valuable insights into long-term trends and fluctuations in precipitation ~~highlighting~~. It highlighted that climate evolution is primarily driven not ~~due to the variation of~~by changes in the maximum values of ~~the~~ climate variables, but rather ~~a variation~~by variations in their frequencies over the years.

~~Rockfall~~Our rockfall analysis ~~showed~~revealed that rockfall frequencies ~~have~~exhibit three main peaks: in November, February-April, and August. ~~In terms of~~Regarding the aspect of the source area, ~~below 1000m.a.s.l., 70% of rockfalls have south-facing slopes; between 1000-2000m.a.s.l., 35% have south-east facing slopes;~~for altitude greater than 2000 m, for group A the predominant component is W while for the group B the W component reduces significantly (from 23% to 7%+7%), the S, SW and ~~above 2000m, 50% of events have north-northwest facing slopes, possibly due~~SE reduces slightly while the N component has significant increment (from 4% to 12% +3%): a pattern potentially linked to permafrost thawing in these high-altitude.

~~Rockfalls~~ The study identified several correlations between rockfall events and ~~high~~ specific climate variables. High-intensity rainfall and rockfalls are correlated in autumn, with monthly and quarterly ~~rainfalls with 12.4% below1000m~~rainfall events showing conditional probabilities of 12.4% below 1000 m and 22.2% at altitudes between ~~1000m~~1000 m and ~~2000m; a~~2000 m. A correlation with ~~air~~ mean air temperatures ~~of 12.7% within range~~was observed: a 12.7% conditional probability for rockfalls with weekly mean temperatures ranging from 21°C to 24°C during the summer season between ~~1000m and 2000m at weekly scale is observed~~1000 m and ~~increment~~2000 m. This conditional probability reaches 2.2% above ~~2000m~~2000 m with ~~a range of temperature~~temperatures ranging from 17.6°C to 20.8°C during the autumn season ~~with Sa=30.~~

~~Rockfalls are correlated with temperature~~ (at a 30-day aggregation scale). Temperature amplitude also showed correlations: in spring below ~~1000m.~~1000 m a.s.l., a~~.s.l. from~~ 28.6% probability was found for amplitudes between 8.8°C ~~to~~and 9.9°C ~~with 28.6% of probability and in~~ . In winter, between ~~1000masl and 2000m.~~1000 m a.s.l. and 2000 m a.s.l., a 5.8% probability was observed for amplitudes in the range of 9°C to 10°C ~~with 5.8% of probability. According to~~.Regarding temperature variation, rockfalls ~~happen~~ in summer between ~~1000m~~1000 m and ~~2000m~~2000 m are correlated with a 14.3% probability with ~~a~~ temperature ~~variation of~~variations from -9°C to -6°C ~~and during~~. During spring ~~season~~ below ~~1000masl with~~1000 m a.s.l., a conditional probability of 20% ~~with~~was found for the maximum range of variation (8.8°C÷11°C).

~~From~~Finally, the analysis of correlations between rockfall events ~~with~~and freeze-thaw cycles and icing periods~~, it is observed how~~ highlighted that the probability results ~~change depending on the~~ are significantly influenced by the chosen calculated ~~timeseries~~time-series (maximum, average, ~~minimum).~~or minimum temperature), emphasizing the importance of detailed temperature data for these phenomena.

Author contributions

FB: meteorological and rockfall data collection and analysis; FB and GD performed the statistical analyses; FB, GD and GC prepared the draft manuscript. PF and GC provided funding, supervised the project and the analyses.

Competing interests

The authors declare that they have no conflict of interest.

References

Allen, S., and Huggel, C.: Extremely warm temperatures as a potential cause of recent high mountain rockfall. Global and Planetary Change, 107, 59-69, 2013.

Angot, A. Sur la decroissance de la temperature dans l'air avec la hauteur. Ciel et Terre, vol. 14, pp. 15-19, 14, 15-19, 1894.

Bajni, G., Camera, C. A., and Apuani, T.: Deciphering meteorological influencing factors for Alpine rockfalls: a case study in Aosta Valley. Landslides, 18(10), 3279-3298, 2021.

Barry, R. G., and Chorley, R. J. Atmosphere, weather and climate. Routledge, 2009.

Bassetti, M., and Borsato, A.: Evoluzione geomorfologica della Bassa Valle dell'Adige dall'Ultimo Massimo Glaciale: sintesi delle conoscenze e riferimenti ad aree limitrofe. Acta Geologica, 82(31), e42, 2005.

Bayes, R. T.: Bayes' Theorem. An essay towards solving a problem in the doctrine of chances, Philosophical, 370-418, 1763.

Bengtsson, L., Semenov, V. A., and Johannessen, O. M.: The early twentieth-century warming in the Arctic—A possible mechanism. Journal of Climate, 17(20), 4045-4057, 2004.

Beniston, M.: Climatic change in mountain regions: a review of possible impacts. Climatic change, 59(1), 5-31, 2003.

Beniston, M.: Mountain weather and climate: a general overview and a focus on climatic change in the Alps. Hydrobiologia, 562, 3-16, 2006.

Berti, M., Martina, M. L. V., Franceschini, S., Pignone, S., Simoni, A., and Pizziolo, M.: Probabilistic rainfall thresholds for landslide occurrence using a Bayesian approach. Journal of Geophysical Research: Earth Surface, 117(F4), 2012.

Böhm, R., Auer, I., Brunetti, M., Maugeri, M., Nanni, T., and Schöner, W.: Regional temperature variability in the European Alps: 1760–1998 from homogenized instrumental time series. International Journal of Climatology: A Journal of the Royal Meteorological Society, 21(14), 1779-1801, 2001.

Bosellini, A., Gianolla, P., and Stefani, M.: Geology of the Dolomites. Episodes Journal of International Geoscience, 26(3), 181-185, 2003.

Brunetti, M., Lentini, G., Maugeri, M., Nanni, T., Auer, I., Bohm, R., and Schoner, W.: Climate variability and change in the Greater Alpine Region over the last two centuries based on multi-variable analysis. International Journal of Climatology, 29(15), 2197-2225, 2009.

Bunce, C. M., Cruden, D. M., and Morgenstern, N. R.: Assessment of the hazard from rock fall on a highway. Canadian Geotechnical Journal, 34(3), 344-356, 1997.

Ceppi, P., Scherrer, S. C., Fischer, A. M., and Appenzeller, C.: Revisiting Swiss temperature trends 1959–2008. International Journal of Climatology, 32(2), 203-213, 2012.

Christensen, J. H., and Christensen, O. B.,: Severe summertime flooding in Europe. Nature, 421(6925), 805-806, 2003.

Corò, D., Galgaro, A., Fontana, A., and Carton, A.: A regional rockfall database: the Eastern Alps test site. Environmental Earth Sciences, 74, 1731-1742, 2015.

Collins, B. D., and Stock, G. M.: Rockfall triggering by cyclic thermal stressing of exfoliation fractures. Nature Geoscience, 9(5), 395-400, 2016.

Courtial-Manent, L., Ravanel, L., Mugnier, J. L., Deline, P., Lhosmot, A., Rabatel, A., ... and Batoux, P.: 18-years of high-Alpine rock wall monitoring using terrestrial laser scanning at the Tour Ronde east face, Mont-Blanc massif. Environmental Research Letters, 19(3), 034037, 2024.

Crosta, G. B., and Agliardi, F.: Parametric evaluation of 3D dispersion of rockfall trajectories. Natural Hazards and Earth System Sciences, 4(4), 583-598, 2004.

Crosta, G. B., Agliardi, F., Frattini, P., and Lari, S.: Key issues in rock fall modeling, hazard and risk assessment for rockfall protection. In *Engineering Geology for Society and Territory-Volume 2: Landslide Processes* (pp. 43-58). Springer International Publishing, 2015.

D'Amato, J., Hantz, D., Guerin, A., Jaboyedoff, M., Baillet, L.,and Mariscal, A.: Influence of meteorological factors on rockfall occurrence in a middle mountain limestone cliff. Natural Hazards and Earth System Sciences, 7587-7630, 2016.

Dal Piaz, G. V., Bistacchi, A., and Massironi, M.: Geological outline of the Alps. Episodes Journal of International Geoscience, 26(3), 175-180, 2003.

Davies, M. C., Hamza, O., and Harris, C.: The effect of rise in mean annual temperature on the stability of rock slopes containing ice-filled discontinuities. Permafrost and periglacial processes, 12(1), 137-144, 2001.

Delonca, A., Gunzburger, Y., and Verdel, T.: Statistical correlation between meteorological and rockfall databases. Natural Hazards and Earth System Sciences, 14(8), 1953-1964, 2014.

Desiato, F., Lena, F., Baffo, F., Suatoni, B., and Toreti, A.: Indicatori del clima in Italia. Ecologia Agraria, U. C., & Romagna, A. E. APAT, Roma, 2005.

Desiato, F., Fioravanti, G., Fraschetti, P., Perconti, W., and Toreti, A.: Climate indicators for Italy: calculation and dissemination, Adv. Sci. Res., 6, 147–150, 2011.

Dodson, R., and Marks, D. Daily air temperature interpolated at high spatial resolution over a large mountainous region. Climate research, 8(1), 1-20, 1997.

Doglioni, C.: Tectonics of the Dolomites (southern Alps, northern Italy). Journal of structural geology, 9(2), 181-193, 1987.

Douglas, G. R.: Magnitude frequency study of rockfall in Co. Antrim, N. Ireland. Earth Surface Processes, 5(2), 123-129, 1980.

Draebing, D., and Krautblatter, M.: The efficacy of frost weather processes in alpine rockwalls. Geophysical Research Letters, 46(12), 6516-6524, 2019.

Đurin, B., Kranjčić, N., Kanga, S., Singh, S. K., Sakač, N., Pham, Q. B., ... and Di Nunno, F.: Application of Rescaled Adjusted Partial Sums (RAPS) method in hydrology–an overview. Advances in civil and architectural engineering, 13(25), 58-72, 2022.

Fei, L., Jaboyedoff, M., Derron, M. H., Choanji, T., and Sun, C.: Multiscale observations of diurnal thermal effects on rock failure and crack dynamics in soft marl layers (La Cornalle molasse rock wall, Switzerland). Engineering Geology, 108159, 2025.

Fischer, L., Kääb, A., Huggel, C., and Noetzli, J.: Geology, glacier retreat and permafrost degradation as controlling factors of slope instabilities in a high-mountain rock wall: the Monte Rosa east face. Natural Hazards and Earth System Sciences, 6(5), 761-772, 2006.

Frattini, P., Crosta, G., Carrara, A., and Agliardi, F.: Assessment of rockfall susceptibility by integrating statistical and physically-based approaches. Geomorphology, 94(3-4), 419-437, 2008.

Frayssines, M., and Hantz, D.: Failure mechanisms and triggering factors in calcareous cliffs of the Subalpine Ranges (French Alps). Engineering Geology, 86(4), 256-270, 2006.

Garbrecht, J., and Fernandez, G. P.: Visualization of trends and fluctuations in climatic records 1. JAWRA Journal of the American Water Resources Association, 30(2), 297-306, 1994.

Gariano, S. L., and Guzzetti, F.: Landslides in a changing climate. Earth-science reviews, 162, 227-252, 2016.

Gasc-Barbier, M., Merrien-Soukatchoff, V., Krzewinski, V., Azemard, P., and Genois, J. L.: Assessment of the influence of natural thermal cycles on dolomitic limestone rock columns: A 10-year monitoring study. Geomorphology, 464, 109353, 2024.

Gobiet, A., Kotlarski, S., Beniston, M., Heinrich, G., Rajczak, J., and Stoffel, M.: 21st century climate change in the European Alps—A review. Science of the total environment, 493, 1138-1151, 2014.

Gruber, S., and Haeberli, W.: Permafrost in steep bedrock slopes and its temperature-related destabilization following climate change. Journal of Geophysical Research: Earth Surface, 112(F2), 2007.

Hilker, N., Badoux, A., ~~and~~& Hegg, C~~.~~. (2009). The Swiss flood and landslide damage database 1972–2007. Natural Hazards and Earth System Sciences, 9(3), 913-925~~, 2009~~.

Huggel, C., Allen, S., Deline, P., Fischer, L., Noetzli, J., and Ravanel, L.: Ice thawing, mountains falling—are alpine rock slope failures increasing?. Geology Today, 28(3), 98-104, 2012.

Hungr, O., Evans, S. G., & Hazzard, J. (1999). Magnitude and frequency of rock falls and rock slides along the main transportation corridors of southwestern British Columbia. *Canadian Geotechnical Journal*, *36*(2), 224-238.

Krautblatter, M., and Moser, M.: A nonlinear model coupling rockfall and rainfall intensity based\newline on a four year measurement in a high Alpine rock wall (Reintal, German Alps). Natural Hazards and Earth System Sciences, 9(4), 1425-1432, 2009.

Krautblatter, M., Funk, D. and Günzel, F. K.: Why permafrost rocks become unstable: a rock–ice-mechanical model in time and space. Earth Surf. Process. Landf. 38, 876–887, 2013.

Letortu, P.: Le recul des falaises crayeuses haut-normandes et les inondations par la mer en Manche centrale et orientale: de la quantification de l'aléa à la caractérisation des risques induits (Doctoral dissertation, Université de Caen), 2013.

Luethi, R., Gruber, S. and Ravanel, L.: Modelling transient ground surface temperatures of past rockfall events: towards a better understanding of failure mechanisms in changing periglacial environments. Geogr. Ann. Ser. A Phys. Geogr. 97, 753–767, 2015.

Macciotta, R., Hendry, M., Cruden, D. M., Blais-Stevens, A., and Edwards, T~~.~~ Quantifying rock fall probabilities and their temporal distribution associated with weather seasonality. Landslides, 14(6), 2025-2039, 2017.

Macciotta, R., Martin, C. D., Edwards, T., Cruden, D. M., and Keegan, T~~.~~ Quantifying weather conditions for rock fall hazard management. Georisk: assessment and management of risk for engineered systems and geohazards, 9(3), 171-186, 2015.

Matsuoka, N., and Sakai, H.: Rockfall activity from an alpine cliff during thawing periods. Geomorphology, 28(3-4), 309-328, 1999.

Nigrelli, G., Fratianni, S., Zampollo, A., Turconi, L., Chiarle, M. The altitudinal temperature lapse rates applied to high elevation rockfalls studies in the Western European Alps. Theoretical and Applied Climatology, 131, 1479-1491, 2018.Nigrelli, G., and Chiarle, M. 1991–2020 climate normal in the European Alps: focus on high-elevation environments. Journal of Mountain Science, 20(8), 2149-2163, 2023.

Nigrelli, G., Paranunzio, R., Turconi, L., Luino, F., Mortara, G., Guerini, M., ... and Chiarle, M.: First national inventory of high-elevation mass movements in the Italian Alps. Computers & Geosciences, 184, 105520, 2024.

Nissen, K. M., Rupp, S., Kreuzer, T. M., Guse, B., Damm, B., & Ulbrich, U.: Quantification of meteorological conditions for rockfall triggers in Germany. Natural Hazards and Earth System Sciences, 22(6), 2117-2130, 2022.

Noetzli, J., Hoelzle, M., and Haeberli, W.: Mountain permafrost and recent Alpine rock-fall events: a GIS-based approach to determine critical factors. In Proceedings of the 8th International Conference on Permafrost (Vol. 2, pp. 827-832). Zürich: Swets & Zeitlinger Lisse, 2003.

Noetzli, J., and Gruber, S.: Transient thermal effects in Alpine permafrost. The Cryosphere, 3(1), 85-99, 2009.

Padulano, R., Rianna, G., and Santini, M.: Datasets and approaches for the estimation of rainfall erosivity over Italy: A comprehensive comparison study and a new method. Journal of Hydrology: Regional Studies, 34, 100788, 2021.

Palau, R. M., Gisnås, K. G., Solheim, A., and Gilbert, G. L.: Regional-scale analysis of weather-related rockfall triggering mechanisms in Norway, and its sensitivity to climate change. *Natural Hazards and Earth System Sciences Discussions*, *2024*, 1-27, 2024.

Palladino, M. R., Viero, A., Turconi, L., Brunetti, M. T., Peruccacci, S., Melillo, M., ... and Guzzetti, F.: Rainfall thresholds for the activation of shallow landslides in the Italian Alps: the role of environmental conditioning factors. Geomorphology, 303, 53-67, 2018.

Paranunzio, R., and Marra, F.: Open gridded climate datasets can help investigating the relation between meteorological anomalies and geomorphic hazards in mountainous areas. Global and Planetary Change, 232, 104328, 2024.

Paranunzio, R., Chiarle, M., Laio, F., Nigrelli, G., Turconi, L. and Luino, F.: New insights in the relation between climate and slope failures at high-elevation sites. Theoretical and Applied Climatology, 137:1765-1784, 2019.

Paranunzio, R., Laio, F., Chiarle, M., Nigrelli, G. and Guzzetti, F.: Climate anomalies associated with the occurence of rockfalls at high-elevation in the Italian Alps, 2016.

Paranunzio, R., Laio, F., Nigrelli, G., and Chiarle, M.: A method to reveal climatic variables triggering slope failures at high elevation. Natural Hazards, 76, 1039-1061, 2015.

Pepin, N., Bradley, R.S., Diaz, H.F. et al (2015) Elevation-dependent warming in mountain regions of the world. Nat Clim Chang 5:424–430. doi:10.1038/nclimate2563.

Pepin, N. C., Arnone, E., Gobiet, A., Haslinger, K., Kotlarski, S., Notarnicola, C., ... and Adler, C.: Climate changes and their elevational patterns in the mountains of the world. Reviews of Geophysics, 60(1), e2020RG000730, 2022.

Perret, S., Stoffel, M., and Kienholz, H.: Spatial and temporal rockfall activity in a forest stand in the Swiss Prealps—a dendrogeomorphological case study. Geomorphology, 74(1-4), 219-231, 2006.

Ravanel, L., Magnin, F. and Deline, P. Impacts of the 2003 and 2015 summer heatwaves on permafrost-affected rock-walls in the Mont Blanc massif. Sci. Total Environ. 609, 132–143, 2017.

Rupp, S., and Damm, B.: A national rockfall dataset as a tool for analysing the spatial and temporal rockfall occurrence in Germany. Earth Surface Processes and Landforms, 45(7), 1528-1538, 2020.

Salzmann, N., Nötzli, J., Hauck, C., Gruber, S., Hoelzle, M., and Haeberli, W.: Ground surface temperature scenarios in complex high-mountain topography based on regional climate model results. Journal of Geophysical Research: Earth Surface, 112(F2), 2007.

Sandersen, F., Bakkehøi, S., Hestnes, E., and Lied, K.: The influence of meteorological factors on the initiation of debris flows, rockfalls, rockslides and rockmass stability. Publikasjon-Norges Geotekniske Institutt, 201, 97-114, 1997.

Sass, O., and Oberlechner, M.: Is climate change causing increased rockfall frequency in Austria?. Natural Hazards and Earth System Sciences, 12(11), 3209-3216, 2012.

Scavia, C., Barbero, M., Castelli, M., Marchelli, M., Peila, D., Torsello, G., and Vallero, G.: Evaluating rockfall risk: Some critical aspects. Geosciences, 10(3), 98, 2020.

Schär, C., Vidale, P. L., Lüthi, D., Frei, C., Häberli, C., Liniger, M. A., and Appenzeller, C.: The role of increasing temperature variability in European summer heatwaves. Nature, 427(6972), 332-336, 2004.

Schmidli, J., and Frei, C.: Trends of heavy precipitation and wet and dry spells in Switzerland during the 20th century. International Journal of Climatology: A Journal of the Royal Meteorological Society, 25(6), 753-771, 2005.

Stoffel, M., and Huggel, C.: Effects of climate change on mass movements in mountain environments. Progress in physical geography, 36(3), 421-439, 2012.

Stoffel, M., Trappmann, D. G., Coullie, M. I., Ballesteros Cánovas, J. A., and Corona, C.: Rockfall from an increasingly unstable mountain slope driven by climate warming. Nature Geoscience, 17(3), 249-254, 2024.

Stull, R. B.: Meteorology for scientists and engineers: a technical companion book with Ahrens' Meteorology Today, 2000.

Trigila, A., Iadanza, C., and Guerrieri, L. The IFFI project (Italian landslide inventory): Methodology and results. Guidelines for mapping areas at risk of landslides in Europe, 23, 15, 2007.

Valagussa, A., Frattini, P., and Crosta, G. B.: Earthquake-induced rockfall hazard zoning. Engineering Geology, 182, 213-225, 2014.

Varnes, D. J.: Slope movement types and processes. Special report, 176, 11-33, 1978.

Viani, C., Chiarle, M., Paranunzio, R., Merlone, A., Musacchio, C., Coppa, G. and Nigrelli, G.: An integrated approach to investigate climate-driven rockfall occurence in high alpine slope: the Bessanese glacial basin, Western Italian Alps. Journal of Mountain Sience 17(11), 2020.

Volkwein, A., Schellenberg, K., Labiouse, V., Agliardi, F., Berger, F., Bourrier, F., ... and Jaboyedoff, M.: Rockfall characterisation and structural protection–a review. Natural Hazards and Earth System Sciences, 11(9), 261, 2011.

Weidner, L., Walton, G., & Phillips, C.. Investigating the influences of precipitation, snowmelt, and freeze-thaw on rockfall in Glenwood Canyon, Colorado using terrestrial laser scanning. Landslides, 21(9), 2073-2091, 2024

Wang, J., Guan, Y., Wu, L., Guan, X., Cai, W., Huang, J., ... and Zhang, B.: Changing lengths of the four seasons by global warming. Geophysical Research Letters, 48(6), e2020GL091753.7-2651, 2021.

Widmann, M., and Schär, C.: A principal component and long-term trend analysis of daily precipitation in Switzerland. International Journal of Climatology: A Journal of the Royal Meteorological Society, 17(12), 1333-1356, 1997.

World Meteorological Organization.: Calculation of monthly and annual 30-year standard normals. WCDP 10, WMO-TD 341, 1989.

~~Zhao, T., Crosta, G.B., Utili, S., and De Blasio F.V.: Investigation of rock fragmentation during rockfalls and rock avalanches via 3-D discrete element analyses. J. Geophys. Res. Earth Surf., 122, 678-695, 2017.~~